Title
Regulation of Trafficking of AMPA-type Glutamate Receptors

Author
Lee, Boram

Publication Date
2021

Peer reviewed|Thesis/dissertation

Regulation of Trafficking of AMPA-type Glutamate Receptors

By

BORAM LEE
DISSERTATION

Submitted in partial satisfaction of the requirements for the degree of

DOCTOR OF PHILOSOPHY

in

Biomedical Engineering

in the

OFFICE OF GRADUATE STUDIES

of the

UNIVERSITY OF CALIFORNIA

DAVIS

Approved:

Johannes W. Hell, Chair

Yang K. Xiang

Manuel F. Navedo

Committee in Charge

2021

Abstract

Synaptic transmission is mediated by diverse ion channels and receptors and the fine regulation of those ion channels and receptors determines physiological functions in the brain. Thus, molecular mechanisms of function and regulation of them have been extensively studied to understand how neurons work.

AMPA-type glutamate receptor (AMPAR) is responsible for the most fast excitatory transmission in the brain. Phosphorylation and surface insertion of AMPARs is essential for augmentation of long-term potentiation (LTP) which is the physiological correlate of learning and memory. AMPAR and β_2 adrenergic receptor (β_2AR) form functional supramolecular signaling complexes and stimulation of β_2AR enhances phosphorylation and trafficking of AMPARs through G_S protein, adenylyl cyclase (AC), and PKA signaling. PKA phosphorylates S845 in the C-terminus of GluA1 subunit. Phosphorylation at S845 augments AMPAR surface expression and postsynaptic targeting. The regulation of AMPARs could be influenced by ligands of β_2ARs or AMPAR-interacting proteins.

Chapter I will review fundamental understandings of synaptic transmission and plasticity and features of AMPARs in neurons. In **chapter II**, regulation of surface insertion of AMPARs by norepinephrine (NE), a ligand of β_2AR, via intracellular β_2AR – AC – PKA signaling will be examined. Also, the role of transporters for NE such as organic cation transporter 3 (OCT3) and plasma membrane monoamine transporter (PMAT) in stimulation of intracellular β_2AR by NE will be investigated. The study in **chapter III** will suggest a novel mechanism of regulating trafficking of AMPARs through their association

with L-type calcium channel, $Ca_V1.2$. In addition, the interaction between AMPAR and $Ca_V1.2$ will be characterized by biochemical experiments. In **chapter IV**, it will be discussed how this study contributes to the understanding of regulation of AMPARs and the development of therapeutics for neuronal disorders.

Acknowledgments

I would like to express my deepest appreciation to everyone who supported me during my PhD journey.

Foremost, I am extremely grateful to my advisor Dr. Johannes W. Hell for his valuable mentoring, support, and patience. He guided me into very interesting research fields, biochemistry and neuroscience. He taught me not only research knowledge and techniques but also scientific attitudes. I also would like to thank Dr. Mary C. Horne for her advice about research. I learned extensive biochemistry and molecular biology skills and knowledge from her.

I also sincerely thank my dissertation committee members, Dr. Yang Kevin Xiang and Dr. Manuel F. Navedo for their support and time for my research and thesis. They provided me with great feedback and encouragement which improved my project.

My gratitude extends to lab mates. I want to thank Karam Kim, Kwun Nok Mimi Man, Peter Bartels, Dhruba Chowdhury, and Anne Hergarden, awesome scientists in the lab for their great advice. I am especially grateful to Peter Henderson for training me. Also, Andrea Coleman and Kyle Ireton, same year graduate students, Jennifer Price and Erik Hammes, BMEGG buddies, and Olivia Buonarati, a former graduate student, nourish my life in the lab. Other Hell lab members, Sheng-Yang Ho, Ariel Jacobi, Zoe Estrada-Tobar, Eric Nguyen, Xiaomin Xing, and Joungho Son, have always supported me.

Finally, I am deeply indebted to my family for the inspiration and unconditional support throughout my journey.

Table of Contents

List of Figures

Chapter I

Backgrounds

Synaptic transmission

The synapse is the contact site between two different neurons, where neurons communicate. The communication process in the synapse is called synaptic transmission. When an action potential reaches an axon terminal of the functionally presynaptic neuron, the plasma membrane at the presynaptic terminal is depolarized and voltage-gated calcium channels are activated. Calcium ion influx through the voltage-gated calcium channels induces release of synaptic vesicles containing neurotransmitter (Dolphin & Lee, 2020). Neurotransmitters such as glutamate or gamma amino butyric acid (GABA) bind to receptors at postsynaptic terminals and stimulate signal transduction in postsynaptic neurons via opening of ligand-gated ion channels (e.g., ionotropic glutamate receptors or $GABA_A$ receptors, respectively) or activation of G-protein coupled receptors (GPCRs). Opening of ion channels causes depolarization of plasma membrane at postsynaptic sites and action potential or activation of voltage-gated ion channels (Voglis & Tavernarakis, 2006). In other words, GPCRs interact with heterotrimeric G proteins which composed of α, β, and γ subunits. Binding of neurotransmitters to GPCRs results in the conformational change of GPCRs and the dissociation of G proteins. Dissociated G_α subunit initiates the cAMP pathway followed by a variety of signal transductions in postsynaptic neurons (S. J. Hill et al., 2010). For example, most of β_2 adrenergic receptor (β_2AR) is associated with G_s protein and stimulation of β_2AR activates adenylyl cyclase (AC) and increases the

production of cAMP. cAMP induces the activation of protein kinase A (PKA) and PKA phosphorylates target proteins (Johnson, 2006; Nguyen & Connor, 2019).

Synaptic plasticity

The strength of synaptic transmission is typically very stable over months if not for a lifetime. However, heightened activity of the presynaptic neurons can lead to a long-lasting or permanent increase or decrease in synaptic strength, which is called long-term potentiation (LTP) or long-term depression (LTD), respectively. Molecular mechanisms of LTP and LTD have been extensively investigated because they regulate neuronal activities, especially learning and memory. N-Methyl-D-aspartate (NMDA) receptor (NMDAR)-dependent LTP and LTD in the CA1 region of the hippocampus are the most considerably studied form of synaptic plasticity. NMDAR-dependent LTP and LTD are triggered by the activation of NMDARs. Activated NMDARs at postsynaptic sites largely increase the influx of Ca^{2+} and stimulate calcium/calmodulin-dependent protein kinase II (CaMKII). Autophosphorylation of CaMKII augments the trafficking of α-amino-3-hydroxy-5-methyl-4-isoxazolepropionic acid (AMPA) receptors on the surface of postsynaptic sites and enhances synaptic transmission which is LTP. By contrast, activation of NMDARs by low frequency stimulation (0.5-5 Hz) induces modest increase in the influx of Ca^{2+} and dephosphorylation of AMPARs by protein phosphatase such as calcineurin (CN) and protein phosphatase 1 (PP1). Dephosphorylated AMPARs are internalized and the synaptic transmission is weakened (Citri & Malenka, 2008; van Bommel & Mikhaylova, 2016; Woolfrey & Dell'Acqua, 2015).

AMPA-type glutamate receptors

Glutamate is the major excitatory neurotransmitter in the brain. Excitatory transmission in glutamatergic synapses is mediated by glutamate receptors; the ligand-gated glutamate receptors are called ionotropic glutamate receptors (iGluRs) and include AMPA- and NMDA- and kainate-type receptors. The glutamate-activated GPCRs are called metabotropic glutamate receptors (mGluRs) and include mGluR1-5. AMPA and NMDA receptors are highly expressed in the postsynaptic density (PSD), which is the protein-dense postsynaptic site proper. By contrast, mGluRs are abundant in both the presynaptic domain and peripheral to the PSD (the perisynaptic space) (Scheefhals & MacGillavry, 2018).

AMPA-type glutamate receptors (AMPAR) mediate fast excitatory transmission responding to the release of glutamate in hundreds of milliseconds (Traynelis et al., 2010). AMPARs are heterotetramers composed of four subunits, GluA1, GluA2, GluA3, and GluA4. GluA4 is expressed low in adult brain. Subunits share common architecture: the extracellular amino-terminal domain (ATD), the extracellular ligand-binding domain (LBD), the transmembrane domain (TMD), and an intracellular carboxyl-terminal domain (CTD) (Greger et al., 2017; Henley & Wilkinson, 2016; Traynelis et al., 2010). Phosphorylation and protein-binding sites exist in the CTD, which play an important role in regulating AMPARs. While GluA1, GluA4, and an alternatively spliced form of GluA2 (GluA2L) have long CTD, GluA2, GluA3, and an alternatively spliced form of GluA4 (GluA4S) contain short CTD (Anggono & Huganir, 2012). The most common form of AMPAR heterotetramers in the forebrain is GluA1 and GluA2 and the second most common form is GluA2 and GluA3 (W. Lu et al., 2009; Wenthold et al., 1996). Ca^{2+}-permeability of

AMPARs is determined by presence and RNA editing of GluA2 subunit. The codon for glutamine (Q) in GluA2 mRNA is converted to arginine (R) by RNA editing mediated by the family of adenosine deaminases that act on RNA (ADARs). Most GluA2 (~99% of total GluA2) are edited (GluA2 (R)) and impermeable to Ca^{2+}. AMPARs lacking GluA2 and having unedited GluA2 (Q) are Ca^{2+}-permeable. Ca^{2+}-permeable AMPARs contribute to excitability in the brain (Wright & Vissel, 2012).

Synaptic expression and function of the AMPAR are critical for neuronal activity and the AMAPR is a potential drug target for various neuronal diseases such as epilepsy and Alzheimer's disease (Dhuriya & Sharma, 2020; Henley & Wilkinson, 2016; H. Zhang & Bramham, 2020). For instance, perampanel (Fycompa®), the selective AMPAR antagonist, is used as an anti-convulsant drug for epilepsy (Frampton, 2015) and amyotrophic lateral sclerosis (ALS) (Akamatsu et al., 2016). Other agonist or antagonist of AMPARs have been investigated as a drug for neuronal diseases (Chang et al., 2012; Dhuriya & Sharma, 2020).

Proteins interacting with the AMPAR

AMPARs associate with many auxiliary proteins and their interaction regulates localization and trafficking of AMPARs. Thus, studying the roles of auxiliary proteins such as Transmembrane AMPAR Regulatory Proteins (TARPs) and cornichon proteins (CNIHs) is essential for understanding function and regulation of AMPARs (Bissen et al., 2019).

Stargazin is the first discovered auxiliary protein of AMPARs. Stargazin is a member of TARPs and also called γ2. TARPs are divided into Type I (γ2, γ3, γ4, and γ8) Type II (γ5 and γ7). Type I TARPs bind to all AMPAR subunits and AMPAR complex can contain only one TARP. TARPs stabilize surface insertion of AMPARs and modulate pharmacology and gating of AMPARs (Bissen et al., 2019; L. Chen et al., 2000; Kato et al., 2010; Tomita et al., 2003). Cornichon homologs (CNIHs) modulate gating and surface expression of AMPARs. CNIH-2 and -3 alter gating of AMPARs by slowing down the deactivation and desensitization of AMPARs (Boudkkazi et al., 2014; Jacobi & von Engelhardt, 2021; Schwenk et al., 2009). Also, the selective binding of CNIH-2 and -3 to GluA1 AMPAR subunit is required for the synaptic expression of GluA1-containing AMPARs and γ8 inhibits the binding to CNIH-2 and -3 to GluA2 and 3 (Herring et al., 2013).

Membrane-associated guanylate kinases (MAGUKs) are a family of scaffolding proteins composed of postsynaptic density 95 (PSD-95), PSD-93, synapse-associated protein 97 (SAP97), and SAP102. The conserved structure of all MAGUK proteins is three PDZ domains and one SH3-GK domain (Bissen et al., 2019; X. Chen et al., 2015). PSD-95 is important for synapse maturation and synaptic plasticity (Beique & Andrade, 2003; El-Husseini et al., 2000; Tomita et al., 2001). Overexpression of PSD-95 increase the number of pre- and postsynapses (El-Husseini et al., 2000) and AMPAR mEPSC (Beique & Andrade, 2003). By contrast, knockout or knockdown of PSD-95 impairs AMPAR mediated synaptic transmission (Elias et al., 2006; Schluter et al., 2006). Also, PSD-95 regulates clustering of AMPARs at synapses (Beique & Andrade, 2003; El-Husseini et al., 2000; Nair et al., 2013) and interaction of stargazin and PSD-95 plays essential role in

regulation of surface insertion of AMPARs. (Bats et al., 2007; L. Chen et al., 2000; Nicoll et al., 2006; Schnell et al., 2002). SAP97 directly binds to GluA1 subunit and mediates transmission and trafficking of AMPARs from the Golgi network to the plasma membrane (Howard et al., 2010; Leonard et al., 1998; Waites et al., 2009).

Synapse differentiation-induced gene 1 (SynDIG1) is identified as an additional AMPAR auxiliary protein by microarray (Diaz et al., 2002). SynDIG1 interacts with AMPAR and regulates development of excitatory synaptic transmission (Kalashnikova et al., 2010; Lovero et al., 2013). However, SynDIG1 does not affect gating or surface insertion of AMPAR like other AMPAR auxiliary proteins (Lovero et al., 2013). SynDIG4 colocalizes with GluA1-containing AMPAR at extrasynaptic sites (Kirk et al., 2016). In contrast to SynDIG1, expression of SynDIG4 influences AMPAR gating kinetics in a subunit-dependent manner. SynDIG4 decreases desensitization of GluA1 homomers but not heteromeric GluA1/2 (Matt et al., 2018).

Functional complex of AMPAR and β_2AR

AMPAR forms a complex with β_2AR, G_S protein, adenylyl cyclase (AC), and protein kinase A (PKA) and its synaptic activity and expression are regulated by localized cAMP signaling. β_2AR is associated with AMPAR via PSD-95, A-Kinase Anchoring Protein 5 (AKAP5), SAP97, and PKA (Buonarati et al., 2019; Joiner et al., 2010; Man et al., 2020; Patriarchi et al., 2018). PSD-95 interacts with AMPAR by binding to the C terminus of auxiliary AMPAR subunits, TARPs (Schnell et al., 2002) and the third PDZ domain of PSD-95 is connected to the C terminus of β_2AR (Joiner et al., 2010; D. Wang et al., 2010).

The homolog of PSD-95, SAP97, directly binds to the C terminus of GluA1 AMPAR subunit through its PDZ domain (Leonard et al., 1998) and also interacts with AKAP5 via the SH3-GK modules (Bhattacharyya et al., 2009; Colledge et al., 2000; Tavalin et al., 2002). SAP97 associated with AKAP5 binds to AC (Willoughby et al., 2010; M. Zhang et al., 2013) and recruits protein phosphatase-2B (PP2B) and PKA (Colledge et al., 2000; Tavalin et al., 2002). Stimulation of β_2AR initiates G_S protein – AC – cAMP – PKA signaling and PKA phosphorylates S845 in GluA1. Phosphorylation at S845 enhances channel activity (Banke et al., 2000), surface insertion (He et al., 2009), and postsynaptic targeting (Esteban et al., 2003; Huganir & Nicoll, 2013; Oh et al., 2006) of AMPARs.

Chapter II

Augmentation of Surface Insertion of the AMPA-type Glutamate Receptor by Intracellular Signaling by NE via the β_2 Adrenergic Receptor

Introduction

Norepinephrine (NE) and its transporters

Norepinephrine (NE), which is also called noradrenaline, is a neurotransmitter released from the locus coeruleus. NE underlies alertness, emotional arousal, sleep regulation, learning, and memory. NE is synthesized from tyrosine and released from noradrenergic terminals (Ranjbar-Slamloo & Fazlali, 2019; Ross & Van Bockstaele, 2020; Wassal et al., 2009; Zhou, 2004). NE acts as an endogenous ligand for G-protein coupled receptors, α- and β-adrenergic receptors, and induces adrenergic signaling, which modulates neuronal excitability and synaptic transmission (O'Dell et al., 2015). The rest of NE in synaptic cleft is taken by other neurons or degraded.

Monoamine neurotransmitters such as NE, dopamine, and serotonin cannot penetrate the plasma membrane by passive diffusion (Bochain et al., 1981; J. Wang, 2016). Thus, monoamine transporters are important for clearance of monoamine neurotransmitters from the synaptic cleft and surrounding regions that are reached by these

neurotransmitters, which act over wider ranges than fast neurotransmitter such as glutamate or GABA. There are two different clearance systems of monoamine neurotransmitter, uptake$_1$ and uptake$_2$ (Eisenhofer, 2001; Grundemann et al., 1998). Uptake$_1$ system is mainly responsible for the re-uptake of monoamine neurotransmitters into presynaptic neurons and mediated by Na^+- and Cl^--dependent, high affinity (K_d = 0.27 μM), and low capacity (V_{max} = 1.22 nmol/min/g tissue) transporters, norepinephrine transporter (NET), dopamine transporter (DAT), and serotonin transporter (SERT), which are members of the solute carrier 6 family (Gasser, 2019; Jayanthi & Ramamoorthy, 2005; Nemeroff & Owens, 2004; Vieira & Wang, 2021). On the other hand, transporters in uptake$_2$ system are Na^+- and Cl^--independent and have low affinity (K_d = 252 μM) and high capacity (V_{max} = 100 nmol/min/g tissue). The organic cation transporter 3 (OCT3) and the plasma membrane monoamine transporter (PMAT) are main components of the uptake$_2$ system in the brain with some contributions also by OCT2 (Duan & Wang, 2010; Gasser, 2019; Matthaeus et al., 2015; Vieira & Wang, 2021). Thus, NE can be transported into neurons through the plasma membrane by OCT3, PMAT, and NET.

Organic cation transporters (OCTs) constitute the SLC22 transporter family which consists of three isoforms: OCT1 (SLC22A1), OCT2 (SLC22A2), and OCT3 (SLC22A3). OCTs are expressed in various tissues such as liver and kidney. In the brain, OCT2 and OCT3 is abundantly and broadly expressed whereas the expression level of OCT1 is very low in the brain (Courousse & Gautron, 2015; Duan & Wang, 2010; Gasser et al., 2009; Vialou et al., 2004; Wu et al., 1998). Also, OCT3 is found in endosomal membrane as well as plasma membrane. This suggests that both extracellular and intracellular NE can be transported by OCT3 (Gasser et al., 2017). Dysfunction of OCT3 causes disorders in

anxiety, stress, and dopaminergic neurotoxicity (Courousse & Gautron, 2015; H. Koepsell, 2021).

The plasma membrane monoamine transporter (PMAT) is encoded by SLC29A4 gene and mostly localized at plasma membrane as implicated by its name. PMAT is distributed in multiple tissues such as brain, heart, kidney, and liver (Duan & Wang, 2010; Engel et al., 2004). In addition, PMAT is expressed in diverse neuronal cells, pyramidal neurons, interneurons, granular neurons, and Purkinje cells and localized in cell bodies, dendrites, and axons (Dahlin et al., 2007; Engel et al., 2004). Neuronal disorders such as autism, depression, and Parkinson's disease are associated with PMAT (Vieira & Wang, 2021).

Both OCT3 and PMAT contribute to clearance of monoamines by uptake$_2$ system. While norepinephrine, histamine, and epinephrine are mainly transported by OCT3 in peripheral organs, PMAT is the major transporter for 5-HT and dopamine in central nervous system (Duan & Wang, 2010). In addition, both are inhibited by decynium 22 (D22) (IC_{50} value for hOCT3: 0.1 µM and K_i value for hPMAT: 0.1 µM) (Duan & Wang, 2010; Engel et al., 2004; Hayer-Zillgen et al., 2002). On the other hand, OCT3 is readily blocked by corticosterone (CORT) (IC_{50} value for hOCT3: 0.12-0.62 µM and for rat OCT3: 4.9 µM) (Hermann Koepsell, 2021) and lopinavir (LOPI) is more selective to PMAT compared to OCT3 (IC_{50} value for PMAT: 1.4 µM) (Duan et al., 2015).

The norepinephrine transporter (NET), one of the monoamine transporters of the uptake$_1$ system, is more selective for NE than dopamine and expressed in the brain, peripheral nervous system, adrenal gland, and placenta (Kristensen et al., 2011). In both neurons and endocrine cells, NETs are localized at plasma membrane and intracellular vesicles (Matthies et al., 2009). The function of NET is important for the regulation of noradrenergic

signaling pathways and neuronal functions such as attention, learning and sleep. Therefore, the NET inhibitor, Desipramine (DESI) is used as an antidepressant drug. K_i value of DESI for NET inhibition is 7.36 nM (Zhou, 2004). The other inhibitor for NET, atomoxetine, is used to treat attention-deficit hyperactivity disorder (ADHD) and its K_i value for NET is 5 nM (Bymaster et al., 2002).

Trafficking of AMPARs

Postsynaptic localization of AMPARs is important for fast and efficient synaptic transmission. Especially, receptors having a low-affinity for their ligands such as AMPARs (EC_{50} is ~100 to 1000 μM) should be localized close to the site where neurotransmitters are released (Groc & Choquet, 2020). Overall surface expression of AMPARs is regulated by synaptic plasticity. During LTP, AMPARs are inserted into the surface by exocytosis while LTD induces the endocytosis of AMPARs (Buonarati et al., 2019; Choquet, 2018; Diering & Huganir, 2018; Henley & Wilkinson, 2016; Herring & Nicoll, 2016; Patriarchi et al., 2018; Shepherd & Huganir, 2007). In addition, diffusion of AMPARs to postsynaptic sites where they become trapped upon augmented calcium influx and LTP and interaction of AMPARs with auxiliary proteins such as stargazing and PSD-95 is required for the reversibly stabilization of AMPARs in the plasma membrane (Choquet, 2018).

Newly synthesized and recycled AMPARs are delivered by recycling endosomes (Bowen et al., 2017). The retromer complex is an important component of endosomes and play key roles in recognizing cargos including various GPCRs such as β_2ARs (Choy et al., 2014). The retromer complex is composed of vacuole protein sorting (VPS) trimer and

sorting nexins (SNXs). Vps35/Vps26/Vps29 trimers mediate the cargo selection. SNXs have Bin/Amphiphysin/Rvs (BAR) domains (SNX-BAR proteins) to assemble and stabilize tubules for the formation of endosomal vesicles (Seaman, 2012; Vagnozzi & Pratico, 2019). Trafficking of AMPARs during LTP is impaired in VPS35 knockdown (KD) cells (Temkin et al., 2017) and surface insertion of AMPARs and β_2ARs is mediated by SNX27 (Hussain et al., 2014; Loo et al., 2014; Temkin et al., 2011).

Dysregulation of the trafficking of AMPARs results in abnormal synaptic transmission and neuronal disorders (Groc & Choquet, 2020; Henley & Wilkinson, 2013; Jurado, 2017). For example, soluble amyloid beta (Aβ) oligomers disrupt the trafficking of AMPARs and increase the endocytosis of AMPARs. Thus, in Alzheimer's disease (AD), the surface expression of AMPARs is reduced (Walsh & Selkoe, 2007; Zhao et al., 2010). Stabilization of AMPARs on the surface is altered in Huntington's disease, which causes impaired neuronal activity (H. Zhang et al., 2018)

Phosphorylation of AMPAR GluA1 subunit at S845 by stimulation of β_2AR increases surface insertion (He et al., 2009) and postsynaptic targeting (Esteban et al., 2003; Huganir & Nicoll, 2013; Oh et al., 2006) of AMPARs. Disruption of interaction between AMPAR and β_2AR blocks the increase in phosphorylation at S845, in surface expression of GluA1, and in AMPAR-mediated EPSCs induced by β_2AR signaling (Joiner et al., 2010) Surface insertion of AMPARs in endosomal vesicles should be induced by intracellular β_2AR – cAMP – PKA signaling. Then, how can NE reach intracellular β_2ARs and induce trafficking of intracellular AMPARs? Previous data suggested that NE is transported into cytosol and lumen of intracellular vesicles via OCT3 to stimulate intracellular β_2AR

(Irannejad et al., 2017; Tsvetanova & von Zastrow, 2014). Based on previous studies, I hypothesized that **AMPARs are inserted into the surface upon stimulation of intracellular β_2ARs, which is induced by NE transported into cytosol via its cognate transporters** (Figure 1). I examined whether inhibition of transporters for NE, OCT3, PMAT, and NET, affects phosphorylation and surface expression of AMPARs by NE. I also investigated the change in interaction of the AMPAR and its auxiliary proteins, SNX27, and VPS35 by NE.

Result

Inhibition of OCT3 and PMAT, but not NET decreases NE-induced phosphorylation at S845 in GluA1

To investigate the role of transporters for NE in regulation of AMPAR phosphorylation via β_2AR signaling, transporters for NE were pharmacologically blocked by their inhibitors (D22, CORT, LOPI, and DESI) and the change in phosphorylation at S845 in GluA1 after the treatment of NE with or without inhibitors for the transporters was analyzed by immunoblotting with phospho-specific antibodies. Phosphorylation at S831 in GluA1 was also examined to monitor potential but a priori unexpected effects on the signaling via CaMKII or PKC, the two kinases that phosphorylate S831 (Barria et al., 1997; Mammen et al., 1997; Roche et al., 1996). The effect of inhibition of OCT3 and PMAT by D22 on phosphorylation at S845 was analyzed by immunoprecipitation (IP) of GluA1 and immunoblotting of pS845, pS831, and GluA1 (Figure 2A). Mouse forebrain slices were pre-incubated with ACSF containing vehicle (DMSO) or 100 nM D22 for 5min at 32°C and incubated with 1 μM of NE with or without 100 nM of D22 for 10min at 32°C. The results of probing pS845 and pS831 after the IP of GluA1 showed that NE increased phosphorylation at S845 but not S831. D22 partially inhibited the upregulation of phosphorylation of S845 by NE treatment. D22 alone did not affect the change in phosphorylation of GluA1 (Figure 2B). However, this result implicates that OCT3 or PMAT mediates a portion of NE-induced S845 phosphorylation without differentiating between the two transporters. Thus, I applied CORT, an OCT3-selective inhibitor, or LOPI, a

PMAT-selective inhibitor, to forebrain slices and analyzed the change in phosphorylation of GluA1 at S845 and S831 by IP of GluA1 and immunoblotting for pS845, pS831, and GluA1. Treatment with 10 μM CORT impeded the augmentation in NE-induced phosphorylation at S845 while phosphorylation at S845 was not changed by CORT alone (Figure 3). In addition, a similar result was found in the blotting from forebrain slices treated with 1 μM NE with or without 10 μM LOPI. Phosphorylation at S845 but not S831 was increased by NE, which was inhibited but again not fully blocked by inhibiting PMAT with LOPI (Figure 4). Similarly, it was tested whether blocking the high affinity and low-capacity NE transporter NET by 1 μM of DESI influences NE-induced phosphorylation of S845 in forebrain slices (Figure 5). In contrast to the treatment of D22, CORT, and LOPI, DESI did not impair NE-induced phosphorylation at S845 (Figure 5B). Also, phosphorylation at S831 was not changed by either NE or inhibitors for OCT3, PMAT, or NET. These results demonstrated that NE has to be transported into neurons via OCT3 and PMAT, not NET, to stimulate intracellular β_2ARs and induces phosphorylation of GluA1 at S845.

Blocking βARs by membrane-impermeable inhibitor, sotalol, significantly reduces phosphorylation of AMPARs

The membrane impermeable βAR antagonist, sotalol (Baker, 2005; M. L. Chen & Yu, 2009; Liu et al., 2012) was used to inhibit stimulation of extracellular β_2AR and explore the change in phosphorylation of GluA1 by only intracellular β2AR. Forebrain slices from wild type mice were pre-incubated with ACSF containing vehicle (DMSO) or Sotalol then incubated with vehicle (DMSO) or 1 μM of norepinephrine (NE) with or without 100 μM of

sotalol. After the treatment, Triton X-100 lysates were prepared for immunoprecipitation with control IgG or anti-GluA1 antibody and sequential immunoblotting with anti-pS845, pS831, and GluA1 antibodies. The quantitative analysis of phosphorylation of GluA1 showed that NE-induced phosphorylation at both S845 and S831 substantially declined by treatment with sotalol. (Figure 6). While inhibition of OCT3 and PMAT by D22, CORT, and LOPI affected only phosphorylation at S845, blocking extracellular βARs by sotalol decreased phosphorylation of GluA1 at both S845 and S831. Also, the reduction in NE-induced phosphorylation of GluA1 was much larger in NE and sotalol-treated slices than in NE and D22, CORT, or LOPI-treated slices. This unexpected effect of sotalol could be because sotalol inhibits not only β adrenergic receptors but also potassium channels (Baker, 2005; Doggrell & Brown, 2000; Funck-Brentano, 1993; Mubarik et al., 2021).

Surface expression of AMPARs is regulated by activity of OCT3 and PMAT

Immunostaining of surface expressed GluA1 (sGluA1) was conducted to investigate the surface insertion of GluA1 in NE-treated cultured hippocampal neurons. D22, CORT, or LOPI was incubated with NE to test whether surface insertion of GluA1 also requires the function of OCT3 and PMAT. Hippocampal neuron culture was treated with vehicle (DMSO) or 1 μM NE with or without 10 nM D22, fixed, incubated with the primary antibody against the extracellular N-terminus of GluA1 for surface labeling (sGluA1), permeabilized with PBS containing 0.25% Triton X-100, and incubated with antibodies against PSD-95 and MAP2B, followed by respective secondary antibody labeling. PSD-95 and MAP2B are markers for postsynaptic sites and dendrites (Figure 7A). GluA1 that is expressed on the surface of postsynaptic sites was quantified by counting the number of PSD-95 puncta

which colocalized with sGluA1 puncta (Figure 7B). The quantification is shown as the ratio of the number of sGluA1-colocalized to the total PSD-95 puncta. In NE-treated hippocampal neurons, the surface expression of GluA1 was increased compared to the control. When D22 was applied with NE, the expression level of sGluA1 was fully blocked. D22 itself had no effect. Next, I treated CORT or LOPI in hippocampal neuron culture and analyzed the change in surface expression of GluA1 by immunostaining of sGluA1, PSD-95, and MAP2B. Incubation of 1 μM NE with 10 μM CORT blocked 86% of NE-induced surface expression of GluA1, while CORT alone did not affect the expression level of sGluA1 (Figure 8). Figure 9A showed representative images of immunostaining with hippocampal neurons incubated with vehicle (DMSO) or 1 μM NE with or without 10 μM LOPI. Higher surface expression of GluA1 was observed in NE-treated neurons but the effect of NE was almost totally blocked by LOPI (96%) (Figure 9B). These results are consistent with the immunoblotting of pS845 and indicate that transport of NE via OCT3 and PMAT is necessary for the stimulation of intracellular β_2ARs and trafficking of AMPARs to the surface.

NE-induced phosphorylation at S845 is lower in OCT3 KO than wild-type (WT) mouse neurons

Given the data of immunoblotting of S845 and immunostaining of sGluA1 in hippocampal neurons treated with NE with or without OCT3 or PMAT inhibitors, NE cannot stimulate intracellular β_2ARs and induce phosphorylation of intracellular AMPARs in the absence of OCT3. Thus, I compared NE-induced phosphorylation at S845 in WT and OCT3 KO mice (Figure 10). Forebrain slices were prepared and incubated with ACSF containing

vehicle (water) or 1 μM NE for 10 min at 32°C. Proteins were extracted from the brain slices with the Triton X-100 lysis buffer and cleared by ultracentrifugation. Control IgG or anti-GluA1 antibody was used for immunoprecipitation with the lysate. Phosphorylation at S845 and total GluA1 was probed by anti-pS845 and GluA1 antibodies. The level of phosphorylation of GluA1 at S845 was analyzed by densitometry of phosphoserine bands and normalization to total GluA1 bands. Phosphorylation at S845 was increased in both WT and OCT3 KO neurons by NE treatment. However, the increase of phosphorylation at S845 in WT was much larger than in OCT3 KO.

Change in interaction of GluA1 and its auxiliary proteins, PSD-95, SNX27, and VPS35 during trafficking of AMPARs by NE

Auxiliary proteins of the AMPAR and PSD-95 support stabilization of AMPARs on the surface (Bissen et al., 2019) and retromer-associated sorting nexin protein, SNX27, and retromer complex protein, VPS35 regulate trafficking of AMPARs interacting with AMPAR subunits (Loo et al., 2014; Temkin et al., 2017). Therefore, I examined whether the interaction between GluA1 and auxiliary proteins of AMPARs (Stargazin, SynDIG1, and SynDIG4), PSD-95, SNX27, and VPS35 is a potential molecular mechanism that boosts trafficking of AMPARs to the cell surface upon treatment with NE (Figure 11). 1 μM NE was applied to forebrain slices for 10 min at 32°C and the slices were lysed with 1% Triton X-100 lysis buffer. Co-immunoprecipitation (co-IP) of GluA1 was performed with the lysate of slices followed by immunoblotting for Stargazin, PSD-95, SynDIG1, SynDIG4, SNX27, VPS35, and GluA1. Interaction between GluA1 and other proteins was not

significantly changed by NE. Co-IP of GluA1 and SNX27 in NE-treated samples showed increasing tendency but not significant.

Discussion

Most of the fast excitatory neurotransmission is mediated by AMPARs at postsynaptic sites. Synaptic plasticity is defined by changes in the number, composition, and activity of synaptic AMPARs (Henley & Wilkinson, 2016; Traynelis et al., 2010). Thus, precise regulation of AMPARs is very important for neuronal activities. The activity and the surface insertion of AMPARs are regulated by β_2AR – cAMP – PKA signaling (Joiner et al., 2010). Stimulation of β_2AR results in phosphorylation at S845 in GluA1 by PKA and increases surface expression (He et al., 2009) and postsynaptic targeting of AMPARs (Esteban et al., 2003; Huganir & Nicoll, 2013). However, it is not clear how NE triggers intracellular signaling by stimulating intracellular β_2AR and how stimulation of intracellular β_2ARs by NE is associated with the trafficking of intracellular AMPARs to the surface of neurons. Membrane-impermeable ligands of β_2ARs such as NE have to enter neurons via their transporters to bind to intracellular β_2ARs. For example, one of ligands of the β_2AR, NE enter neurons through OCT3, PMAT, and NET (Duan & Wang, 2010; Irannejad et al., 2017; Kristensen et al., 2011; Tsvetanova & von Zastrow, 2014). In this study, I showed the importance of the transport of NE into neurons for regulation of the trafficking of AMPARs via β_2 adrenergic receptor signaling and which transporter plays a role in the transport of NE into postsynaptic neurons.

I found that NE has to be transported into neurons via OCT3 and PMAT, but not NET to stimulate intracellular β_2AR by analyzing the change in phosphorylation at S845 by the

treatment of NE in forebrain slices with or without inhibition of OCT3, PMAT, or NET. When D22, the inhibitor for OCT3 and PMAT was pre-incubated and treated with NE, NE-induced phosphorylation at S845 was partially blocked. D22 alone did not affect the NE-induced phosphorylation at S845. Phosphorylation at S831 was not changed by NE and D22. It suggests that the change in phosphorylation of GluA1 at S845 is mediated by β_2AR – cAMP – PKA signaling rather than other pathways including NE – α_1AR – PLCβ – PKC signaling. This result indicates that blocking the transport of NE by the inhibition of OCT3 and PMAT impedes stimulation of intracellular β_2ARs and phosphorylation of GluA1 at S845, which induces surface insertion of AMPARs. Nevertheless, D22 is not specific inhibitor for either OCT3 or PMAT. IC_{50} values of D22 for both OCT3 and PMAT are about 0.1 μM (Engel & Wang, 2005; Hayer-Zillgen et al., 2002). It means that this result cannot clarify which transporter mediates phosphorylation at S845. Therefore, the specific inhibitor for OCT3, corticosterone (CORT, IC_{50}: 0.29 μM (Hayer-Zillgen et al., 2002)) or for PMAT, lopinavir (LOPI, IC_{50}: 1.4 μM (Duan et al., 2015)) was used to distinguish the role of OCT3 and CORT in inducing higher phosphorylation of GluA1 by β_2AR signaling. Consistent with the change in phosphorylation at S845 by NE treatment with D22, application of CORT or LOPI with NE impaired the increase in NE-induced phosphorylation at S845 and did not affect phosphorylation at S831. These experiments confirmed that OCT3 and PMAT transport NE into cytosol of neurons and NE in the cytosol can stimulate intracellular β_2AR. Given the quantitative analysis of NE-induced phosphorylation at S845, 50% of NE-induced phosphorylation at S845 was decreased by D22. It infers that 50% of phosphorylation of GluA1 at S845 results from the stimulation of intracellular β_2AR and AMPARs. It was also tested if inhibition of NET affects the NE-

induced phosphorylation at S845. Forebrain slices were pre-incubated with the NET inhibitor, desipramine (DESI, IC_{50}: 1.2 nM (Roubert et al., 2001)), and incubated with NE. Contrary to D22, CORT, and LOPI, DESI did not decrease NE-induced phosphorylation at S845 when it was treated with NE. These results could be due to different subcellular localization and roles of the transporters in NE clearance system, $uptake_1$ and $uptake_2$. NET is majorly expressed in presynaptic sites and play crucial role in reuptake of NE (Kristensen et al., 2011; Matthies et al., 2009), while OCT3 and PMAT are broadly distributed in neurons and transport NE into cytosol (Dahlin et al., 2007; Duan & Wang, 2010; Engel et al., 2004; Gasser et al., 2009). NE which is transported into postsynaptic sites of glutamatergic neurons can trigger intracellular β_2AR – cAMP – PKA signaling and phosphorylation of intracellular AMPARs by PKA. Collectively, the data suggest that OCT3 and PMAT, but not NET are associated with stimulation of intercellular β_2AR and phosphorylation of AMPARs.

In previous experiments using total lysate of forebrain slices, I was not able to avoid the increase in phosphorylation of GluA1 at S845 by β_2AR signaling from extracellular β_2ARs, which is activated by free NE in synaptic cleft. In order to examine the change in phosphorylation of GluA1 by only stimulation of intracellular β_2AR, I used the membrane impermeable βAR antagonist, sotalol (Baker, 2005; M. L. Chen & Yu, 2009; Liu et al., 2012). Sotalol was used to pre-treat forebrain slices before application of NE to prevent the stimulation of surface β_2AR by NE. I assumed that the effect of sotalol on the decrease in NE-induced phosphorylation at S845 would be complementary to that of D22. Since D22 caused the 50% of reduction of NE-induced phosphorylation at S845, which should

be from intracellular signaling, the other 50% triggered by the extracellular β_2AR signaling might be blocked by sotalol. However, the decrease in NE-induced phosphorylation at S845 was about 80% which is much higher than expected. In addition, phosphorylation at S831 was reduced when NE was treated with sotalol. This unanticipated result can be explained by the broad effect of sotalol. Sotalol is not selective to only β_2ARs and β_1ARs and potassium channels are also inhibited by sotalol (Baker, 2005; Doggrell & Brown, 2000; Funck-Brentano, 1993; Li & Dong, 2010; Mubarik et al., 2021). Moreover, since I used the high concentration of sotalol (100 μM), some of them could penetrate the plasma membrane and inhibit intracellular β_2ARs. In order to distinguish the phosphorylation by intracellular and extracellular β_2AR signaling, the drug treatment condition should be finely adjusted or subcellular fractionation can be performed.

Furthermore, I examined whether the surface expression of AMPARs is changed by inhibition of OCT3 and PMAT by immunostaining of hippocampal neurons which were treated with NE with or without D22, CORT, or LOPI. NE augmented the surface expression of GluA1 near postsynaptic sites. D22 and LOPI completely blocked the increase in surface insertion of AMPARs by NE and about 86% of increase in surface expression of GluA1 was blocked by CORT. These data provide one more piece of evidence that both OCT3 and PMAT transport NE into cytosol and result in surface insertion of AMAPRs. Interestingly, the decrease in NE-induced surface expression of GluA1 by D22, CORT, and LOPI was much larger than in NE-induced phosphorylation at S845. Different methodological approaches might cause these results. Since AMPARs from whole lysate was IPed for the immunoblotting of phosphorylation at S845, both

extracellular and intracellular AMPAR phosphorylation was quantified. Even though phosphorylation of intracellular AMPARs was decreased by inhibition of OCT3 and PMAT, phosphorylation of extracellular AMPARs still can be increased by NE. Thus, phosphorylation at S845 in NE and inhibitor (D22, CORT, and LOPI) treated groups was higher than in the control group. By contrast, for the immunostaining results, only the population of newly inserted AMPARs were quantified as increase in surface expression of GluA1 by NE. Thus, the effect of inhibitors on the NE-induced surface insertion of AMPARs was more significant than on the NE-induced phosphorylation of GluA1. If subcellular fractionation is performed and only phosphorylation of GluA1 in cytosol or endosomal vesicles was quantified, difference between NE and NE+inhibitor groups should be larger. Also, it is intriguing that as little as 10 nM D22 impaired the effect of NE on surface insertion of AMPAR because the IC_{50} and K_i value of D22 for ectopically expressed hOCT3 and hPMAT are 0.1 μM is (Duan & Wang, 2010; Engel et al., 2004; Hayer-Zillgen et al., 2002). However, the IC_{50} values of D22 for NE uptake by the endogenous $uptake_2$ system was 2.4-6.6 nM as measured for the uptake of [^{3}H] MPP^+ into cultured cerebellar granule neurons (J. E. Hill et al., 2011; Shang et al., 2003). Given these data, it is plausible that 10 nM D22 is enough to inhibit the uptake of NE into neurons by endogenous OCT3 and PMAT. Perhaps reconstituting OCT3 and PMAT in HEK293 and MDCK is not complete and components are missing that would otherwise yield a lower IC_{50} value.

In order to verify that NE needs OCT3 to be transported into neurons and stimulate intracellular βARs, NE-induced phosphorylation at S845 in WT and OCT3 KO was

analyzed. Phosphorylation as S845 in the basal condition was similar in WT and OCT3 KO mice, but the augmentation of phosphorylation at S845 by NE in WT was four times larger than in OCT3 KO although the P-value of the standard t-test was not significant. Since NE is not able to enter neurons through OCT3 and stimulate intracellular βARs in OCT3 KO, NE-induce phosphorylation at S845 was lower in OCT3 KO compared to WT. On the other hands, the magnitude of the reduction of phosphorylation at S845 in OCT3 KO is surprisingly large considering the decrease in NE-induced phosphorylation at S845 by pharmacological inhibition of OCT3 by CORT. This result might be a hint at additional mechanisms such as reduced NE availability in OCT3 KO mice. Also, PMAT can compensate the absence of OCT3 in OCT3 KO mice.

Interaction between AMPARs and auxiliary proteins (Stargazin, SynDIG1, and SynDIG4), PSD-95, SNX27, and VPS35 is important for surface insertion and stabilization of AMPARs. Especially, it has been shown that the binding of GluA1 and SNX27 increases during the glycine-induced chemical LTP (Loo et al., 2014). Hence, I presumed that interaction of GluA1 with auxiliary proteins, PSD-95, SNX27, and VPS35 would be altered by NE. However, NE did not change the interaction between AMPARs and auxiliary proteins, PSD-95, and VPS35. Only SNX27 showed an increasing tendency in interaction with GluA1 in NE-treated brain slices. These results suggest that AMPARs with auxiliary proteins form a complex in the endosomal vesicles and they might be inserted to the surface together as the complex. Therefore, their interaction between AMPARs and auxiliary proteins is not altered during the trafficking of AMPARs. On the other hand, although the P-value was not significant, increased co-IP of SNX27 with GluA1 by NE is

consistent with findings from previous studies (Hussain et al., 2014; Loo et al., 2014). In this respect, this result shows the important role of binding of GluA1 to SNX27 for trafficking of AMPARs. I assumed that the interaction of GluA1 and VPS35 would increase because VPS35 is required for the surface insertion of AMPARs. Nevertheless, co-IP of VPS35 with GluA1 was not influenced by NE. This result shows that the binding of the AMPAR and VPS trimer including VPS35 is stable in the endosomal vesicle, not changing during the trafficking of AMPARs. In addition, co-IP was conducted with whole lysate from brain slices as explained previously. Thus, I cannot distinguish the interaction of the AMPAR and auxiliary proteins, PSD-95, SNX27, and VPS35 in different subcellular domains such as endosomes and plasma membrane. If their interactions were analyzed after subcellular fractionation, the co-IP might have shown different results for different fractions.

Taken together, my results suggest a new mechanism of regulation of AMPAR trafficking which is induced by NE via stimulation of intracellular β_2AR (Figure 12). NE is released from noradrenergic neurons and diffuses to dendritic regions of glutamatergic neurons. Some stimulate extracellular adrenergic receptors (α and β) and others are transported into cytosol of neurons through OCT3 or PMAT. The NE in the cytosol can enter endosomal vesicles via OCT3 or PMAT and binds to intracellular β_2AR which forms a functional complex with the AMPAR in endosomal vesicles. Binding of NE to the β_2AR induces the β_2AR – cAMP – PKA signaling and S845 in GluA1 subunit is phosphorylated by PKA. Then, the phosphorylated AMPAR is inserted to the plasma membrane. NET contributes to the reuptake of NE around the terminals of noradrenergic neurons.

Other monoamines such as dopamine, serotonin, and histamine also can be transported by OCT3 and PMAT (Courousse & Gautron, 2015; Duan & Wang, 2010; J. Wang, 2016). Therefore, function of OCT3 and PMAT could be crucial to the regulation of signaling from other monoamine receptors such as dopamine and serotonin receptors. In addition, the transport of dopamine via OCT3 and PMAT might be able to control the trafficking of AMPARs through D1 like receptor signaling because stimulation of D1 like receptors fosters phosphorylation and trafficking of AMPARs (Chao et al., 2002; Price et al., 1999; Sun et al., 2008). Considering diverse functions of OCT3 and PMAT, their effects on the regulation of neurotransmitter receptors and ion channels in neurons should be further analyzed.

Trafficking of AMPARs is very important for synaptic transmission and plasticity, learning and memory and it is dysregulated in neuronal disorders (Groc & Choquet, 2020; Henley & Wilkinson, 2013; Jurado, 2017). NE is essential for cognitive functions such as attention, learning, and memory (Ross & Van Bockstaele, 2020; Wassal et al., 2009). Moreover, it is considered that function of NE is involved in the pathology of Alzheimer's disease (Friedman et al., 1999; Gannon et al., 2015; Ross et al., 2015). Accordingly, this study reveals an important molecular mechanism of the regulation of trafficking of AMPARs by NE via intracellular β_2AR – cAMP – PKA signaling, which can be therapeutic targets for various neuronal diseases. We may be able in the future to manipulate the function of OCT3 and PMAT to control surface expression of AMPARs and treat neuronal diseases.

Figures

Figure 1

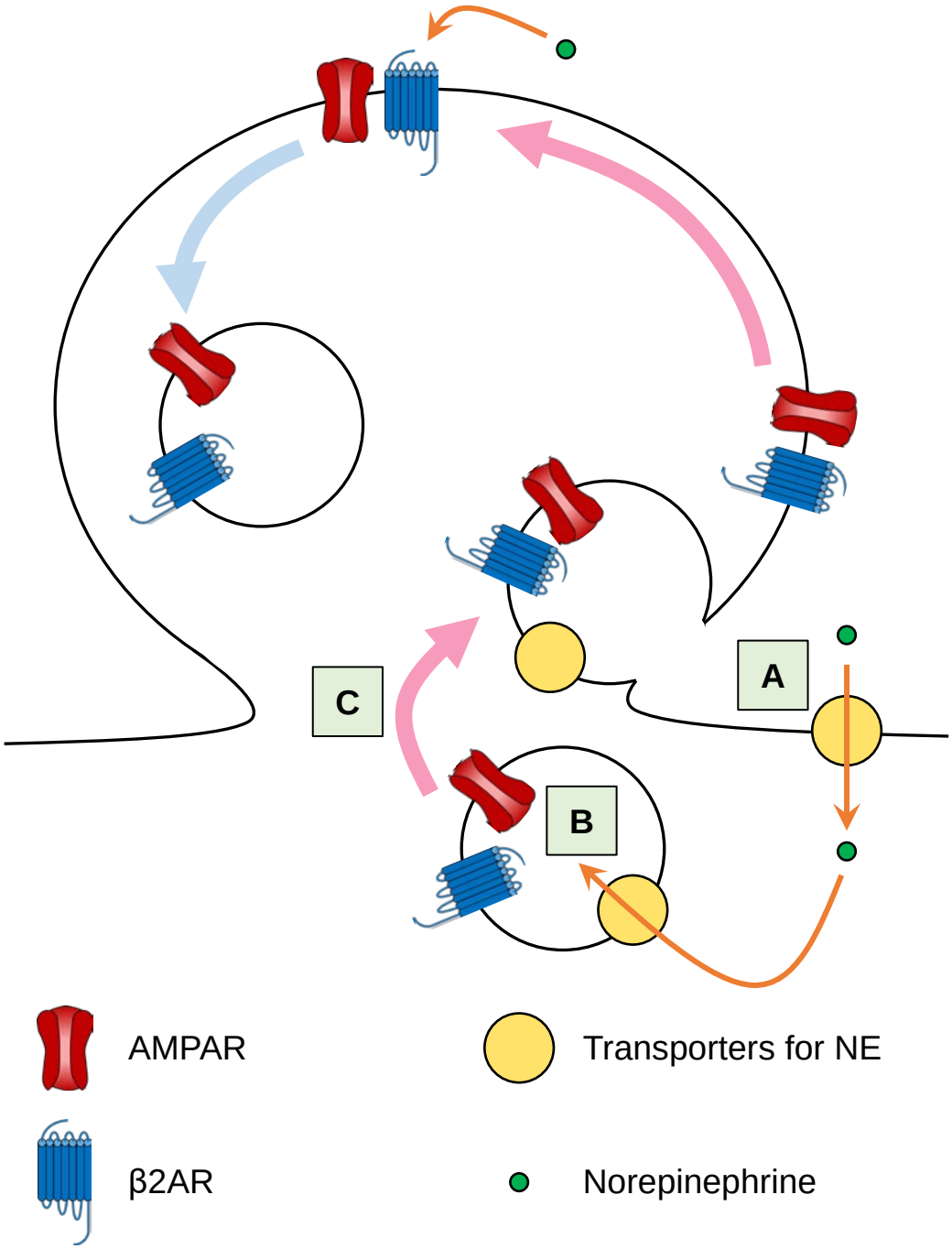

Figure 1. Model of regulation of AMPAR trafficking via β2AR signaling

I proposed the model of surface insertion of AMPARs by NE via β_2AR signaling. (A) NE can access to β_2AR in cytosol through transporters for NE. OCT3, PMAT, or NET might play role in the transport of NE. (B) Stimulation of intracellular β_2AR which is associated with AMPARs activates cAMP – PKA signaling and induces phosphorylation of GluA1 at S845 by PKA. (C) Phosphorylated AMPARs are inserted into the surface of neurons and diffused to the spine.

Figure 2

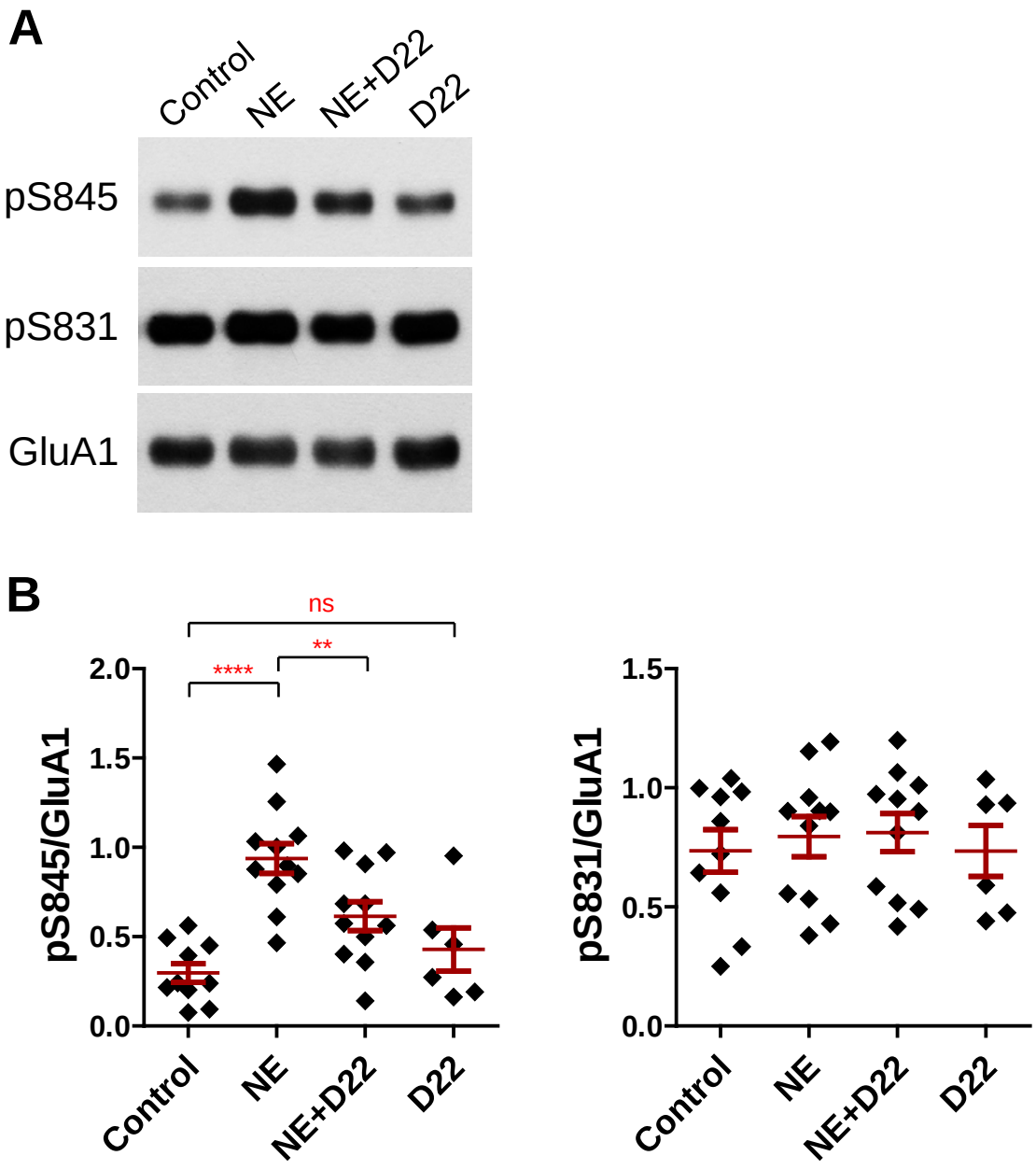
A
Control
NE
NE+D22
D22
pS845
pS831
GluA1
B
ns
**
****
pS845/GluA1
2.0
1.5
1.0
0.5
0.0
Control
NE
NE+D22
D22
pS831/GluA1
1.5
1.0
0.5
0.0
Control
NE
NE+D22
D22

Figure 2. Decynium22 (D22) blocks increase in NE-induced phosphorylation at S845

(A) Forebrain slices from wild type mice were pre-incubated with ACSF containing vehicle (DMSO) or OCT3 and PMAT blocker, Decynium22 (D22) then incubated with vehicle (DMSO) or 1 μM of norepinephrine (NE) with or without 100 nM of D22. After the treatment, Triton X-100 lysates were prepared for immunoprecipitation with control IgG or anti-GluA1 antibody and sequential immunoblotting with anti-pS845, pS831, and GluA1 antibodies.

(B) For quantification of phosphorylation of GluA1 at Ser845 and Ser831, phosphorylated serine signals were normalized to the amount of total GluA1. ($n \geq 6$ from 6 mice, given as mean±SEM; the one-way ANOVA test was used to analyze significance of difference between all groups and significant differences between control vs NE, NE vs NE+D22, and control vs D22 are determined by Fisher's least significant difference (LSD) post-hoc test; **$p<0.01$, ****$p<0.0001$, ns: not significant)

Figure 3

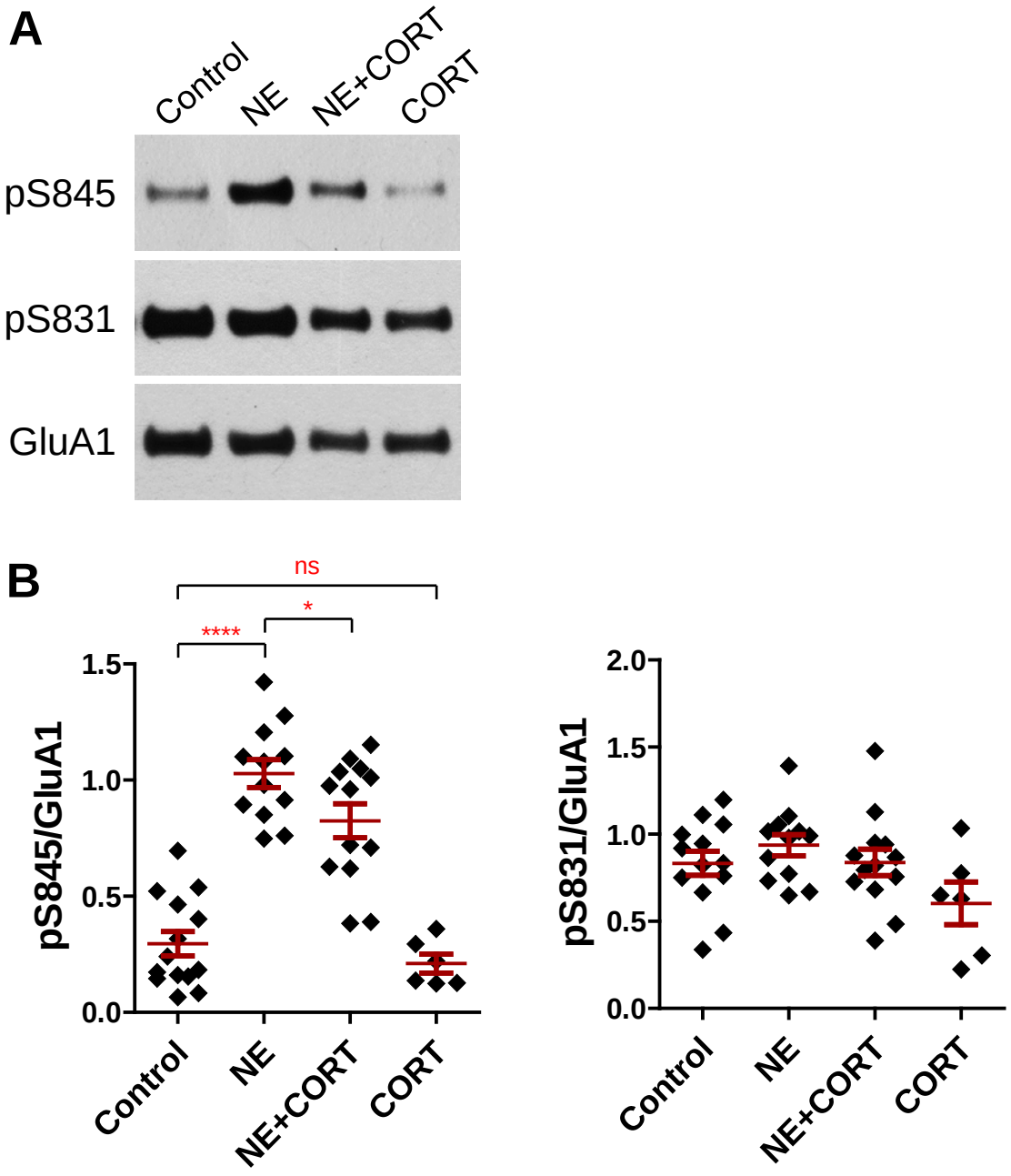
A
Control
NE
NE+CORT
CORT
pS845
pS831
GluA1
B
ns
*
****
pS845/GluA1
1.5
1.0
0.5
0.0
Control
NE
NE+CORT
CORT
pS831/GluA1
2.0
1.5
1.0
0.5
0.0
Control
NE
NE+CORT
CORT

Figure 3. Corticosterone (CORT) blocks increase in NE-induced phosphorylation at S845

(A) Forebrain slices from wild type mice were pre-incubated with ACSF containing vehicle (DMSO) or OCT3 blocker, Corticosterone (CORT) then incubated with vehicle (DMSO) or 1 μM of norepinephrine (NE) with or without 10 μM of CORT. After the treatment, Triton X-100 lysates were prepared for immunoprecipitation with control IgG or anti-GluA1 antibody and sequential immunoblotting with anti-pS845, pS831, and GluA1 antibodies. (B) For quantification of phosphorylation of GluA1 at Ser845 and Ser831, phosphorylated serine signals were normalized to the amount of total GluA1. ($n \geq 6$ from 7 mice, given as mean±SEM; the one-way ANOVA test was used to analyze significance of difference between all groups and control vs NE, NE vs NE+CORT, and control vs CORT are determined by Fisher's least significant difference (LSD) post-hoc test; *$p<0.05$, ****$p<0.0001$, ns: not significant)

Figure 4

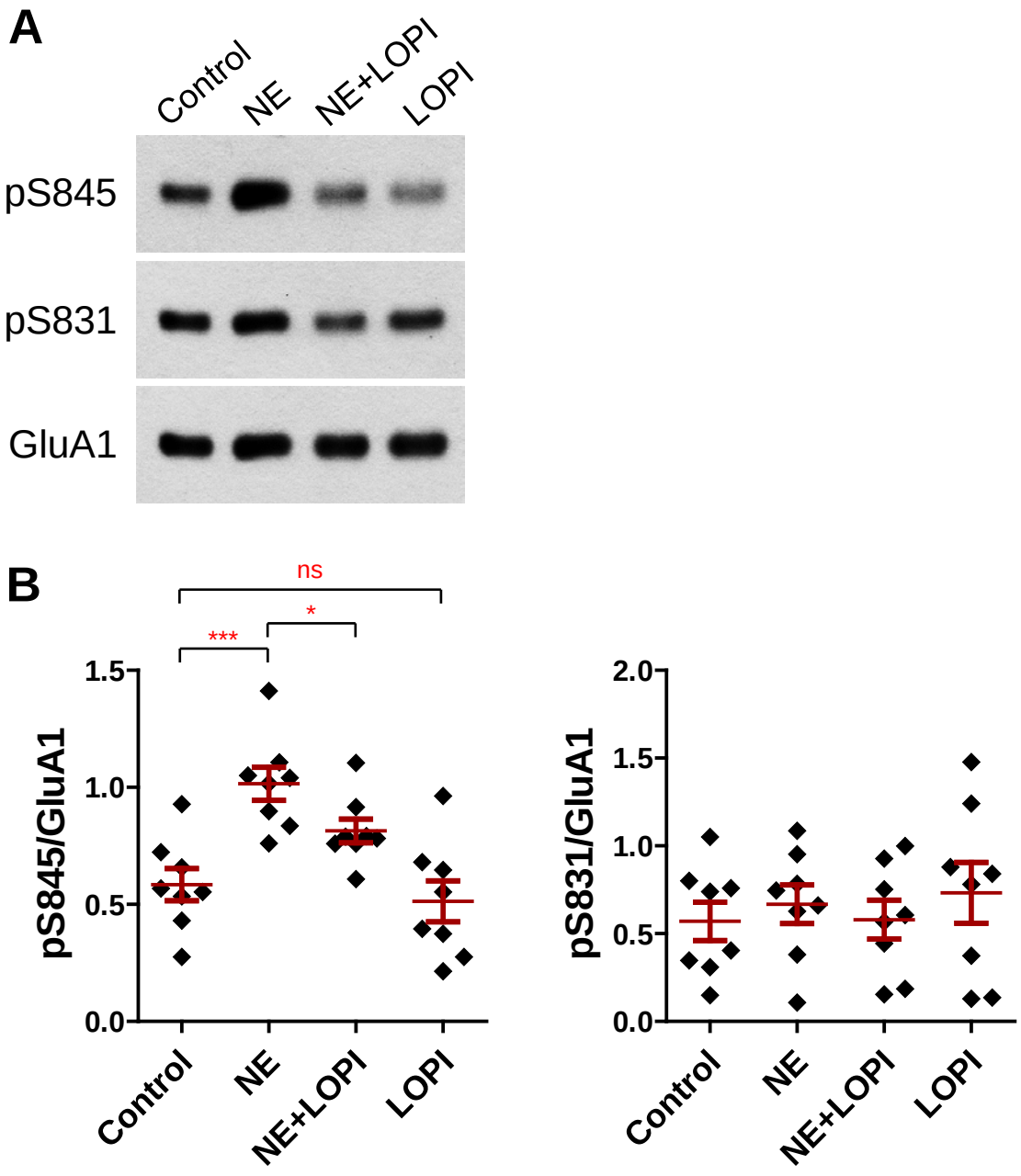
A
Control
NE
NE+LOPI
LOPI
pS845
pS831
GluA1
B
ns
*
***
pS845/GluA1
1.5
1.0
0.5
0.0
Control
NE
NE+LOPI
LOPI
pS831/GluA1
2.0
1.5
1.0
0.5
0.0
Control
NE
NE+LOPI
LOPI

Figure 4. Lopinavir (LOPI) blocks increase in NE-induced phosphorylation at S845

(A) Forebrain slices from wild type mice were pre-incubated with ACSF containing vehicle (DMSO) or PMAT blocker, Lopinavir (LOPI) then incubated with vehicle (DMSO) or 1 μM of norepinephrine (NE) with or without 10 μM of LOPI. After the treatment, Triton X-100 lysates were prepared for immunoprecipitation with control IgG or anti-GluA1 antibody and sequential immunoblotting with anti-pS845, pS831, and GluA1 antibodies.

(B) For quantification of phosphorylation of GluA1 at Ser845 and Ser831, phosphorylated serine signals were normalized to the amount of total GluA1. ($n \geq 8$ from 3 mice, given as mean±SEM; the one-way ANOVA test was used to analyze significance of difference between all groups and control vs NE, NE vs NE+LOPI, and control vs LOPI are determined by Fisher's least significant difference (LSD) post-hoc test; *$p<0.05$, ***$p<0.001$, ns: not significant)

Figure 5

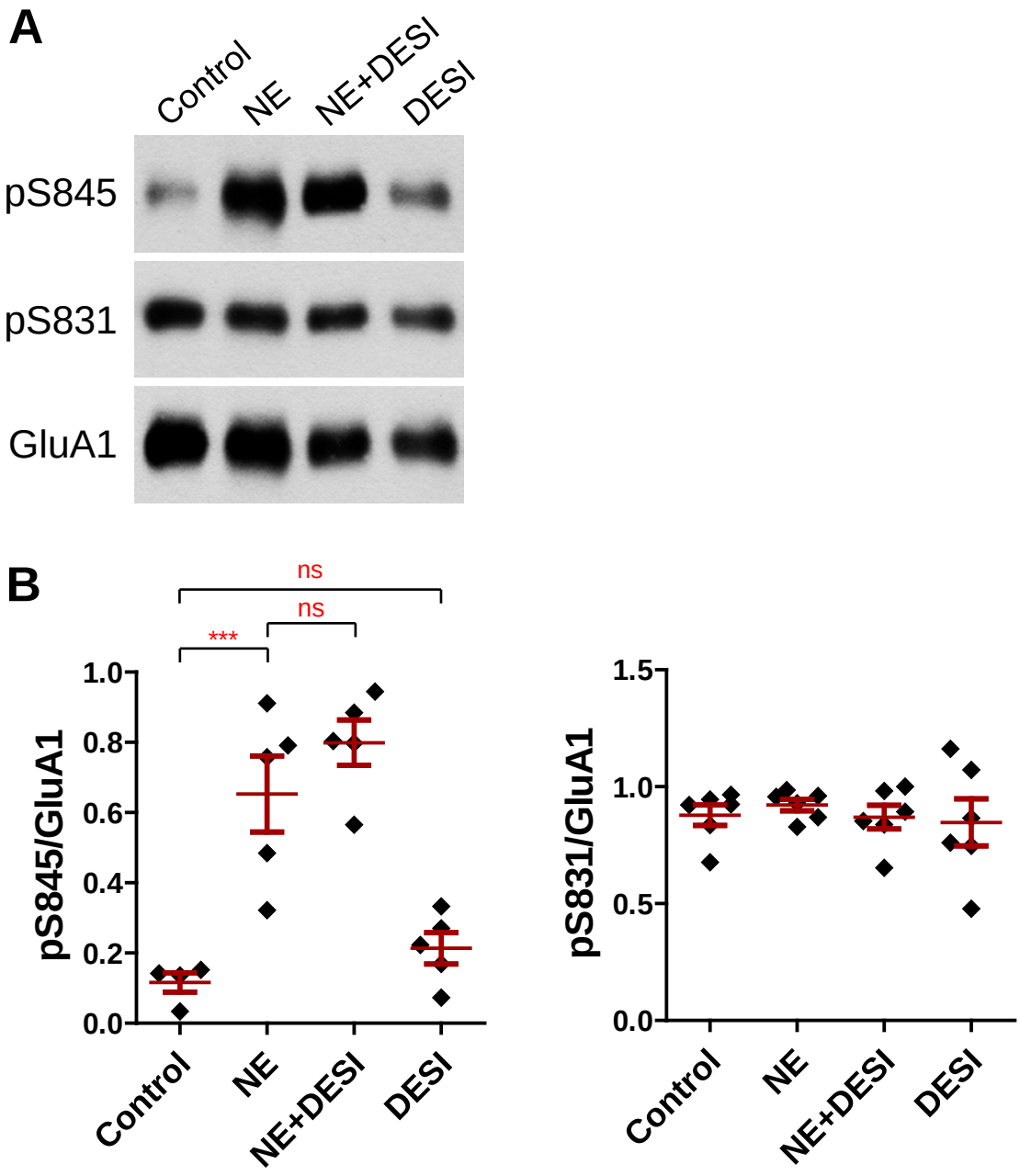
A
Control
NE
NE+DESI
DESI
pS845
pS831
GluA1
B
ns
ns
***
pS845/GluA1
1.0
0.8
0.6
0.4
0.2
0.0
Control
NE
NE+DESI
DESI
pS831/GluA1
1.5
1.0
0.5
0.0
Control
NE
NE+DESI
DESI

Figure 5. Desipramine (DESI) does not affect NE-induced phosphorylation at S845

(A) Forebrain slices from wild type mice were pre-incubated with ACSF containing vehicle (water) or norepinephrine transporter blocker, Desipramine (DESI) then incubated with vehicle (water) or 1 μM of norepinephrine (NE) with or without 1 μM of DESI. After the treatment, Triton X-100 lysates were prepared for immunoprecipitation with control IgG or anti-GluA1 antibody and sequential immunoblotting with anti-pS845, pS831, and GluA1 antibodies.

(B) Phosphorylation of GluA1 at S845 and S831 was quantified by densitometry of the bands and normalized to total GluA1 expression. ($n \geq 5$ from 5 mice, given as mean±SEM; the one-way ANOVA test was used to analyze significance of difference between all groups and control vs NE, NE vs NE+DESI, and control vs DESI are determined by Fisher's least significant difference (LSD) post-hoc test; ***$p<0.001$, ns: not significant)

Figure 6

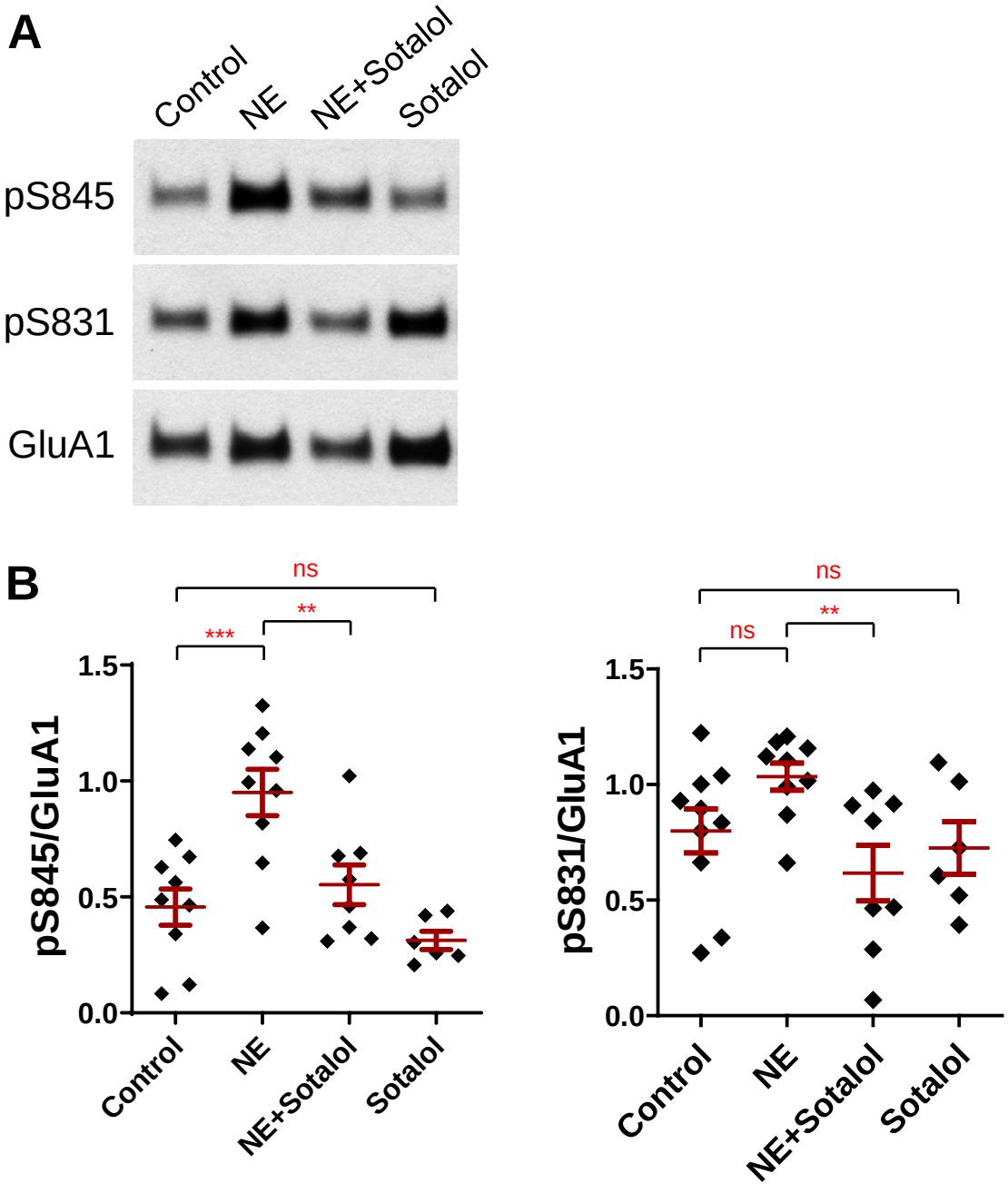
A
Control
NE
NE+Sotalol
Sotalol
pS845
pS831
GluA1
B
ns
**
***
pS845/GluA1
1.5
1.0
0.5
0.0
Control
NE
NE+Sotalol
Sotalol
ns
**
ns
pS831/GluA1
1.5
1.0
0.5
0.0
Control
NE
NE+Sotalol
Sotalol

Figure 6. NE-induced phosphorylation of GluA1 at S845 and S831 in the mouse brain slices incubated with NE ± membrane impermeable β adrenergic receptor inhibitor, Sotalol

(A) Forebrain slices from wild type mice were pre-incubated with ACSF containing vehicle (DMSO) or membrane impermeable β adrenergic receptor inhibitor, Sotalol then incubated with vehicle (DMSO) or 1 μM of norepinephrine (NE) with or without 100 μM of Sotalol. After the treatment, Triton X-100 lysates were prepared for immunoprecipitation with control IgG or anti-GluA1 antibody and sequential immunoblotting with anti-pS845, pS831, and GluA1 antibodies.

(B) Phosphorylation of GluA1 at S845 and S831 was quantified by densitometry of the bands and normalized to total GluA1 expression. ($n \geq 5$ from 5 mice, given as mean±SEM; the one-way ANOVA test was used to analyze significance of difference between all groups and control vs NE, NE vs NE+Sotalol, and control vs Sotalol are determined by Fisher's least significant difference (LSD) post-hoc test; $^{**}p<0.01$, $^{***}p<0.001$, ns: not significant)

Figure 7

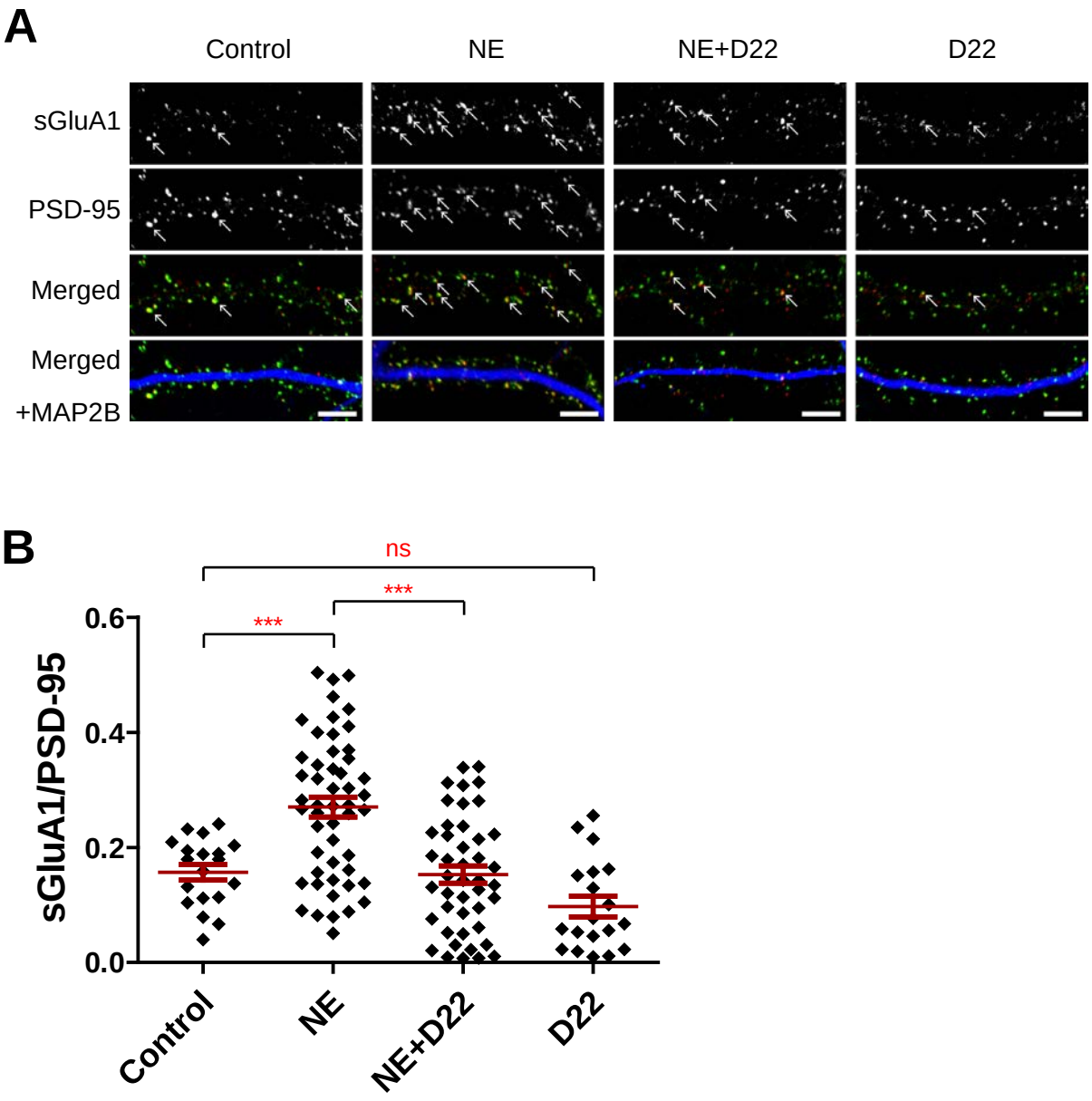
A
Control
NE
NE+D22
D22
sGluA1
PSD-95
Merged
Merged
+MAP2B
B
ns
***
***
sGluA1/PSD-95
0.6
0.4
0.2
0.0
Control
NE
NE+D22
D22

Figure 7. Decynium22 (D22) blocks increase in NE-induced surface expression of GluA1 in hippocampal neurons

(A) Vehicle (DMSO, Control) or NE (1 μM) were applied with or without D22 (10 nM) to dissociated hippocampal culture (HCs). Surface GluA1 (sGluA1, red), PSD-95 (green), and MAP2B (blue) were labelled with fluorophore-conjugated antibodies. PSD-95 was used as a postsynaptic site marker and MAP2B as a dendritic shaft marker. (Scale bar, 5μm)

(B) Quantitative analysis of surface GluA1 puncta at postsynaptic sites, which was colocalized with PSD-95 puncta. NE treatment increased surface expression of GluA1 but the effect of NE was impeded by D22 ($n \geq 19$ from four preparations, given as mean±SEM; the one-way ANOVA test was used to analyze significance of difference between all groups and significance of differences between control vs NE, NE vs NE+D22, and control vs D22 were determined by Tukey's post-hoc test; ***$p<0.001$, ns: not significant)

Figure 8

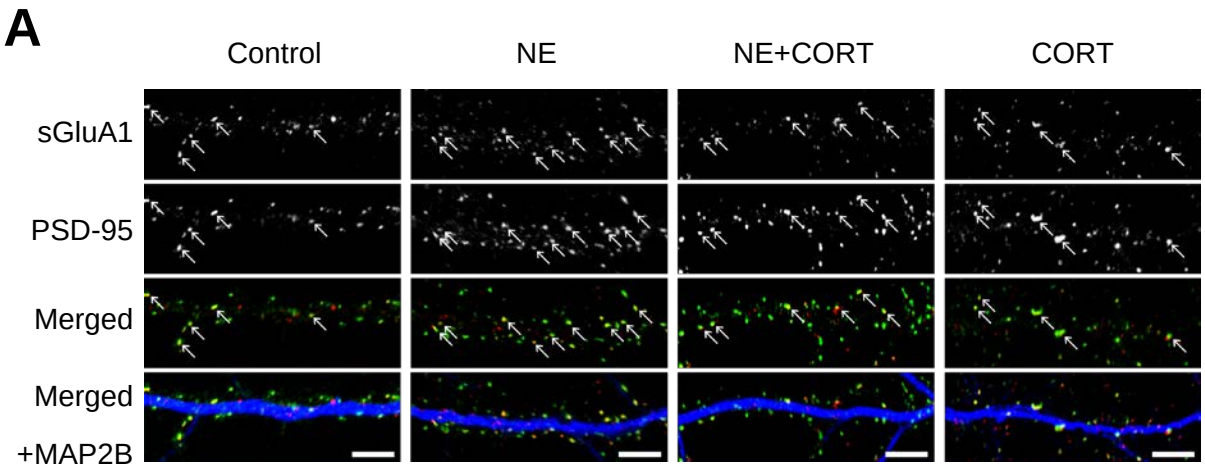
A
Control
NE
NE+CORT
CORT
sGluA1
PSD-95
Merged
Merged
+MAP2B

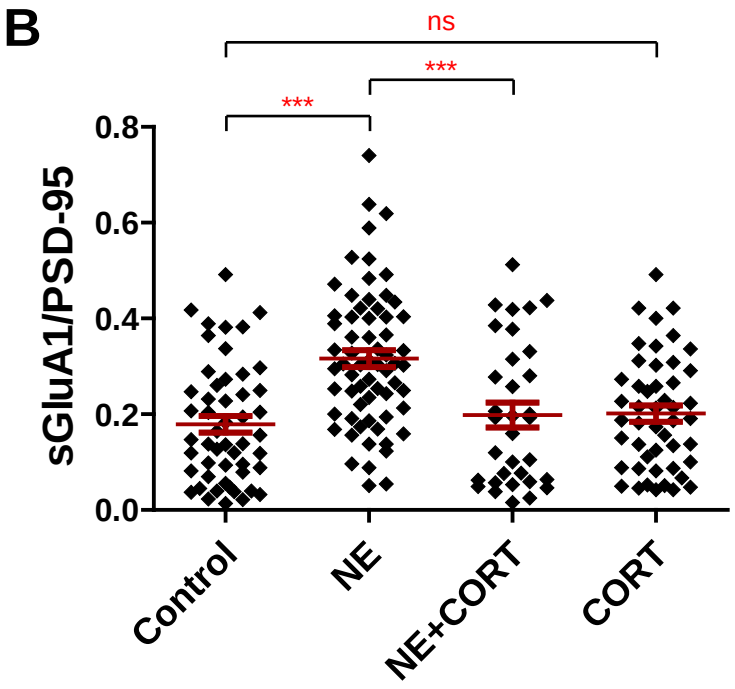
B
ns
***
***
sGluA1/PSD-95
0.8
0.6
0.4
0.2
0.0
Control
NE
NE+CORT
CORT

Figure 8. Corticosterone (CORT) blocks increase in NE-induced surface expression of GluA1 in hippocampal neurons

(A) Vehicle (DMSO, Control) or NE (1 μM) were applied with or without CORT (10 μM) to dissociated hippocampal culture (HCs). Surface GluA1 (sGluA1, red), PSD-95 (green), and MAP2B (blue) were labelled with fluorophore-conjugated antibodies. PSD-95 was used as a postsynaptic site marker and MAP2B as a dendritic shaft marker. (Scale bar, 5μm)

(B) Quantitative analysis of surface GluA1 puncta at postsynaptic sites, which was colocalized with PSD-95 puncta. NE treatment increased surface expression of GluA1 but the effect of NE was impeded by CORT ($n \geq 33$ from five preparations, given as mean±SEM; the one-way ANOVA test was used to analyze significance of difference between all groups and significance of differences between control vs NE, NE vs NE+CORT, and control vs CORT are determined by Tukey's post-hoc test; ***$p<0.001$, ns: not significant)

Figure 9

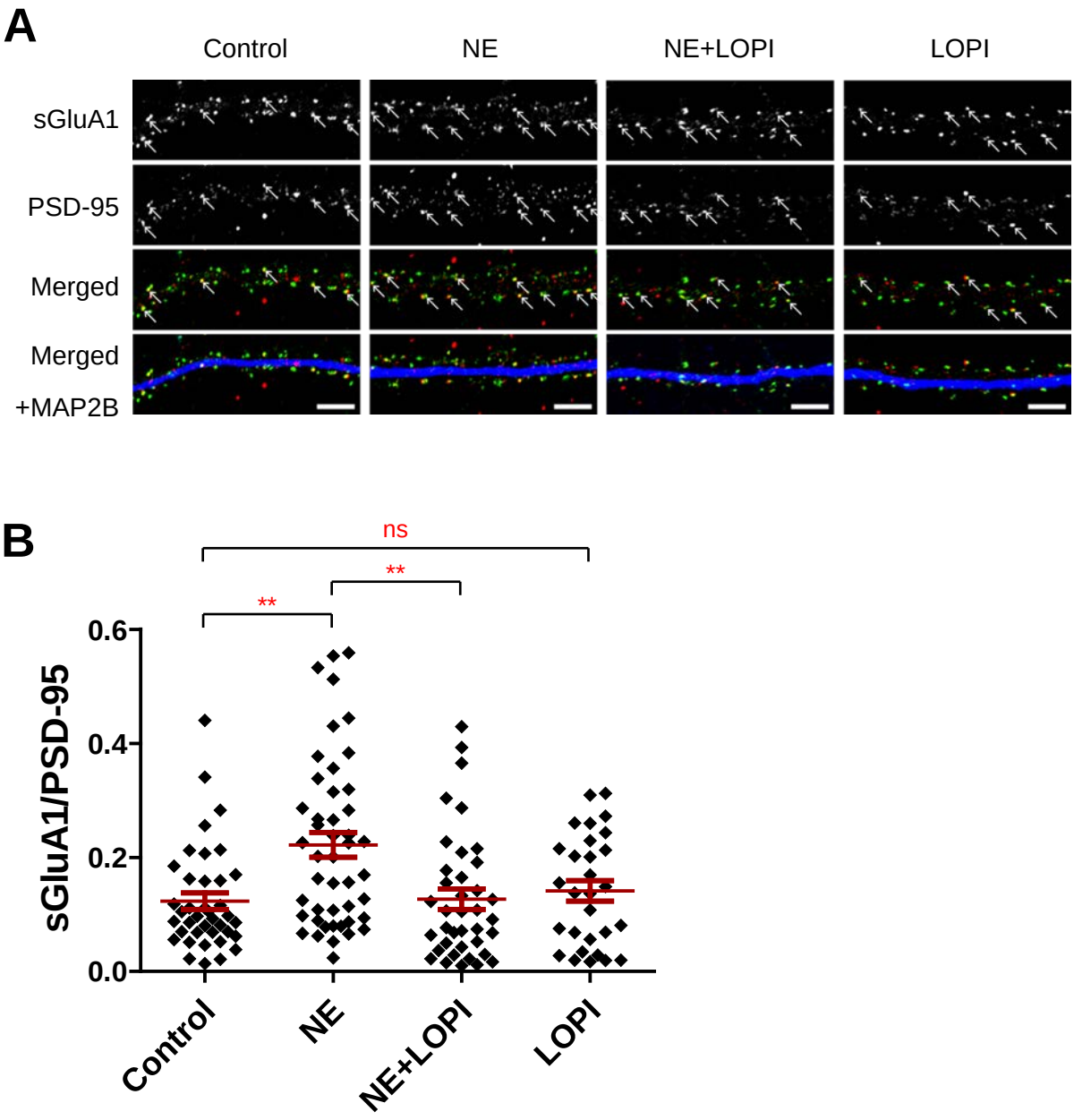
A
Control
NE
NE+LOPI
LOPI
sGluA1
PSD-95
Merged
Merged
+MAP2B
B
ns
**
**
sGluA1/PSD-95
0.6
0.4
0.2
0.0
Control
NE
NE+LOPI
LOPI

Figure 9. Lopinavir (LOPI) blocks increase in NE-induced surface expression of GluA1 in hippocampal neurons

(A) Vehicle (DMSO, Control) or NE (1 μM) were applied with or without LOPI (10 μM) to dissociated hippocampal culture (HCs). Surface GluA1 (sGluA1, red), PSD-95 (green), and MAP2B (blue) were labelled with fluorophore-conjugated antibodies. PSD-95 was used as a postsynaptic site marker and MAP2B as a dendritic shaft marker. (Scale bar, 5μm)

(B) Quantitative analysis of surface GluA1 puncta at postsynaptic sites, which was colocalized with PSD-95 puncta. NE treatment increased surface expression of GluA1 but the effect of NE was impeded by LOPI ($n \geq 29$ from four preparations, given as mean±SEM; the Kruskal-Wallis test was used to analyze significance of difference between all groups and significance of differences between control vs NE, NE vs NE+LOPI, and control vs LOPI are determined by Dunn's multiple comparison post-hoc test; $^{**}p<0.01$, ns: not significant)

Figure 10

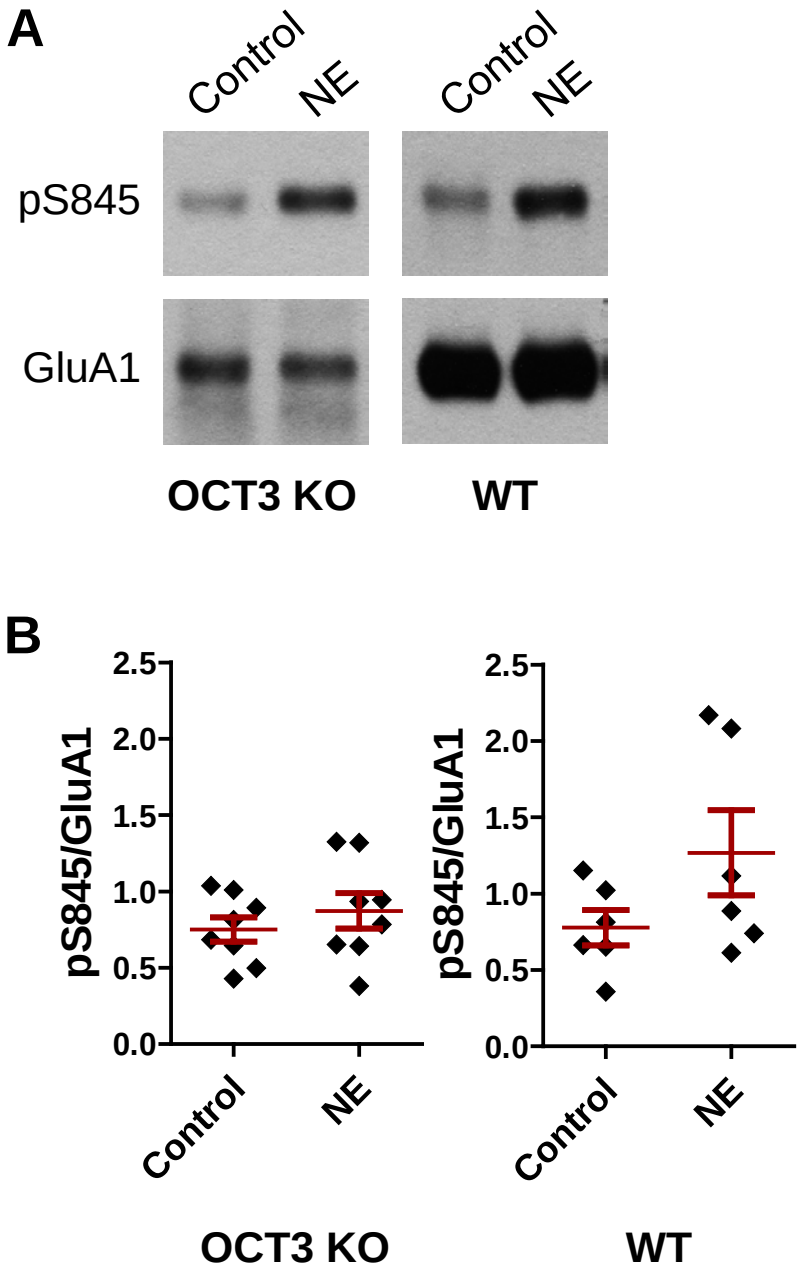
A
Control
NE
Control
NE
pS845
GluA1
OCT3 KO
WT
B
pS845/GluA1
2.5
2.0
1.5
1.0
0.5
0.0
Control
NE
pS845/GluA1
2.5
2.0
1.5
1.0
0.5
0.0
Control
NE
OCT3 KO
WT

Figure 10. Phosphorylation of GluA1 at S845 in OCT3 KO and WT mice

Mouse brain slices from OCT3 KO or wild type mice were extracted with 1% Triton X-100 after 1 μM NE treatment. Non-soluble materials from the lysate were removed by ultracentrifugation before immunoprecipitation with control IgG or antibody against GluA1 and immunoblotting with antibodies against pS845 and GluA1. Phosphoserine signal was quantified by film densitometry and normalized to total GluA1 ($n \geq 6$ from two mice of each strain, given as mean±SEM).

Figure 11

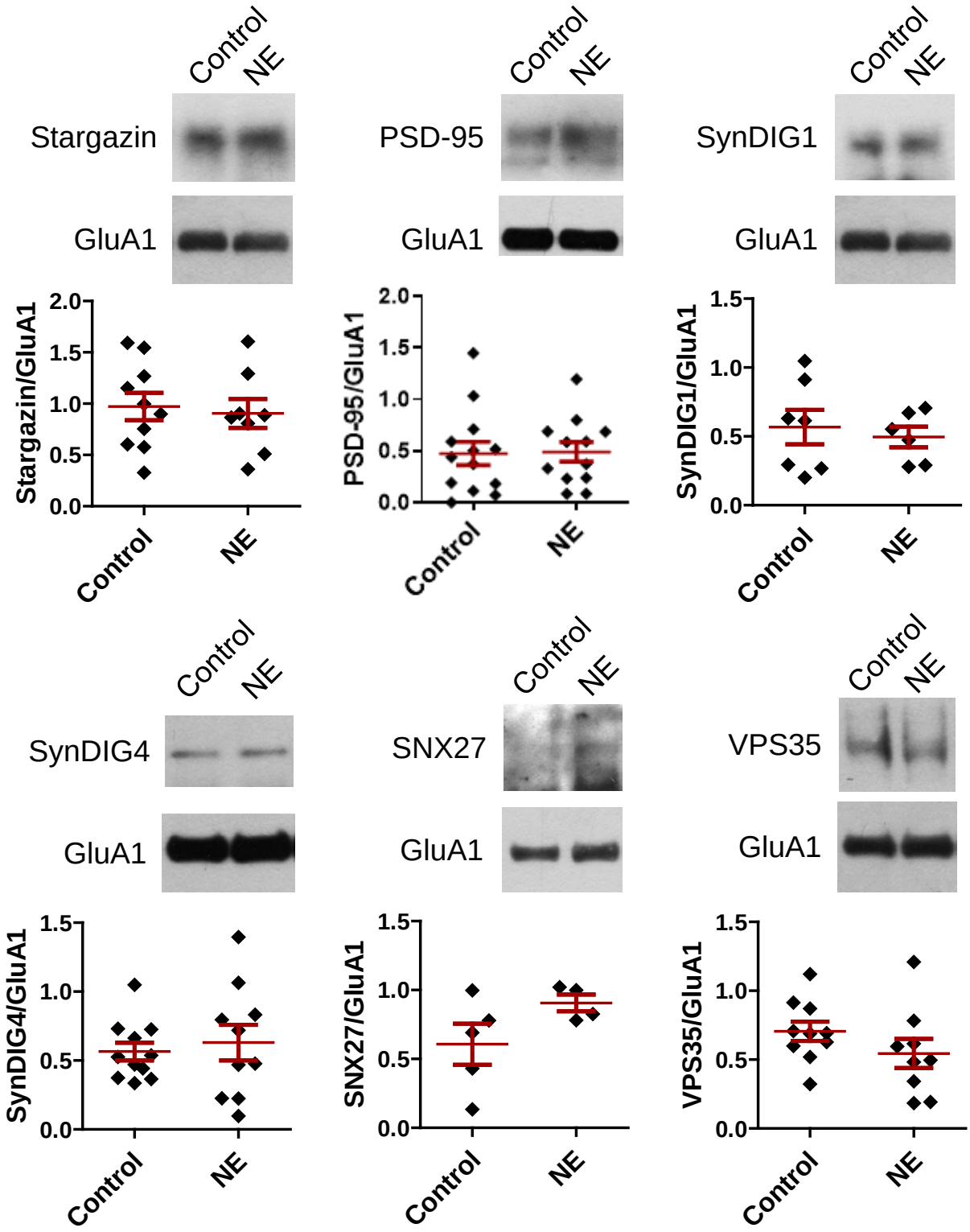
Control
NE
Stargazin
GluA1
Stargazin/GluA1
2.0
1.5
1.0
0.5
0.0
Control
NE
PSD-95
GluA1
PSD-95/GluA1
SynDIG1
GluA1
SynDIG1/GluA1
SynDIG4
GluA1
SynDIG4/GluA1
SNX27
GluA1
SNX27/GluA1
VPS35
GluA1
VPS35/GluA1

Figure 11. Change in interaction of GluA1 and AMPAR-interacting proteins by NE

Co-immunoprecipitation of GluA1 with Stargazin, PSD-95, SynDIG1, SynDIG4, SNX27, and VPS35. After treatment with vehicle or NE (1 μM), the mouse brain slices were extracted with 1% Triton X-100 and cleared by ultracentrifugation before immunoprecipitation with control IgG or antibody against GluA1 and immunoblotting with antibodies against Stargazin, PSD-95, SynDIG1, SynDIG4, SNX27, VPS35, and GluA1. The amount of each protein was quantified by film densitometry and normalized to total GluA1 (n≥4, given as mean±SEM).

Figure 12

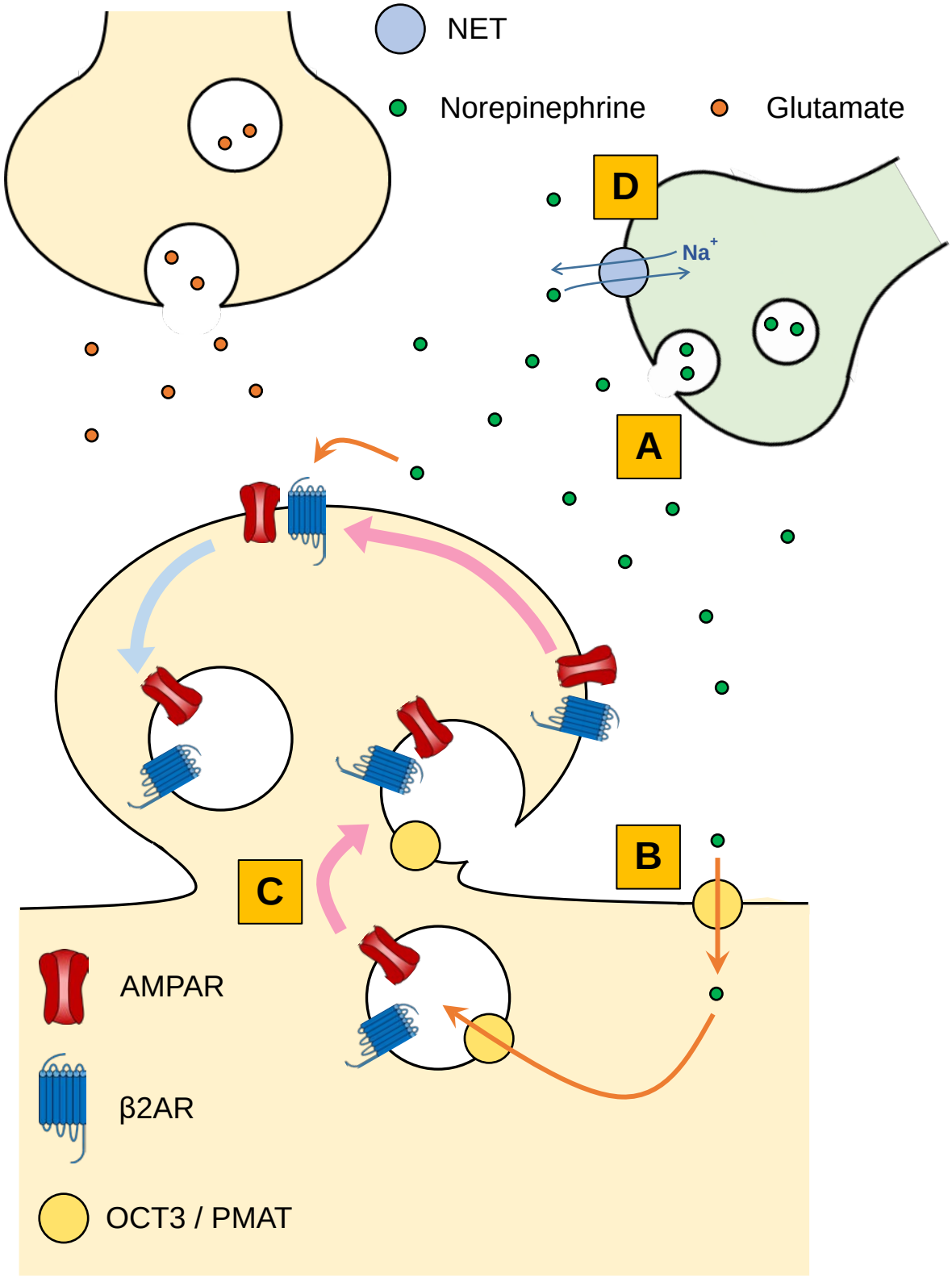

Figure 12. A schematic model of the regulation of surface insertion of AMPARs by NE through the intracellular β_2AR – cAMP – PKA signaling

The mechanism how NE and its transporters, OCT3 and PMAT, play role in the regulation of trafficking of AMPARs by activating the intracellular β_2AR – cAMP – PKA signlaing is proposed based on key findings in this study.

(A) Release of NE from noradrenergic neurons and diffusion of NE into synapses

(B) Transport of NE into cytosol of glutamatergic neurons and then into endosomal vesicles via OCT3 and PMAT

(C) Stimulation of the β_2AR which is associated with the AMPAR by NE followed by phosphorylation and surface insertion of the AMPAR

(D) Reuptake of remaining NE in synaptic cleft into noradrenergic neurons via NET

Chapter III

Interaction of the AMPA-type Glutamate Receptor with the Voltage-gated L-type Calcium Channel, $Ca_V1.2$

Introduction

L-type calcium channels, $Ca_V1.2$

Calcium (Ca^{2+}) is a secondary messenger playing important roles in neuronal excitability, neurotransmitter release, synaptic plasticity, and gene transcription (Berridge, 1998; Brini et al., 2014). Voltage- and ligand-gated calcium channels are major sources of Ca^{2+} influx. Voltage-gated calcium channels (VGCCs) are open when the plasma membrane is depolarized and external Ca^{2+} enters neurons via VGCCs. VGCCs are composed of a pore-forming α_1 subunit and auxiliary subunits, $\alpha_2\delta$, β, and γ subunits and classified into high- and low-voltage gated calcium channels. High-voltage gated calcium channels are subdivided into long-lasting L-type calcium channels (Ca_V1) and N-, P/Q-, and R-type calcium channels (Ca_V2). Low-voltage gated calcium channels are called T-type calcium channels (Ca_V3) (Catterall, 2011; Dolphin, 2016; Simms & Zamponi, 2014).

L-type calcium channels are encoded by four different Ca_V1 genes, $Ca_V1.1$ (CACNA1S), $Ca_V1.2$ (CACNA1C), $Ca_V1.3$ (CACNA1D), and $Ca_V1.4$ (CACNA1F) (Catterall et al., 2005; Ertel et al., 2000). While $Ca_V1.1$ and $Ca_V1.4$ are mainly expressed in skeletal muscle and

retina, $Ca_V1.2$ and $Ca_V1.3$ are ubiquitously expressed in the brain, heart, endocrine cells, and smooth muscle (Calin-Jageman & Lee, 2008; Hell et al., 1993; Striessnig et al., 2014). In the brain, $Ca_V1.2$ is much more expressed than $Ca_V1.3$ (Sinnegger-Brauns et al., 2004; Sinnegger-Brauns et al., 2009). Also, $Ca_V1.2$ is essential for synaptic plasticity, LTP (Grover & Teyler, 1990; Moosmang et al., 2005; Patriarchi et al., 2016; Qian et al., 2017) and LTD (Bolshakov & Siegelbaum, 1994). Dysfunction and mutation of $Ca_V1.2$ have been linked to neuronal diseases such as schizophrenia, depression, autism, and bipolar disorder (Kabir et al., 2017; Nanou & Catterall, 2018; Splawski et al., 2004). For instance, three different missense mutations in pore-forming α_1 subunit of $Ca_V1.2$ causes Timothy Syndrome (Han et al., 2019). Proteolytic cleavage of the C-terminus of $\alpha_1 1.2$ about 300 residues upstream of its C-terminus by the Ca^{2+}-stimulated protease calpain creates two different forms of $\alpha_1 1.2$, the 230-250 kDa long form and 190-210 kDa short form (Hell et al., 1996). In addition, $\alpha_1 1.2$ is extensively cleaved by calpain- and ubiquitin/proteasome-mediated mechanisms (Michailidis et al., 2014). The deletion of the distal C- terminus of $\alpha_1 1.2$ enhances the current density of $Ca_V1.2$ 4-6 times (Wei et al., 1994).

Like AMPAR, $Ca_V1.2$ is also associated with β_2AR, adenylyl cyclase (AC), and protein kinase A (PKA) and regulated by cAMP signaling (Davare et al., 2001; Man et al., 2020; Patriarchi et al., 2018; Patriarchi et al., 2016; Qian et al., 2017). The C-terminus of $\alpha_1 1.2$ binds to the C terminus of β_2AR (Patriarchi et al., 2016). While AMPAR is linked to AKAP5 via SAP97, AKAP5 binds to three different sites of $\alpha_1 1.2$, the N-terminus, the loop between domain I and II, and the C-terminus (Davare et al., 1999; Hall et al., 2007; Oliveria et al., 2007). Also, two short motifs near the C-terminus of AKAP5 interact with PP2B and PKA (Colledge et al., 2000; Leonard et al., 1998; Tavalin et al., 2002) and the

N-terminus of AKAP5 associates with the AC (Efendiev et al., 2010; Willoughby et al., 2010). PP2A and PP2B also bind directly to the C-terminus of $\alpha_1$1.2 (Hall et al., 2006; Xu et al., 2010). Stimulation of β_2AR – AC – cAMP – PKA signaling causes phosphorylation of $\alpha_1$1.2 at S1700 and S1928 by PKA (De Jongh et al., 1996; Fuller et al., 2010; Kamp & Hell, 2000). Phosphorylation at S1928 enhances activity of Ca_V1.2 in neurons (Qian et al., 2017) and vascular smooth muscle cells (Nystoriak et al., 2017) but not in the heart (Lemke et al., 2008). Moreover, interaction of Ca_V1.2 and β_2AR is essential for prolonged theta tetanus LTP (PTT-LTP) and β_2AR is dissociated by phosphorylation at S1928 (Patriarchi et al., 2016; Qian et al., 2017).

Functional coupling of AMPAR and Ca_V1.2

Previous studies showed the functional coupling of AMPAR and VGCCs. Co-expression of Ca_V2.1 and AMPAR changed activities of Ca_V2.1 and AMPAR (Kang et al., 2006). In addition, activity of ventral tegmental area (VTA) Ca_V1.3 modulated cocaine and depressive-like behavior through CP-AMPAR signaling (Martinez-Rivera et al., 2017). More interestingly, the activity of L-type calcium channels stabilizes surface insertion of AMPARs by regulating the mode of recycling endosome fusion (Hiester et al., 2017). These findings suggest that Ca_V1.2 is also functionally associated with AMPAR. In support of this notion, LTP indued by a theta tetanus requires Ca^{2+} influx through Ca_V1.2 that is triggered by AMPAR-mediated depolarization of the postsynaptic site. This LTP requires phosphorylation of both, AMPAR (on S845 in GluA1) and Ca_V1.2 (S1928) to augment the activity of both channels (Qian et al., 2017).

I discovered that AMPAR GluA1 and GluA2 subunits and $Ca_V1.2$ robustly co-immunoprecipitate (co-IP) from brain lysate and when co-expressed in HEK293 cells. These data suggest that $Ca_V1.2$ and AMPAR physically interact to form a functional unit. I hypothesize that **surface expression upon exocytosis of AMPARs requires their interaction with $Ca_V1.2$ mediating localized Ca^{2+} influx**. This study will define a structural and functional interaction between AMPARs and $Ca_V1.2$ in neurons, which will provide a novel paradigm for surface insertion of ion channels.

Result

$Ca_V1.2$ and AMPAR GluA1 and GluA2 subunits interact in the mouse brain

I assumed that $Ca_V1.2$ and AMPAR physically interact to be functionally coupled. Thus, I performed co-immunoprecipitation (co-IP) of $Ca_V1.2$ and AMPAR GluA1 and GluA2 subunits using mouse brain lysate. The mouse brain was lysed with 1% Triton X-100 buffer and the lysate was used for co-IP with anti-$Ca_V1.2$ antibody and immunoblotting of $Ca_V1.2$, AMPAR GluA1 and GluA2 subunit, and NMDAR GluN2A subunit. GluA1 and GluA2 were detected with $Ca_V1.2$ in the immunoprecipitated mouse brain lysate (Figure 1A) but GluN2A was not immunoprecipitated with $Ca_V1.2$ (Figure 1B). This result shows that $Ca_V1.2$ associates with AMPAR, but not NMDAR in the mouse brain.

$Ca_V1.2$ co-immunoprecipitates with GluA1 and GuA2 when co-expressed in HEK293 cells

To examine whether $Ca_V1.2$ interacts with AMPAR directly or via other proteins, I expressed rat neuronal $Ca_V1.2$ and rat AMPAR subunits in HEK293 cells which do not have endogenous $Ca_V1.2$ and AMPAR. $\alpha_1 1.2$ pore-forming subunit was expressed with $\alpha_2\delta$ and β2a auxiliary subunits. The HEK293 cells were extracted with Triton X-100 buffer and cleared by ultracentrifugation. Anti-$Ca_V1.2$, GluA1, and GluA2 antibodies were used for IP and immunoblotting. When $Ca_V1.2$, GluA1, and GluA2 are overexpressed in HEK293 cells and co-IP was conducted with anti-$Ca_V1.2$, GluA1, or GluA2 antibody, they

immunoprecipitated together. Also, GluA1 and GluA2 were detected with $Ca_V1.2$ when $Ca_V1.2$ was expressed with either GluA1 or GluA2 (Figure 2). These results suggest that GluA1 and GluA2 can be associated with $Ca_V1.2$ independently. Moreover, intensity of co-IPed GluA1 and GluA2 bands were weaker when they were coexpressed than when expressed separately. It implies that GluA1 and GluA2 competitively interact with $Ca_V1.2$. On the other hand, alternative splicing generates slightly different $Ca_V1.2$ in various tissues. Thus, I tested if isoform of $Ca_V1.2$ from other tissues also interact with GluA1. Human smooth muscle $Ca_V1.2$ ($hCa_V1.2(9*/-33)$) was overexpressed with or without β2a and $\alpha_2\delta$ subunits in HEK293 cells (Figure 3). The absence of β2a and $\alpha_2\delta$ subunits did not impair the expression of $Ca_V1.2$. GluA1 was overexpressed with $hCa_V1.2(9*/-33)$ in HEK293 cells. HEK293 cell lysates were immunoprecipitated with anti-GluA1 antibody and immunoblotted with anti- $Ca_V1.2$, GluA1, or GluA2 antibody. $hCa_V1.2(9*/-33)$ was also detected with GluA1. The co-IP of GluA1 with $hCa_V1.2(9*/-33)$ was not altered by the absence of β2a and $\alpha_2\delta$ subunits. Next, I performed co-IP of several different $Ca_V1.2$ with GluA1 in HEK293 cells in order to investigate the interaction of $Ca_V1.2$ from different tissues and GluA1 (Figure 4). Human neuronal ($hCa_V1.2(18a)$), cardiac ($hCa_V1.2(1a8a)$), smooth muscle ($hCa_V1.2(9*/-33)$), and rat neuronal (rat $nCa_V1.2$-HA, CFP) were overexpressed with or without GluA1 in HEK293 cells. $Ca_V1.2$ and GluA1 were probed by immunoblotting. All $Ca_V1.2$ co-IPed with GluA1.

$Ca_V1.3$ also interact with GluA1 when co-expressed in HEK293 cells

It is predictable that $Ca_V1.3$ also associates with GluA1 because $Ca_V1.3$ is a close homologue of $Ca_V1.2$ (Catterall et al., 2005; Zuccotti et al., 2011). Therefore, I

investigated the co-IP of $Ca_V1.3$ with GluA1 in HEK293 cells (Figure 5). Rat neuronal $Ca_V1.3$ with or without β2a and $\alpha_2\delta$ subunits was expressed with GluA1 in HEK293 cells. Triton X-100 lysates of HEK293 cells were used for co-IP and immunoblotting using anti-$Ca_V1.3$ or GluA1 antibody. Expression of $Ca_V1.3$ was not affected by absence of β2a and $\alpha_2\delta$ subunits and $Ca_V1.3$ and GluA1 were detected together when they are coexpressed.

$Ca_V1.2$ interact with AMPAR subunits GluA1, GluA2, and GluA3, but not kainate receptor subunit GluK2

Due to the sequence and structure homology of AMPAR and kainate receptor (Traynelis et al., 2010), it could be possible that kainate receptor interact with $Ca_V1.2$. Therefore, interaction of AMPAR and kainate receptor with $Ca_V1.2$ by co-IP (Figure 6). AMPAR GluA1, GluA2, and GluA3 subunits and kainate receptor GluK2 subunit were overexpressed with rat neuronal $Ca_V1.2$ in HEK293 cells. The HEK293 cells were lysed with 1% Triton X-100 solution and the Triton X-100 extracts were used for co-IP with anti-GluA1 antibody and immunoblotting with anti-$Ca_V1.2$, GluA1, GluA2, GluA3, and GluK2 antibody. Anti-GluA3 antibody which was used for the immunoblotting binds to the N-terminus of GluA3 (amino acid 245 to 451). Since almost all sequences of the epitope is shared by GluA1 and GluA2, not only GluA3 but also GluA1 and GluA2 were probed by the anti-GluA3 antibody. All AMPAR subunits, GluA1, GluA2 and GluA3, co-IPed with $Ca_V1.2$, while GluK2 was not detected with $Ca_V1.2$. This finding suggests that AMPAR but not kainate receptor interact with $Ca_V1.2$.

Activity of calcium channels is required for NE-induced surface insertion of AMPARs

The previous study showed the regulation of AMPAR trafficking by calcium channels (Hiester et al., 2017). In addition, co-IP results suggest that AMPAR and $Ca_V1.2$ are associated. Given these findings, I supposed that NE-induced surface insertion of GluA1 is also regulated by calcium channels. Change in NE-induced surface insertion of GluA1 by inhibition of calcium channels was analyzed by immunostaining of surface GluA1 (Figure 7). Cultured hippocampal neurons were pre-incubated with the vehicle (water) or calcium channel blocker, isradipine (ISRA, 10 μM), and treated with 1 μM NE with or without 10 μM ISRA. The surface GluA1 (sGluA1) was stained in fixed hippocampal neurons with the primary antibody against the extracellular N-terminus of GluA1, followed by the permeabilization with PBS containing 0.25% Triton X-100. PSD-95 and MAP2B were co-labeled as markers for postsynaptic sites and dendrites. Overlap of PSD-95 and sGluA1 represents the surface expression of GluA1 on postsynaptic sites. Consistent with immunostaining results in chapter II, NE augmented the surface insertion of GluA1. Also, NE-induced surface insertion of GluA1 is totally blocked by ISRA. It suggests that activity of calcium channels is required for the trafficking of AMPARs by NE.

Discussion

Both AMPAR and $Ca_V1.2$ are abundantly expressed in the brain (Calin-Jageman & Lee, 2008; Hell et al., 1993; Traynelis et al., 2010), cluster in postsynaptic sites (Craig et al., 1993; Di Biase et al., 2011), and take important roles in synaptic transmission and plasticity. They similarly form functional complexes with β_2AR, AC, and PKA and stimulation of β_2AR enhances activity of AMPAR and $Ca_V1.2$ inducing phosphorylation of GluA1 and $\alpha_1$1.2 subunits by PKA. Phosphorylation of GluA1 at S845 and $\alpha_1$1.2 at S1928 is required for LTP (Lee et al., 2000; Patriarchi et al., 2016; Qian et al., 2017). Given the ubiquitous expression and functional coupling of AMPAR and $Ca_V1.2$, I investigated their physical interaction and regulation of trafficking of AMPARs by calcium channels.

The first important finding is that AMPAR and $Ca_V1.2$ interact in the mouse brain lysate. Co-IP with anti-$Ca_V1.2$ antibody and immunoblotting for $Ca_V1.2$, GluA1, GluA2, and GluN2A was performed with Triton X-100 lysates of the mouse brain. Both GluA1 and GluA2 were detected with $Ca_V1.2$ in the same sample. Contrary to GluA1, GluN2A did not co-IP with $Ca_V1.2$, which represents that $Ca_V1.2$ association with AMPAR is specific and not due to non-specific effects such as incomplete solubilization of the NMDAR. To confirm the interaction of AMPAR with $Ca_V1.2$, I conducted co-IP with HEK293 cells overexpressing $Ca_V1.2$, GluA1, and GluA2. Since HEK293 cells does not express endogenous $Ca_V1.2$ and AMPAR, HEK293 cells were used to verify the interaction with different combinations of overexpression of those proteins. Three different co-IPs was

carried out with anti-$Ca_V1.2$, GluA1, or GluA2 antibody. When $Ca_V1.2$, GluA1, and GluA2 were expressed altogether in HEK293 cells, GluA1 as well as GluA2 co-IPed with $Ca_V1.2$ regardless of the antibody used for the co-IP. This result does not clarify if either GluA1 or GluA2 directly interacts with $Ca_V1.2$ because GluA1 and GluA2 are forming the AMPAR complex. Even if only GluA1 is linked to $Ca_V1.2$, GluA2 which is in the same complex with the GluA1 also can be co-IPed. Thus, another co-IP with $Ca_V1.2$ and GluA1 or GluA2 expressing HEK293 cells was performed. When only $Ca_V1.2$ and GluA1 were expressed in HEK293 cells, they were detected together. GluA2 also co-IPed with $Ca_V1.2$ in the absence of GluA1. These data showed that GluA1 and GluA2 interact with $Ca_V1.2$ separately. In addition, the intensity of co-IPed GluA1 and GluA2 bands were changed by different expression combinations, while the intensity of co-IPed $Ca_V1.2$ bands were constant. In the absence of GluA1 or GluA2, the co-IP of GluA2 or GluA1 with $Ca_V1.2$ was stronger. It could be because GluA1 and GluA2 influence each other when they are co-expressed in HEK293 cells. On the other hand, GluA1 and GluA2 might competitively interact with $Ca_V1.2$ sharing the binding sites.

To examine if different alternative splicing forms of $Ca_V1.2$ from various tissues changes their interaction with AMPARs, $Ca_V1.2$ from the brain, the heart, and smooth muscle was overexpressed in HEK293 cells for the co-IP with GluA1. First, $Ca_V1.2$ from human smooth muscle ($hCa_V1.2$(9*/-33)) was overexpressed with GluA1 in HEK293 cells and also co-IPed with GluA1. Interestingly, co-IP of $hCa_V1.2$(9*/-33) with GluA1 was not changed by the absence of β2a and $\alpha_2\delta$ subunits. It indicates that β2a and $\alpha_2\delta$ subunits do not mediate the interaction of GluA1 and $Ca_V1.2$. Secondly, I tested if four different

alternative splicing forms of $Ca_V1.2$ associate with GluA1. Human neuronal (h$Ca_V1.2$(18a)), cardiac (h$Ca_V1.2$(1a8a)), smooth muscle (h$Ca_V1.2$(9*/-33)), and rat neuronal (rat n$Ca_V1.2$-HA, CFP) were co-IPed with GluA1. Collectively, these results infer that $Ca_V1.2$ interacts with AMPAR in various tissues.

Considering the high homology between $Ca_V1.2$ and $Ca_V1.3$, I tested if $Ca_V1.3$ interacts with AMPAR. When rat neuronal $Ca_V1.3$ and GluA1 were coexpressed in HEK293 cells, they immunoprecipitated together. The expression and co-IP of $Ca_V1.3$ was not impacted by the absence of β2a and $\alpha_2\delta$ subunits. Since the interaction of AMPAR with $Ca_V1.2$ and $Ca_V1.3$ does not require β2a and $\alpha_2\delta$ subunits, the conserved regions of $Ca_V1.2$ and $Ca_V1.3$ could be critical for the binding to AMPAR GluA1 or GluA2. Furthermore, the kainate receptor is another kind of glutamate receptor and a homologue of AMPAR. Therefore, co-IP of AMPAR and kainate receptor subunits with $Ca_V1.2$ was analyzed with HEK293 cells which are transfected with $Ca_V1.2$, GluA1, GluA2, GluA3, or GluK2. GluA1, GluA2, and GluA3 were detected with $Ca_V1.2$. By contrast, GluK2 did not co-IPed with $Ca_V1.2$. This result showed that $Ca_V1.2$ is associated with AMPAR, but not kainate receptor.

To investigate the role of calcium channels in regulation of AMPARs, I analyzed the change in NE-induced surface expression of GluA1 by inhibition of calcium channels. Corresponding to the previous study (Hiester et al., 2017), the treatment of calcium channel blocker, isradipine (ISRA), completely blocked the NE-induced surface insertion

of GluA1. This finding supports the hypothesis that Ca^{2+} influx via calcium channels is essential for the trafficking of AMPARs to the surface.

Given that AMPAR co-IPed with $Ca_V1.2$ and trafficking of AMPARs was impaired by calcium channel blocker, I speculate that AMPAR and $Ca_V1.2$ are physically associated and their interaction is important for the stabilization of surface inserted AMPARs. AMPARs might be closely localized with $Ca_V1.2$ at postsynaptic sites and Ca^{2+} influx through the $Ca_V1.2$ which is interacting with the AMPAR modulates the activity of the AMPAR. Based on results of co-IP of GluA1, GluA2, and GluA3 with $Ca_V1.2$, $Ca_V1.2$ associates with different forms of AMPARs, GluA1/GluA2 or GluA2/GluA3 heteromer, GluA1 or GluA2 homomer. Moreover, $Ca_V1.3$ also interacts with GluA1. Further studies are necessary to examine if interaction between $Ca_V1.2$ or $Ca_V1.3$ and different AMPAR subunits have unique physiological roles in synaptic transmission and plasticity. In addition, the binding site of AMPAR and $Ca_V1.2$ should be determined to investigate the molecular characteristics and function of their interaction. It is possible to use amino acid sequence alignment to predict the binding site. Since both $Ca_V1.2$ and $Ca_V1.3$ co-IPed with GluA1 and have short extracellular loops, the binding site should be in conserved regions in cytosolic loops, C-termini, or transmembrane domains of $Ca_V1.2$ and $Ca_V1.3$. I used the sequence alignment tool from EMBL-EBI, Clustal Omega (Goujon et al., 2010; Sievers et al., 2011), for amino acid sequence alignment of $Ca_V1.2$ and $Ca_V1.3$ (Figure 8). Amino acids in cytosolic loops and proximal region of C-termini of $Ca_V1.2$ and $Ca_V1.3$ are conserved and might mediate the interaction of $Ca_V1.2$ and $Ca_V1.3$ with AMPAR. Amino acid sequences of GluA1, GluA2, GluA3, and GluK2 were also aligned using

Clustal Omega (Figure 9). Amino acids shared by GluA1, GluA2, and GluA3 but not GluK2 might be part of the binding site because the co-IP of GluK2 with $Ca_V1.2$ was not observed. Transmembrane domains of the four proteins are highly conserved. On the other hand, 12 amino acids in the long cytosolic domain between M1 and M2, six amino acids in the short cytosolic domain between M2 and M3, and 13 amino acids in C-termini are common in GluA1, GluA2, GluA3, and GluK2. Among common amino acids, three amino acids in the cytosolic domain between M1 and M2, five amino acids in the cytosolic domain between M2 and M3, and five amino acids in the C-terminus are not conserved in GluK2. These amino acids could mediate the association of AMPAR and $Ca_V1.2$. Especially, the five amino acids in the C-terminus are located near the transmembrane domain. In addition, it is possible that GluA1 and GluA2 are linked to $Ca_V1.2$ via other proteins considering that they form complexes with β_2AR through PSD-95, SAP97, and other binding partners. For instance, p97, a type II AAA ATPase also called valonsin-containing protein, directly binds to the N-terminus of GluA1 and regulates the formation and surface insertion of GluA1 homomeric AMPARs (Ge et al., 2019). N-ethylmaleimide–sensitive fusion protein (NSF), a member of AAA ATPase family, mediates AMPAR synaptic transmission and trafficking of AMPARs by binding to the C-terminus of GluA2 (Nishimune et al., 1998; Shi et al., 2001). Given the roles of p97 and NSF, AMPAR could interact with $Ca_V1.2$ via p97 or NSF. If the binding site is determined, it could be tested whether interruption of interaction of GluA1 and GluA2 with $Ca_V1.2$ alters the surface insertion of AMPARs. Disruption of the interaction between AMPAR and $Ca_V1.2$ using peptides blocking their binding site and mutant GluA1, GluA2, and $Ca_V1.2$ without the

binding site might result in reduction of surface expression of AMPARs, which will show the pivotal role of $Ca_V1.2$ in regulation of trafficking of AMPARs.

Function and dysfunction of AMPAR and $Ca_V1.2$ have been implicated many physiological processes in the brain including synaptic plasticity, learning, and neural disorders such as Alzheimer's disease, autism, and schizophrenia. Trafficking of AMPARs is also critical for neuronal activity and dysregulated in pathological conditions. In the present study, I investigated the physical and functional association of AMPAR and $Ca_V1.2$ in neurons and its effects on the surface insertion of AMPARs. Understanding the formation of a functional complex between AMPAR and $Ca_V1.2$ will reveal the new mechanisms of neuronal activity via those two ion channels, which can be a promising therapeutic target for various neuronal disorders.

Figures

Figure 1

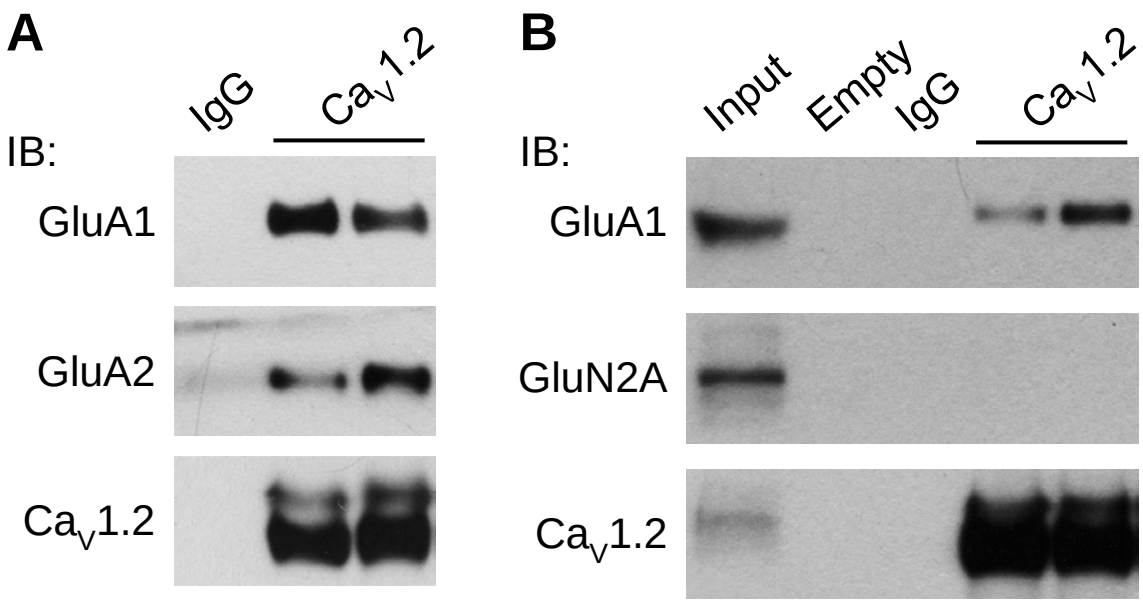

Figure 1. Co-immunoprecipitation (co-IP) of AMPAR GluA1 and GluA2 subunits but not the NMDAR GluN2A subunit with $Ca_V1.2$ from the mouse brain lysate

$Ca_V1.2$ was immunoprecipitated from the mouse brain extracted with 1% Triton X-100 buffer and cleared by ultracentrifugation. SDS-PAGE separated immunoprecipitated lysates and was followed by immunoblotting for $Ca_V1.2$ and GluA1, GluA2 (A), or GluN2A (B). IP with control IgG was negative. Total lysate (input) was loaded as positive control for GluN2A probing (B). GluA1 and GluA2 (A) but not GluN2A (B) co-IPed with $Ca_V1.2$.

Figure 2

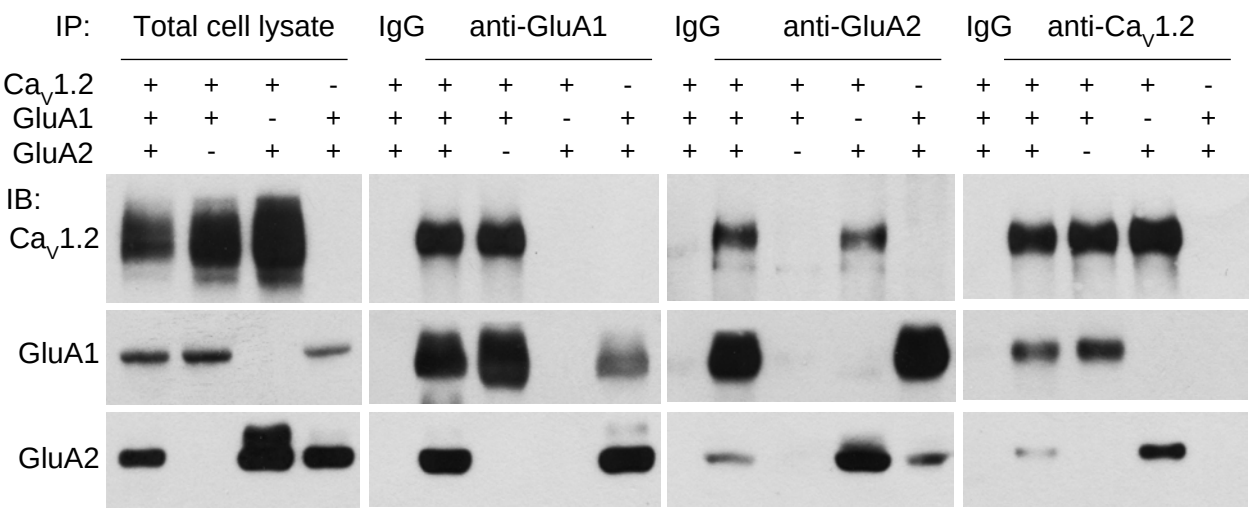
IP:
Total cell lysate
IgG
anti-GluA1
IgG
anti-GluA2
IgG
anti-CaV1.2
CaV1.2
GluA1
GluA2
IB:
CaV1.2
GluA1
GluA2

Figure 2. GluA1 and GluA2 co-immunopreciptate with rat neuronal $Ca_V1.2$ from HEK293 cells

HEK293 cells were transfected with rat GluA1 or GluA2 and rat neuronal $Ca_V1.2$. The cells were lysed with 1% Triton X-100 solution before immunoprecipitation and immunoblotting with anti-GluA1, GluA2, or $Ca_V1.2$ antibody.

Figure 3

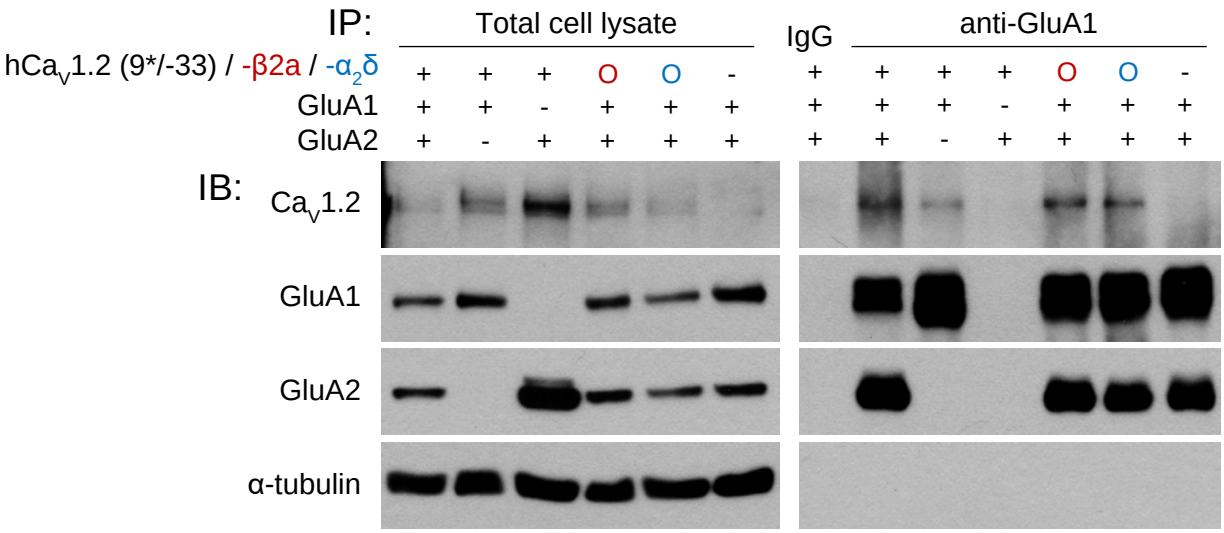
IP:
Total cell lysate
IgG
anti-GluA1
hCaV1.2 (9*/-33) / -β2a / -α2δ
GluA1
GluA2
IB:
CaV1.2
GluA1
GluA2
α-tubulin

Figure 3. GluA1 co-immunopreciptates with human smooth muscle $Ca_V1.2$ from HEK293 cells

Human smooth muscle $Ca_V1.2$ ($hCa_V1.2$ (9*/-33)) was overexpressed with or without its subunit protein, β2a or $\alpha_2\delta$ in HEK293 cells. The absence of β2a or α2δ subunit does not affect the co-immunoprecipitation of GluA1 or GluA2 with $Ca_V1.2$.

Figure 4

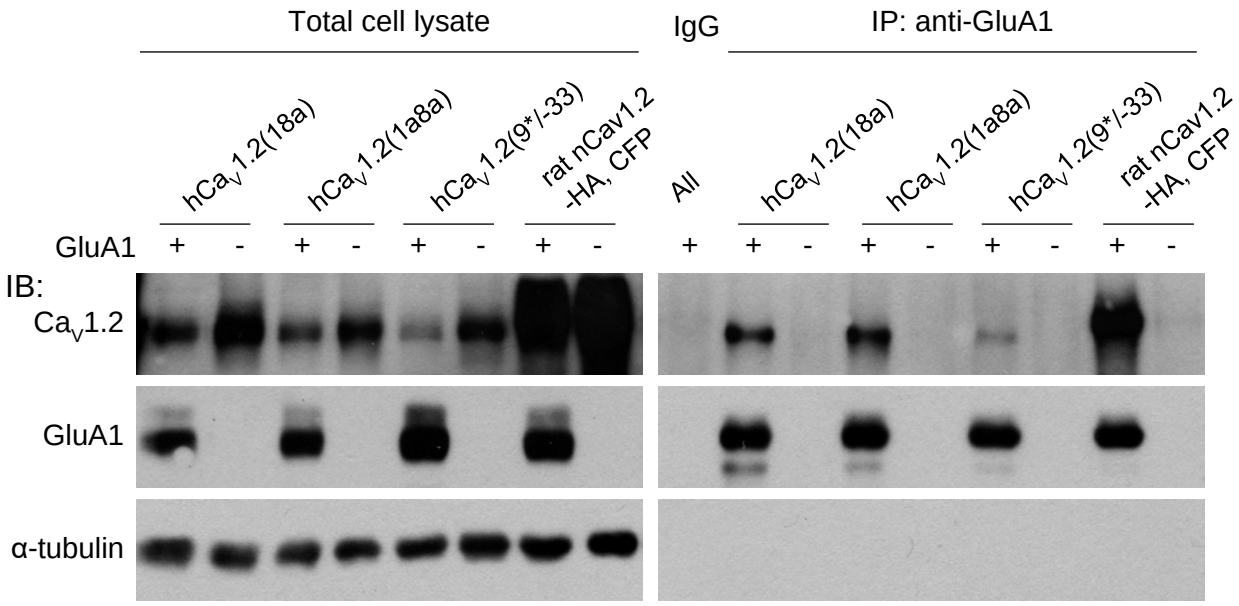
Total cell lysate
IgG
IP: anti-GluA1
hCaV1.2(18a)
hCaV1.2(1a8a)
hCaV1.2(9*/-33)
rat nCav1.2 -HA, CFP
All
GluA1
+ - + - + - + - + + - + - + - + -
IB:
CaV1.2
GluA1
α-tubulin

Figure 4. Interaction of human and rat $Ca_V1.2$ and GluA1 from HEK293 cells

HEK293 cells was transfected with splicing variants of human $Ca_V1.2$ (18a, brain; 1a8a, heart; 9*/-33, smooth muscle) or rat neuronal $Ca_V1.2$ tagged with HA and CFP and GluA1 and solubilized by 1% Triton X-100 solution before immunoprecipitation of GluA1, SDS-PAGE, and immunoblotting for $Ca_V1.2$ and GluA1. All different human and rat $Ca_V1.2$ co-IPed with GluA1.

Figure 5

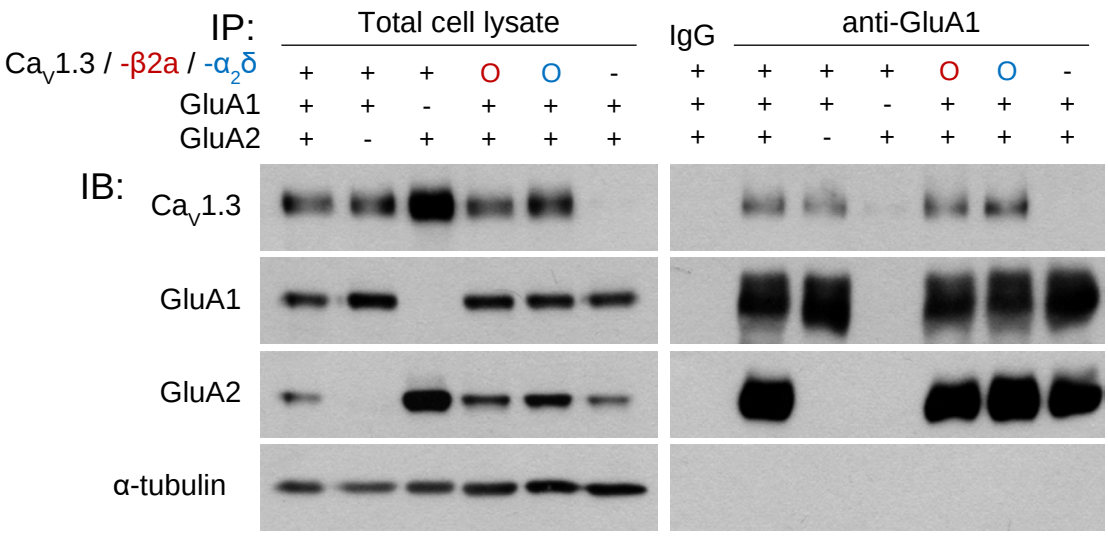
IP:
Total cell lysate
IgG
anti-GluA1
CaV1.3 / -β2a / -α2δ
+ + + O O - + + + + O O -
GluA1
+ + - + + + + + + - + + +
GluA2
+ - + + + + + + - + + + +
IB:
CaV1.3
GluA1
GluA2
α-tubulin

Figure 5. GluA1 and GluA2 co-immunopreciptate with rat neuronal $Ca_V1.3$ from HEK293 cells

HEK293 cells overexpressing rat neuronal $Ca_V1.3$ and GluA1 or GluA2 were extracted 1% Triton X-100 solution before immunoprecipitation and immunoblotting with anti-GluA1, GluA2, or $Ca_V1.3$ antibody. $Ca_V1.3$ was transfected with or without its subunit protein, β2a or $\alpha_2\delta$ in HEK293 cells. The absence of β2a or $\alpha_2\delta$ subunit decreases the expression of $Ca_V1.3$.

Figure 6

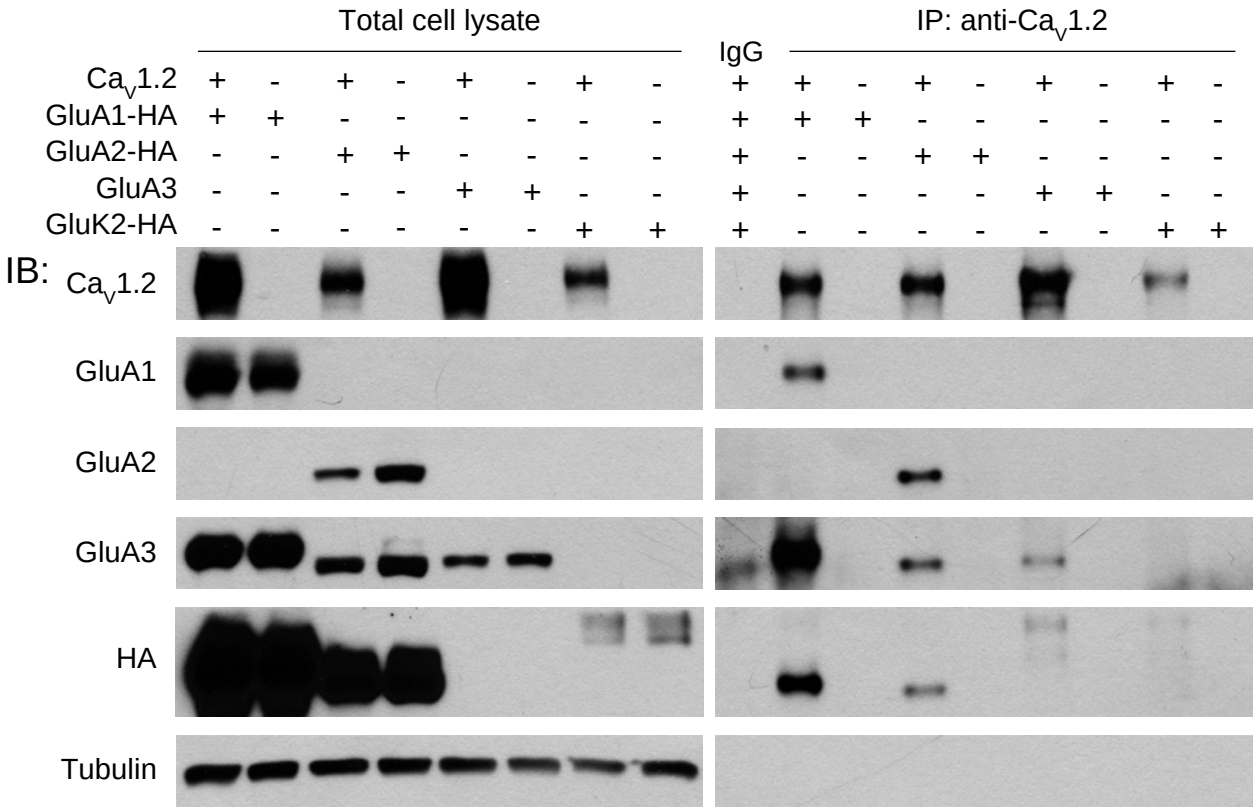
Total cell lysate
IgG
IP: anti-Ca$_V$1.2
Ca$_V$1.2 + - + - + - + - + + - + - + - + -
GluA1-HA + + - - - - - - + + + - - - - - -
GluA2-HA - - + + - - - - + - - + + - - - -
GluA3 - - - - + + - - + - - - - + + - -
GluK2-HA - - - - - - + + + - - - - - - + +
IB:
Ca$_V$1.2
GluA1
GluA2
GluA3
HA
Tubulin

Figure 6. $Ca_V1.2$ interacts with GluA1, GluA2, and GluA3 but not GluK2 from HEK293 cells

Interaction between $Ca_V1.2$ and AMPA receptor (GluA1, GluA2, and GluA3) or kainate receptor subunit (GluK2) was examined by immunoprecipitation with anti-$Ca_V1.2$ antibody. GluA1, GluA2, GluA3 or GluK2 was co-expressed with $Ca_V1.2$ in HEK293 cells and the cell extract was used for immunoprecipitation and immunoblotting. AMPA receptor subunits (GluA1, GluA2, and GluA3) but not kainate receptor subunit, GluK2 co-IPed with $Ca_V1.2$. Anti-GluA3 N-terminus antibody also detects GluA1 and GluA2 because the sequence of GluA3 N-terminus is almost identical to those of GluA1 and GluA2.

Figure 7

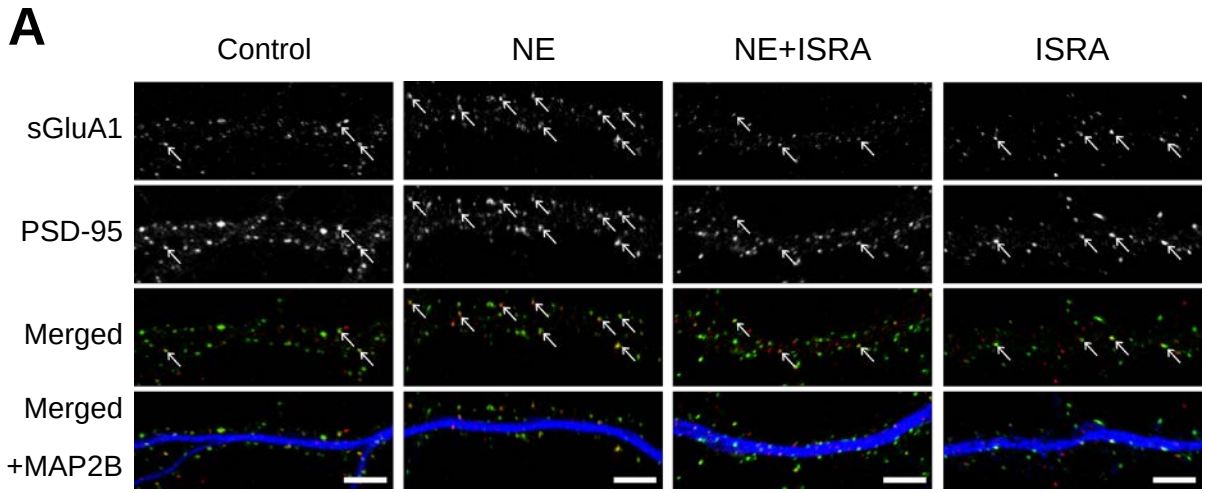
A
Control
NE
NE+ISRA
ISRA
sGluA1
PSD-95
Merged
Merged
+MAP2B

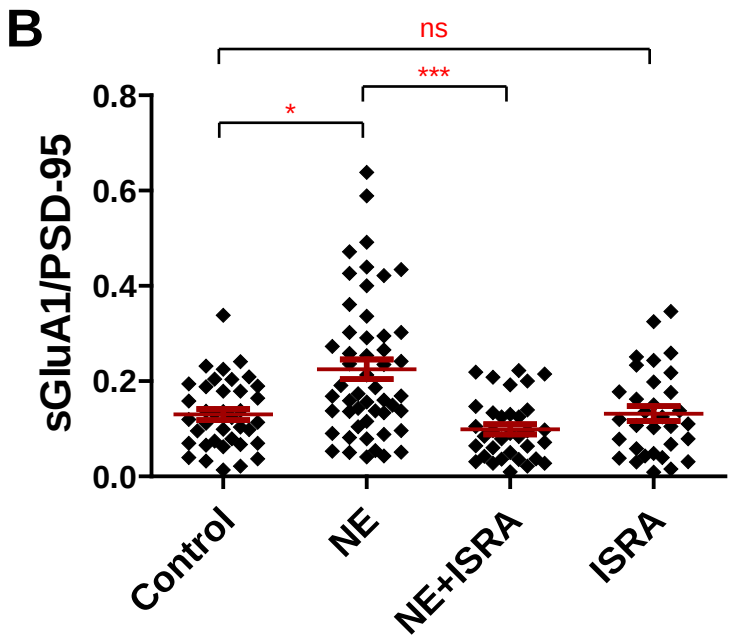
B
ns
***
*
sGluA1/PSD-95
0.8
0.6
0.4
0.2
0.0
Control
NE
NE+ISRA
ISRA

Figure 7. Blocking calcium channels with isradipine (ISRA) prevents increase in NE-induced surface expression of GluA1 in hippocampal neurons

(A) Vehicle (water, Control) or NE (1 μM) were applied with or without isradipine (ISRA) (10 μM) to dissociated hippocampal culture (HCs). Surface GluA1 (sGluA1, red), PSD-95 (green), and MAP2B (blue) were labelled with fluorophore-conjugated antibodies. PSD-95 was used as a postsynaptic site marker and MAP2B as a dendritic shaft marker. (Scale bar, 5μm)

(B) Quantitative analysis of surface GluA1 puncta at postsynaptic sites, which was colocalized with PSD-95 puncta. NE treatment increased surface expression of GluA1 but the effect of NE was impeded by ISRA ($n \geq 32$ from four preparations, given as mean±SEM; the Kruskal-Wallis test was used to analyze significance of difference between all groups and significance of differences between control vs NE, NE vs NE+ISRA, and control vs ISRA are determined by Dunn's multiple comparison post-hoc test; *$p<0.05$, ***$p<0.001$, ns: not significant)

Figure 8


CLUSTAL O(1.2.4) multiple sequence alignment
CaV1.2 (NP_036649.2)
CaV1.3 (NP_058994.1)
CaV1.2 MIRAFAQPSTPPYQPLSSCLSEDTERKFKGKVVHEAQLNCFYISPGGSNYGSPRPAHANM 60
CaV1.3 MMM--------------MM--------MMKKMQHQRQQQE--DHANEANYARGT-----R 31
CaV1.2 NANAAAGLAPEHIPTPGAALSWQAAIDAARQAKLMGSAGNATI-STVSSTQRKRQQYGKP 119
CaV1.3 LPISGEGPTSQPNSSKQTVLSWQAAIDAARQAKAAQTMSTSAPPPVGSLSQRKRQQYAKS 91
CaV1.2 KKQGGTTATRPPRALLCLTLKNPIRRACISIVEWKSFEIIILLTIFANCVALAIYIPFPE 179
CaV1.3 KKQGNSSNSRPARALFCLSLNNPIRRACISIVDWKPFDIFILLAIFANCVALAIYIPFPE 151
CaV1.2 DDSNATNSNLERVEYLFLIIFTVEAFLKVIAYGLLFHPNAYLRNGWNLLDFIIVVVGLFS 239
CaV1.3 DDSNSTNHNLEKVEYAFLIIFTVETFLKIIASGLLLHPNASVRNGWNLLDFVIVIVGLFS 211
CaV1.2 AILEQATK-ADGANALGGKGAGFDVKALRAFRVLRPLRLVSGVPSLQVVLNSIIKAMVPL 298
CaV1.3 VILEQLTKETEGGNHSSGKSGGFDVKALRAFRVLRPLRLVSGVPSLQVVLNSIIKAMVPL 271
CaV1.2 LHIALLVLFVIIIYAIIGLELFMGKMHKTCYNQEGIIDVPAEEDPSPCALETGHGRQCQN 358
CaV1.3 LHIALLVLFVIIIYAIIGLELFIGKMHKTCFFADS--DIVAEEDPAPCAFSGNGRQCAAN 329
CaV1.2 GTVCKPGWDGPKHGITNFDNFAFAMLTVFQCITMEGWTDVLYWMQDAMGYELPWVYFVSL 418
CaV1.3 GTECRSGWVGPNGGITNFDNFAFAMLTVFQCITMEGWTDVLYWVNDAIGWEWPWVYFVSL 389
Loop I-II
CaV1.2 VIFGSFFVLNLVLGVLSGEFSKEREKAKARGDFQKLREKQQLEEDLKGYLDWITQAEDID 478
CaV1.3 IILGSFFVLNLVLGVLSGEFSKEREKAKARGDFQKLREKQQLEEDLKGYLDWITQAEDID 449
CaV1.2 PENEDEGMDEDKPRNMSMPTSETESVNTENVAGGDIEGENCGARLAH------------ 525
CaV1.3 PENEEEGGEEG-KRNTSMPTSETESVNTENVSGEGETQGCCGSLWCWWKRRGAAKTGPSG 508
CaV1.2 ---RISKSKFSRYWRRWN 540
CaV1.3 CRRWGQAISKSKLRSHGAREALCVCRCSLESLVKLWTSRFSAHLQAAYVRPYSRRWRRWN 568
CaV1.2 RFCRRKCRAAVKSNVFYWLVIFLVFLNTLTIASEHYNQPHWLTEVQDTANKALLALFTAE 600
CaV1.3 RFNRRRCRAAVKSVTFYWLVIVLVFLNTLTISSEHYNQPDWLTQIQDIANKVLLALFTCE 628
CaV1.2 MLLKMYSLGLQAYFVSLFNRFDCFIVCGGILETILVETKIMSPLGISVLRCVRLLRIFKI 660
CaV1.3 MLVKMYSLGLQAYFVSLFNRFDCFVVCGGITETILVELELMSPLGVSVFRCVRLLRIFKV 688
CaV1.2 TRYWNSLSNLVASLLNSVRSIASLLLLLFLFIIIFSLLGMQLFGGKFNFDEMQTRRSTFD 720
CaV1.3 TRHWTSLSNLVASLLNSMKSIASLLLLLFLFIIIFSLLGMQLFGGKFNFDETQTKRSTFD 748

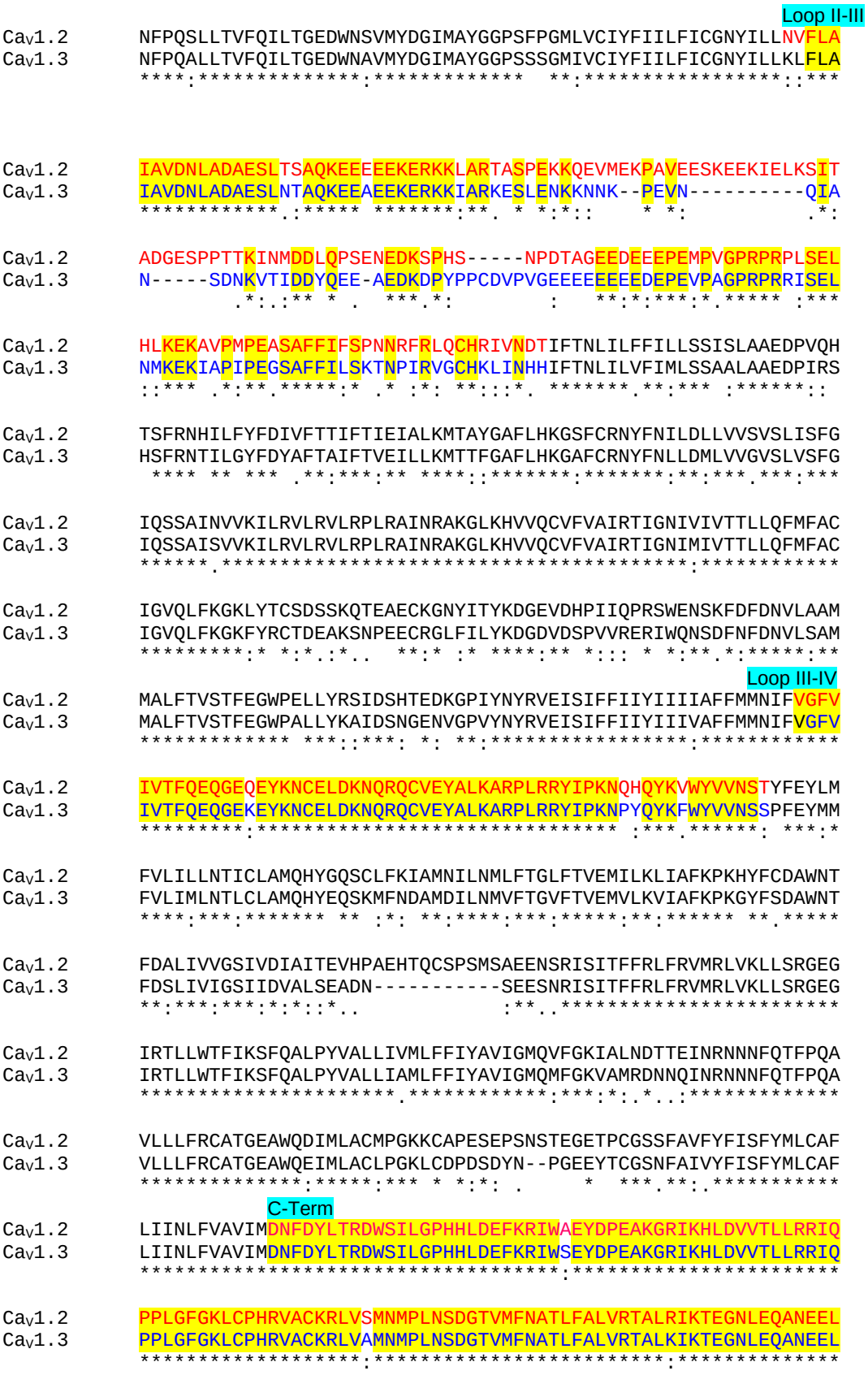
Loop II-III
Cav1.2 NFPQSLLTVFQILTGEDWNSVMYDGIMAYGGPSFPGMLVCIYFIILFICGNYILLNVFLA 780
Cav1.3 NFPQALLTVFQILTGEDWNAVMYDGIMAYGGPSSSGMIVCIYFIILFICGNYILLKLFLA 808
Cav1.2 IAVDNLADAESLTSAQKEEEEEKERKKLARTASPEKKQEVMEKPAVEESKEEKIELKSIT 840
Cav1.3 IAVDNLADAESLNTAQKEEAEEKERKKIARKESLENKKNNK--PEVN----------QIA 856
Cav1.2 ADGESPPTTKINMDDLQPSENEDKSPHS-----NPDTAGEEDEEEPEMPVGPRPRPLSEL 895
Cav1.3 N-----SDNKVTIDDYQEE-AEDKDPYPPCDVPVGEEEEEEEEDEPEVPAGPRPRRISEL 910
Cav1.2 HLKEKAVPMPEASAFFIFSPNNRFRLQCHRIVNDTIFTNLILFFILLSSISLAAEDPVQH 955
Cav1.3 NMKEKIAPIPEGSAFFILSKTNPIRVGCHKLINHHIFTNLILVFIMLSSAALAAEDPIRS 970
Cav1.2 TSFRNHILFYFDIVFTTIFTIEIALKMTAYGAFLHKGSFCRNYFNILDLLVVSVSLISFG 1015
Cav1.3 HSFRNTILGYFDYAFTAIFTVEILLKMTTFGAFLHKGAFCRNYFNLLDMLVVGVSLVSFG 1030
Cav1.2 IQSSAINVVKILRVLRVLRPLRAINRAKGLKHVVQCVFVAIRTIGNIVIVTTLLQFMFAC 1075
Cav1.3 IQSSAISVVKILRVLRVLRPLRAINRAKGLKHVVQCVFVAIRTIGNIMIVTTLLQFMFAC 1090
Loop III-IV
Cav1.2 MALFTVSTFEGWPELLYRSIDSHTEDKGPIYNYRVEISIFFIIYIIIIAFFMMNIFVGFV 1195
Cav1.3 MALFTVSTFEGWPALLYKAIDSNGENVGPVYNYRVEISIFFIIYIIIVAFFMMNIFVGFV 1210
Cav1.2 IVTFQEQGEQEYKNCELDKNQRQCVEYALKARPLRRYIPKNQHQYKVWYVVNSTYFEYLM 1255
Cav1.3 IVTFQEQGEKEYKNCELDKNQRQCVEYALKARPLRRYIPKNPYQYKFWYVVNSSPFEYMM 1270
Cav1.2 FVLILLNTICLAMQHYGQSCLFKIAMNILNMLFTGLFTVEMILKLIAFKPKHYFCDAWNT 1315
Cav1.3 FVLIMLNTLCLAMQHYEQSKMFNDAMDILNMVFTGVFTVEMVLKVIAFKPKGYFSDAWNT 1330
Cav1.2 FDALIVVGSIVDIAITEVHPAEHTQCSPSMSAEENSRISITFFRLFRVMRLVKLLSRGEG 1375
Cav1.3 FDSLIVIGSIIDVALSEADN----------SEESNRISITFFRLFRVMRLVKLLSRGEG 1379
Cav1.2 IRTLLWTFIKSFQALPYVALLIVMLFFIYAVIGMQVFGKIALNDTTEINRNNNFQTFPQA 1435
Cav1.3 IRTLLWTFIKSFQALPYVALLIAMLFFIYAVIGMQMFGKVAMRDNNQINRNNNFQTFPQA 1439
Cav1.2 VLLLFRCATGEAWQDIMLACMPGKKCAPESEPSNSTEGETPCGSSFAVFYFISFYMLCAF 1495
Cav1.3 VLLLFRCATGEAWQEIMLACLPGKLCDPDSDYN--PGEEYTCGSNFAIVYFISFYMLCAF 1497
C-Term
Cav1.2 LIINLFVAVIMDNFDYLTRDWSILGPHHLDEFKRIWAEYDPEAKGRIKHLDVVTLLRRIQ 1555
Cav1.3 LIINLFVAVIMDNFDYLTRDWSILGPHHLDEFKRIWSEYDPEAKGRIKHLDVVTLLRRIQ 1557
Cav1.2 PPLGFGKLCPHRVACKRLVSMNMPLNSDGTVMFNATLFALVRTALRIKTEGNLEQANEEL 1615
Cav1.3 PPLGFGKLCPHRVACKRLVAMNMPLNSDGTVMFNATLFALVRTALKIKTEGNLEQANEEL 1617

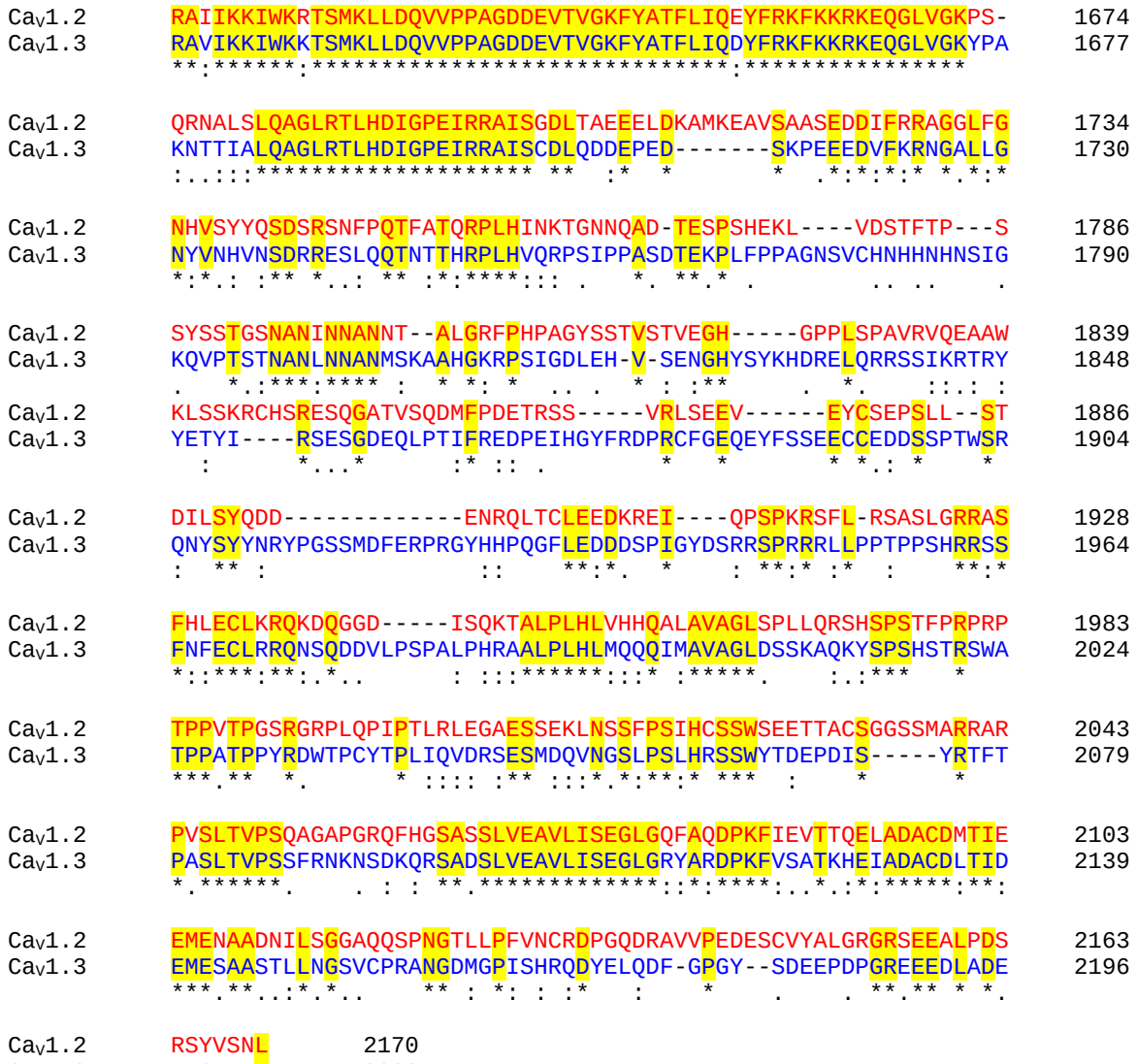
Cav1.2 RAIIKKIWKRTSMKLLDQVVPPAGDDEVTVGKFYATFLIQEYFRKFKKRKEQGLVGKPS- 1674
Cav1.3 RAVIKKIWKKTSMKLLDQVVPPAGDDEVTVGKFYATFLIQDYFRKFKKRKEQGLVGKYPA 1677
Cav1.2 QRNALSLQAGLRTLHDIGPEIRRAISGDLTAEEELDKAMKEAVSAASEDDIFRRAGGLFG 1734
Cav1.3 KNTTIALQAGLRTLHDIGPEIRRAISCDLQDDEPED-------SKPEEEDVFKRNGALLG 1730
Cav1.2 NHVSYYQSDSRSNFPQTFATQRPLHINKTGNNQAD-TESPSHEKL----VDSTFTP---S 1786
Cav1.3 NYVNHVNSDRRESLQQTNTTHRPLHVQRPSIPPASDTEKPLFPPAGNSVCHNHHNHNSIG 1790
Cav1.2 SYSSTGSNANINNANNT--ALGRFPHPAGYSSTVSTVEGH-----GPPLSPAVRVQEAAW 1839
Cav1.3 KQVPTSTNANLNNANMSKAAHGKRPSIGDLEH-V-SENGHYSYKHDRELQRRSSIKRTRY 1848
Cav1.2 KLSSKRCHSRESQGATVSQDMFPDETRSS-----VRLSEEV------EYCSEPSLL--ST 1886
Cav1.3 YETYI----RSESGDEQLPTIFREDPEIHGYFRDPRCFGEQEYFSSEECCEDDSSPTWSR 1904
Cav1.2 DILSYQDD-------------ENRQLTCLEEDKREI----QPSPKRSFL-RSASLGRRAS 1928
Cav1.3 QNYSYYNRYPGSSMDFERPRGYHHPQGFLEDDDSPIGYDSRRSPRRRLLPPTPPSHRRSS 1964
Cav1.2 FHLECLKRQKDQGGD-----ISQKTALPLHLVHHQALAVAGLSPLLQRSHSPSTFPRPRP 1983
Cav1.3 FNFECLRRQNSQDDVLPSPALPHRAALPLHLMQQQIMAVAGLDSSKAQKYSPSHSTRSWA 2024
Cav1.2 TPPVTPGSRGRPLQPIPTLRLEGAESSEKLNSSFPSIHCSSWSEETTACSGGSSMARRAR 2043
Cav1.3 TPPATPPYRDWTPCYTPLIQVDRSESMDQVNGSLPSLHRSSWYTDEPDIS-----YRTFT 2079
Cav1.2 PVSLTVPSQAGAPGRQFHGSASSLVEAVLISEGLGQFAQDPKFIEVTTQELADACDMTIE 2103
Cav1.3 PASLTVPSSFRNKNSDKQRSADSLVEAVLISEGLGRYARDPKFVSATKHEIADACDLTID 2139
Cav1.2 EMENAADNILSGGAQQSPNGTLLPFVNCRDPGQDRAVVPEDESCVYALGRGRSEEALPDS 2163
Cav1.3 EMESAASTLLNGSVCPRANGDMGPISHRQDYELQDF-GPGY--SDEEPDPGREEEDLADE 2196
Cav1.2 RSYVSNL 2170
Cav1.3 MICITTL 2203

Figure 8. Sequence alignment of $Ca_V1.2$ and $Ca_V1.3$

Amino acid sequence of $Ca_V1.2$ (Reference sequence (RefSeq): NP_036649.2) and $Ca_V1.3$ (RefSeq: NP_058994.1) were aligned using Clustal Omega (Goujon et al., 2010; Sievers et al., 2011). Sequences in intracellular loops and C-termini were colored in red ($Ca_V1.2$) or blue ($Ca_V1.3$) and common sequences of $Ca_V1.2$ and $Ca_V1.3$ were highlight in yellow.

Figure 9

```
CLUSTAL O(1.2.4) multiple sequence alignment


GluK2 (NP_062182.1)
GluA1 (NP_113796.1)
GluA2 (NP_058957.1)
GluA3 (NP_116785.2)

GluK2      MKIISPVLSNLVFSRSIKVLLCLLWIGYS--QGTTHVLRFGGIFEYVESGPMGAEELAFR     58
GluA1      ------------MPYIFAFFCTGFLGAVVGANFPNNIQIGGLFPNQQ----SQEHAAFR     43
GluA2      ---M-------QKIMHISVLLSPVLWGLI-FGVSSNSIQIGGLFPRGA----DQEYSAFR     45
GluA3      --MG-------QSVLRAVFFLVLGLLGHS-HGGFPNTISIGGLFMRNT----VQEHSAFR     46
                              ::     *        : : :**:*          *  ***

GluK2      FAVNTINRNRTLL-PNTTLTYDTQKINLYDSFEASKKACDQLSLGVAAIFGPSHSSSANA     117
GluA1      FALSQLT-------EPPKLLPQIDIVNISDSFEMTYRFCSQFSKGVYAIFGFYERRTVNM     96
GluA2      VGMVQFST------SEFRLTPHIDNLEVANSFAVTNAFCSQFSRGVYAIFGFYDKKSVNT     99
GluA3      FAVQLYNTNQNTTEKPFHLNYHVDHLDSSNSFSVTNAFCSQFSRGVYAIFGFYDQMSMNT     106
           ..:   .           *  . : ::  :**  :   *.*:* ** ****  .  : *

GluK2      VQSICNALGVPHIQTRWKHQVSDNKDSFYVSLYPDFSSLSRAILDLVQFFKWKTVTVVYD     177
GluA1      LTSFCGALHVCFITPSFPV---DTSNQFVLQLRPE---LQEALISIIDHYKWQTFVYIYD     150
GluA2      ITSFCGTLHVSFITPSFPT---DGTHPFVIQMRPD---LKGALLSLIEYYQWDKFAYLYD     153
GluA3      LTSFCGALHTSFVTPSFPT---DADVQFVIQMRPA---LKGAILSLLGYYKWEKFVYLYD     160
           : *:*.:* . .:   :     *    * :.: *    *. *::.:: .::*.... :**

GluK2      DSTGLIRLQELIKAPSRYNLRLKIRQLPAD-----TKDAKPLLKEMKRGKEFHVIFDCSH     232
GluA1      ADRGLSVLQRVLDTAAEKNWQVTAVNILTT----TEEGYRMLFQDLEKKKERLVVVDCES     206
GluA2      SDRGLSTLQAVLDSAAEKKWQVTAINVGNINNDKKDETYRSLFQDLELKKERRVILDCER     213
GluA3      TERGFSVLQAIMEAAVQNNWQVTARSVGNIKD---VQEFRRIIEEMDRRQEKRYLIDCEV     217
             . *:  ** ::.:  . : ::.  .:         :  : :::::.  :*   :.**.

GluK2      EMAAGILKQALAMGMMTEYYHYIFTTLDLFALDVEPYRYSGVNMTGFRILNTENTQVSSI     292
GluA1      ERLNAILGQIVKLEKNGIGYHYILANLGFMDIDLNKFKESGANVTGFQLVNYTDTIPARI     266
GluA2      DKVNDIVDQVITIGKHVKGYHYIIANLGFTDGDLLKIQFGGANVSGFQIVDYDDSLVSKF     273
GluA3      ERINTILEQVVILGKHSRGYHYMLANLGFTDILLERVMHGGANITGFQIVNNENPMVQQF     277
           :    *: * : :      ***:::.*.:    :     .*.*::**::::  :     :

GluK2      IEKWSMERLQAPPKPDSGLLDGFMTTDAALMYDAVHVVSVAVQQFPQMTV--------SS     344
GluA1      MQQWRTSDSRDHTRVDWK----RPKYTSALTYDGVKVMAEAFQSLRRQRIDISRRGNAGD     322
GluA2      IERWSTLEEKEYPGAHTA----TIKYTSALTYDAVQVMTEAFRNLRKQRIEISRRGNAGD     329
GluA3      IQRWVRLDEREFPEAKNA----PLKYTSALTHDAILVIAEAFRYLRRQRVDVSRRGSAGD     333
           :::*     :     .        .  :** :*.: *:: *.: : :  :        ..

GluK2      LQCNRHKPWRFGTRFMSLIKEAHWEGLTGRITFNKTNGLRTDFDLDVISLKEEGLEKIGT     404
GluA1      CLANPAVPWGQGIDIQRALQQVRFEGLTGNVQFNE-KGRRTNYTLHVIEMKHDGIRKIGY     381
GluA2      CLANPAVPWGQGVEIERALKQVQVEGLSGNIKFDQ-NGKRINYTINIMELKTNGPRKIGY     388
GluA3      CLANPAVPWSQGIDIERALKMVQVQGMTGNIQFDT-YGRRTNYTIDVYEMKVSGSRKAGY     392
             .*   **  *  :   :: .: :*::*.: *:   * * :: :.: .:* .* .* *

GluK2      WDPASGLNMTESQKGKPANITDSLSNRSLIVTTILEEPYVLFKKSDKPLYGNDRFEGYCI     464
GluA1      WNEDDKFVPAATD-AQAGGDNSSVQNRTYIVTTILEDPYVMLKKNANQFEGNDRYEGYCV     440
GluA2      WSEVDKMVVTLTE-LPSGNDTSGLENKTVVVTTILESPYVMMKKNHEMLEGNERYEGYCV     447
GluA3      WNEYERFVP-FSD-QQISNDSSSSENRTIVVTTILESPYVMYKKNHEQLEGNERYEGYCV     450
           *.  . :    ::    .. ... .*:: :******.***: **. : : **:*:****:
```

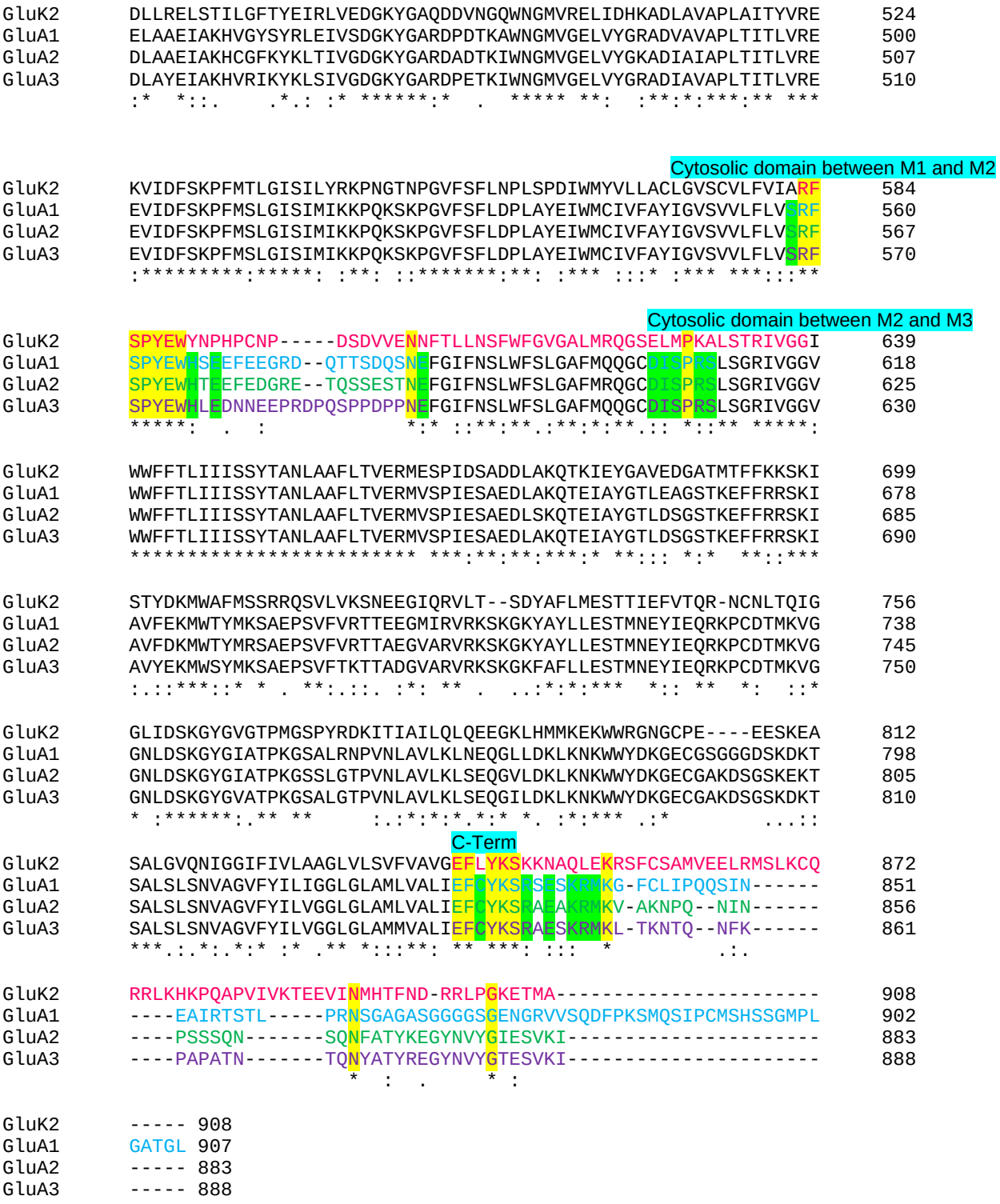

Figure 9. Multiple sequence alignment of GluK2, GluA1, GluA2, and GluA3

Amino acid sequence alignment of GluK2 (RefSeq: NP_062182.1), GluA1 (RefSeq: NP_113796.1), GluA2 (RefSeq: NP_058957.1), and GluA3 (RefSeq: NP_116785.2) using Clustal Omega (Goujon et al., 2010; Sievers et al., 2011). Sequences in cytosolic domains and C-termini are colored in pink (GluK2), light blue (GluA1), green (GluA2), or purple (GluA3). Common sequences in cytosolic domains and C-termini of all four proteins were highlighted in yellow and green highlighted amino acids are conserved in GluA1, GluA2, and GluA3, not in GluK2.

Chapter IV

Concluding Remarks

Neurotransmitters such as glutamate and GABA modulate neuronal activity via neurotransmitter receptors. Stimulation of neurotransmitter receptors initiates signaling pathways in neurons and function and surface expression of neurotransmitter receptors determine synaptic strength. In this respect, extensive researches have characterized the molecular details of activity and postsynaptic localization of AMPARs to understand the fast excitatory transmission and synaptic plasticity. Also, previous studies in the field have shown that AMPAR-interacting proteins regulate function and trafficking of AMPARs. My work suggested two interesting mechanisms of trafficking of AMPARs by investigating the role of transporters for NE (Chapter II) and the interaction of AMPAR with the L-type calcium channel, $Ca_V1.2$ (Chapter III).

In chapter II, I investigated the regulation of AMPAR trafficking by NE via intracellular β_2AR signaling. The important finding in this study is that NE can stimulate the intracellular β_2AR signaling after being transported into cytosol via OCT3 and PMAT, which shows how NE reaches intracellular β_2AR. Also, inhibition of OCT3 and PMAT impaired surface insertion of AMPARs. These findings can explain the molecular mechanisms of enhanced learning and memory by NE in emotional situations. Furthermore, understanding the transport of NE via OCT3 and PMAT for the regulation of AMPARs via intracellular β_2AR signaling will help to discover therapeutic targets for neuronal disorders such as ADHD and Alzheimer's disease.

Next, chapter III revealed the association of AMPAR and $Ca_V1.2$ which are key players in synaptic plasticity. Several co-IP experiments provided evidence of physical interaction of AMPAR GluA1, GluA2, and GluA3 subunits with $Ca_V1.2$ and I found that NE-induced surface expression of AMPARs requires activity of calcium channels.

Even though previous studies have shown the functional coupling of AMPAR and another L-type calcium channels, $Ca_V1.3$ and $Ca_V2.1$ (Kang et al., 2006; Martinez-Rivera et al., 2017), the molecular details of their association remained unclear. My findings suggested that physical association of AMPAR and $Ca_V1.2$, which could be via the direct binding to each other, mediates their functional coupling. Further studies are needed to determine their binding sites to scrutinize molecular mechanisms how activity of calcium channels, especially $Ca_V1.2$, affect the trafficking of AMPARs.

In conclusion, my research elucidates novel mechanisms of trafficking of AMPARs via NE-induced intracellular β_2AR signaling and L-type calcium channel, $Ca_V1.2$. I believe that my findings can answer questions about surface expression of AMPARs at postsynaptic sites and strategies to develop treatments for neuronal diseases.

Chapter V

Materials and Methods

Antibodies

Table A.1. Primary antibodies

Antigen	Host species	Source	Identifier	IB/IF Dilution	IP (µg)
$Ca_V1.2$	Rabbit	Johannes W Hell (Davare et al., 2000)	FP1	IB: 1:1,000 or 1:4,000	4µg
$Ca_V1.3$	Rabbit	Amy Lee at U. Iowa (Gregory et al., 2013)	AB144	IB: 1:200	2µg
GluA1-CT	Rabbit	Johannes W Hell (Joiner et al., 2010; Murphy et al., 2014; M. Zhang et al., 2013)	N/A	IB: (antiserum) 1:10,000 or 1:500,000	(purified antibody) 1µg
GluA1-NT	Rabbit	Calbiochem	PC246	IF: 1:100	N/A
GluA1	Mouse IgG_1	NeuroMab	clone N355/1	IB: (hybridoma culture supernatant) 1:500	N/A
GluA1 pS831	Rabbit	Johannes W Hell (M. Zhang et al., 2013)	N/A	IB: (antiserum) 1:50,000	N/A
GluA1 pS845	Rabbit	Johannes W Hell (Murphy et al., 2014; M. Zhang et al., 2013)	N/A	IB: (antiserum) 1:50,000	N/A
GluA2	Mouse IgG_1	NeuroMab	clone L21/32	IB: 1:500	N/A

GluA2	Rabbit	Robert Wenthold (Wenthold et al., 1992)	N/A	N/A	(anti-serum) 10µl
HA.11 16B12	Mouse IgG1	Covance	MMS-101P	IB: 1:100	N/A
PSD-95	Mouse IgG_{2a}	NeuroMab	clone K28/43	IF: 1:2,000	N/A
PSD-95	Mouse IgG_1	NeuroMab	clone K28/38.1	IB: 1:100	N/A
MAP2B	Mouse IgG_1	BD Transduction Laboratories™	610460, clone 18/MAP2B (RUO)	IF: 1:2,000	N/A
VPS35	Rabbit	Abcam	ab97545	IB: 1:200	N/A
SynDIG1	Mouse $IgG2_a$	NeuroMab	clone L42/17	IB: 1:1,000	N/A
SynDIG4	Mouse $IgG2_a$	NeuroMab	clone L102/45	IB: 1:1,000	N/A
Stargazin	Guinea-pig	Eunjoon Kim at KAIST, South Korea (Choi et al., 2002)	N/A	IB: 1:1,000	N/A
GluN2A	Rabbit	Upstate (Millipore)	06-313	IB: 1:1,000	N/A
α-tubulin	Mouse IgG_1	SantaCruz	sc-32293, clone DM1A	IB: 1:10,000	N/A

Table A. 2. Secondary antibodies and isotype control

Name	Host species	Source	Identifier	IB/IF Dilution	IP (µg)
Peroxidase IgG Fraction Monoclonal Mouse Anti-Rabbit IgG, Light Chain Specific	Mouse IgG_1	Jackson Immuno Research	211-032-171	IB: 1:10,000	N/A
Peroxidase AffiniPure Goat Anti-Mouse IgG, Light Chain Specific	Goat	JacksonImmuno Research	115-035-174	IB: 1:10,000	N/A
Alexa 488 - anti-mouse IgG2a	Goat	Invitrogen	A21131	IF: 1:1,000	N/A
Alexa 555 - anti-rabbit IgG	Goat	Invitrogen	A21428	IF: 1:1,000	N/A
Alexa 647- anti-mouse IgG1	Goat	Invitrogen	A21240	IF: 1:2,000	N/A
Rabbit IgG isotype control	Rabbit	Invitrogen	02-6102	N/A	1-4 µg*

* The rabbit IgG isotype control was used at the same amount as primary antibodies for immunoprecipitation.

DNA constructs

For immunoprecipitation studies with overexpressed proteins in HEK293 cells, various plasmids of $Ca_V1.2$ α1C subunit (Genbank ID: M67515.1) from different origins were transfected in HEK293 cells. A rat neuronal $Ca_V1.2$ α1C subunit construct with an HA tag in the S5-H5 extracellular loop of domain II (Green et al., 2007), which does not affect the properties of the channel (Altier et al., 2002), in pECFP-C1 vector (Clontech) was used (Tseng et al., 2017). Plasmids with human $Ca_V1.2$ α1C subunit from the brain ($hCa_V1.2$(18a)), the heart ($hCa_V1.2$(1a8a)), and smooth muscle ($hCa_V1.2$(9*/-33)) were provided by Tuck Wah Soong at National University of Singapore (Liao & Soong, 2010). A rat neuronal $Ca_V1.3$ α1D subunit construct (Genbank ID: AF370010.1) was a gift from Jörg Striessnig at Universität Innsbruck (Lieb et al., 2012). $Ca_V1.2$ α1C and $Ca_V1.3$ α1D subunits were transfected with rat β2a (Perez-Reyes et al., 1992) and rabbit α2δ subunits (Ellis et al., 1988) in pGWIH vector. Rat GluA1 with HA tag in pRK5 vector, rat GluA2 with HA tag in pRK vector, and rat GluK2 with HA tag in pRK vector are originally from Yael Stern-Bach at the Hebrew University of Jerusalem and subcloned and kindly provided by Elva Diaz at University of California, Davis (Ben-Yaacov et al., 2017; Matt et al., 2018). GluA3 in pCI-neo vector was also used for transfection. The origin of this plasmid was not traceable but the cDNA encoding GluA3 within this plasmid was confirmed by sequencing.

Reagents

Table B. Chemicals

Name	Source	CAS number
(±)-Norepinephrine (+)-bitartrate salt	Sigma-Aldrich	3414-63-9
Corticosterone	Sigma-Aldrich	50-22-6
Decynium 22	Tocris	977-96-8
Acros Organics™ Lopinavir, 98%	Fisher Scientific	192725-17-0
Desipramine hydrochloride	Tocris	58-28-6
Sotalol hydrochloride	Tocris	959-24-0
(−)-Isoproterenol hydrochloride	Sigma-Aldrich	5984-95-2
Isradipine	Tocris	75695-93-1

Table C. Protease and phosphatase inhibitors

Name	Source	CAS number
Protease inhibitors		
phenylmethanesulfonyl fluorid (PMSF)	Sigma-Aldrich	329-98-6
Pepstatin A	Merck Millipore	26305-03-3
Leupeptin	Merck Millipore	103476-89-7
Aprotinin	Merck Millipore	9087-70-1
Phosphatase inhibitors		
Sodium fluoride	Sigma-Aldrich	7681-49-4
Sodium pyrophosphate	Fisher Scientific	13472-36-1
p-nitrophenyl phosphate	Sigma-Aldrich	68189-42-4
Microcystin LR	Calbiochem	101043-37-2

Animals

C57BL/6 wild-type (WT) and OCT3 knockout (KO) mice which were used to analyze phosphorylation of GluA1 were 3–20 week old. Primary hippocampal neuron culture was prepared with E17-19 embryonic Sprague-Dawley rats. All procedures involving animals followed the guidelines for the Care and Use of Laboratory Animals of the National Institutes of Health and had been approved by the Institutional Animal Care and Use Committees (IACUC) at the University of California, Davis.

Preparation of mouse forebrain slices and drug treatment

3–20 week-old C57BL/6 mice were used to test the effect of norepinephrine on phosphorylation of GluA1. After decapitation, the brain was quickly removed from the mouse, placed in the slicing chamber, and submerged in ice-cold slicing buffer (in mM: 10 NaCl, 230 Sucrose, 25.6 $NHCO_3$, 1.2 NaH_2PO_4, 2.5 KCl, 1 $CaCl_2$, 1.3 $MgCl_2$, 10 D-Glucose, saturated with 5% O_2 and 5% CO_2). Slices (400 μm thick) were sectioned by a vibrating microtome (VT1000S, Leica Microsystems, Nussloch, Germany) and transferred to a preincubation chamber with artificial cerebrospinal fluid (ACSF; in mM: 126 NaCl, 25.6 $NHCO_3$, 1.2 NaH_2PO_4, 2.5 KCl, 1 $CaCl_2$, 1,3 $MgCl_2$, 10 D-Glucose, saturated with 95% CO_2 and 5% O_2). The slices were recovered for 1 h at 32 °C before treated with drugs (Y. Lu et al., 2007).

After the recovery period, slices were pre-incubated with vehicle (water or DMSO) or inhibitors, 100 nM of D22, 10 μM of CORT, 10 μM of LOPI, 1 μM of DESI, or 100 μM of

Sotalol for 5 min and then treated with 1 μM of NE with or without inhibitors for 10 min. All drugs were prepared in oxygen-saturated and warm ACSF.

Transfection of HEK293 cells

HEK293 cells were cultured in DMEM-10 (Dulbecco's modified Eagle's medium, Life Technologies) containing 10% fetal bovine serum (FBS, Corning), 1mM Sodium pyruvate, and 1% penicillin/streptomycin at 37 °C in humidified incubators injected with 5% CO_2 and 95% air. HEK293 cells were plated on 100 mm culture dishes. In order to express $Ca_V1.2$, GluA1, GluA2, or GluK2, DNA constructs were transfected in HEK293 cells using calcium phosphate solution or JetPRIME® transfection reagent (Polyplus transfection®, Illkirch, France). $Ca_V1.2$ $\alpha_1 1.2$ subunit is transfected with α2δ and β2a subunits in 1:1:1 ratio.

HEK293 cells grew to 50% confluency at the time of the transfection. 20 μg of DNA constructs were mixed with 50 μl of 2.5 M $CaCl_2$ and sterile water up to 500 μl then 500 μl of HeBS buffer (50 mM HEPES (free acid), 280 mM NaCl, 1.5 mM $Na_2HPO_4 \cdot 7H_2O$, pH 7.11) was added with aerating. The DNA-Calcium phosphate mixture was incubated at room temperature (RT) for 10 min and added to HEK293 cell culture. After 6-7 hour incubation, the media was changed (Jordan et al., 1996; Senatore et al., 2011; Tseng et al., 2017).

JetPRIME® reagent was used as the manufacturer recommended. DNA constructs and JetPRIME® buffer were mixed and JetPRIME® reagent was added (DNA/JetPRIME®

reagent ratio: 1:2). The mixture was incubated at RT for 10 min and applied to the cell culture. Cells were harvested after 24 hours.

Immunoprecipitation (IP) and immunoblotting (IB)

Immunoprecipitation and immunoblotting procedures were described previously (Hall et al., 2007; Hall et al., 2006; Hell et al., 1993).

Mouse forebrain slices and mouse whole brain were lysed in ice-cold 1% Triton X-100 solubilization buffer (in mM; 50 Tris-Cl, pH 7.4, 150 NaCl, 5 EGTA, pH 7.4, 10 EDTA) with protease inhibitors (200 nM phenylmethanesulfonyl fluorid (PMSF), 1 µg/mL pepstatin A, 10 µg/mL leupeptin, and 20 µg/mL aprotinin) and phosphatase inhibitors (25 mM sodium fluoride, 25 mM sodium pyrophosphate, 1 mM p-nitrophenyl phosphate and 4 µM microcystin LR). HEK293 cells were also homogenized in the same ice-cold 1% Triton X-100 buffer without NaCl containing all protease inhibitors. Insolubilized materials was removed by ultracentrifugation (40,000 rpm for 30 min at 4°C).

1 µg of anti-GluA1 antibody, 10 µl of GluA2 antiserum, 4 µg of anti-$Ca_V1.2$ antibody (FP1), or 2 µg of anti-$Ca_V1.3$ antibody was immobilized to 30 µl of protein A Sepharose or protein G Sepharose beads (1:1 mixture of resin and tris buffered saline (TBS)) for immunoprecipitation (IP). The same amount of non-specific IgG isotype control (Invitrogen) was used as a negative control. Triton X-100 extracts were incubated with antibody-bead mixture for 4 hours at 4°C and washed with ice-cold three different IP wash buffers (Table D). IP samples were heated for 15 min at 65°C in the 1.5x SDS-PAGE protein sample buffer (0.09 g/mL SDS, 150 mM Tris-HCl, 0.3 g/mL sucrose, 8.52 mg/mL

DTT, 0.12 mg/mL bromophenol blue) for complete denaturation, separated by SDS-PAGE, transferred onto 0.2 µm polyvinylidene fluoride (PVDF) membranes (BioRad) at 50 V for 600 min in the wet transfer chamber. Input lysate samples were prepared for immunoblotting as IP samples were. The PVDF membrane was blocked by 3% bovine serum albumin (BSA) in TBS with 0.1% tween 20 (TBST) followed by incubation with primary antibodies at RT for 3 hours or at 4°C overnight and with HRP-conjugated secondary antibodies at RT for 1 hour (antibodies and their dilution factors are listed in table A .1 and 2). Immunosignals were detected using chemiluminescent peroxidase substrate (Luminata™ Western HRP Substrate, classico and crescendo (Merck Millipore) and SuperSignal™ West Femto Maximum Sensitivity Substrate (Thermo Fisher Scientific)). When sequential probing was required, the membrane was stripped by incubation with a stripping buffer (15 g/L Glycine, 1 g/L SDS, 10 % Tween 20, pH 2.2) at 55°C for 20 min. Immunoblotting bands were quantified with densitometry using ImageJ software.

Table D. Recipe for IP wash buffers

	Low salt buffer	High salt buffer	10 mM Tris-HCl buffer
Triton X-100	1%	N/A	N/A
NaCl	150 mM	750 mM	N/A
Tris-HCl, pH7.4	10 mM	10 mM	10 mM
EGTA, pH7.4	5 mM	5 mM	5 mM
EDTA	5 mM	5 mM	5 mM

Primary hippocampal cultures

All procedures to prepare hippocampal neuron culture was previously described (C. Y. Chen et al., 2014; Y. Chen et al., 2008; Y. Zhang et al., 2014). Hippocampi was dissected from E17-19 embryonic rats (Sprague-Dawley, Charles River Laboratories). Isolated hippocampi was treated with 0.5mg/ml papain (Roche, Basel, Switzerland) in Hibernate E medium (Gibco) at 37°C for 30 min, washed with Hibernate E medium and the plating media (2% B27 (Gibco) or N21 (R&D systems), 10% horse serum (Geminibio), 10 mM HEPES (Gibco), and 1% Glutamax (Gibco) in Neurobasal medium (Gibco)), and dissociated by a constricted Pasteur pipet. Dissociated neurons in the plating media were seeded on the coverslips coated with 0.1% (w/v) poly-L-lysine. The plating media was replaced with the growth media (2% B27 (Gibco) or N21 (R&D systems) and Glutamax (Gibco) in Neurobasal medium (Gibco)) in four hours. The neurons were ready for the drug treatment in 21 days.

Immunofluorescence (IF)

21 DIV neurons were pre-treated with vehicle (water or DMSO) or inhibitors of OCT3 or PMAT, 100 nM of D22, 10 μM of CORT, or 10 μM of LOPI for 5 min and then treated with 1μM of NE with or without inhibitors for 10 min. All drugs were prepared in neuron conditioned media. After the drug incubation, neuron culture was fixed with 4% paraformaldehyde (PFA) and 4% (w/v) sucrose solution at RT for 5 min, washed with phosphate buffered saline (PBS), and incubated with the blocking buffer (2% glycerol, 2% normal goat serum (Jackson Immuno Research), 5% fetal bovine serum (Corning), 50

mM NH_4Cl in PBS) at RT for 1 hour. In order to stain surface expressed GluA1, anti-GluA1 N-terminus antibody was applied to the neuron culture at 4°C for 2 hours. After washing with PBS for 10 min three times, neurons were permeabilized with 0.25% Triton X-100 containing PBS at RT for 8 min. Antibodies against intracellular proteins, PSD-95 and MAP2B were incubated at RT for 2 hours after blocking at RT for 2 hours. Then, neurons were washed with 0.1% Triton X-100 containing PBS, incubated with blocking buffer at RT for 45 min, and labelled with fluorophore-conjugated secondary antibodies at RT for 2 hours. Antibodies and the dilution factor used for staining was listed in table A. 1 and 2. Coverslips were mounted onto microscope slides with the mounting solution (Mountant, PermaFluor, ThermoScientific) after washing with 0.1% Triton X-100 containing PBS, PBS, and H_2O. Images were acquired by a Leica SP2 confocal microscope.

Statistical analysis

Data are expressed as means ± standard error of the mean (SEM) and analyzed with Excel (Microsoft Corp.) and GraphPad Prism software (GraphPad, San Diego, CA). For normally distributed data, the one-way ANOVA test was used to analyze the statistical difference between more than two different conditions followed by Tukey's or uncorrected Fisher's LSD post-hoc test which compare two different samples. For the nonparametric data, the Kruskal-Wallis test and Dunn's multiple comparison test were used. When the P value is lower than 0.05, data is considered significantly different and the significance is represented by asterisks (*) in figures (*$p<0.05$, **$p<0.01$, ***$p<0.001$).

References

Akamatsu, M., Yamashita, T., Hirose, N., Teramoto, S., & Kwak, S. (2016). The AMPA receptor antagonist perampanel robustly rescues amyotrophic lateral sclerosis (ALS) pathology in sporadic ALS model mice. *Sci Rep, 6*, 28649. doi:10.1038/srep28649

Altier, C., Dubel, S. J., Barrere, C., Jarvis, S. E., Stotz, S. C., Spaetgens, R. L., . . . Bourinet, E. (2002). Trafficking of L-type calcium channels mediated by the postsynaptic scaffolding protein AKAP79. *J Biol Chem, 277*(37), 33598-33603. doi:10.1074/jbc.M202476200

Anggono, V., & Huganir, R. L. (2012). Regulation of AMPA receptor trafficking and synaptic plasticity. *Curr Opin Neurobiol, 22*(3), 461-469. doi:10.1016/j.conb.2011.12.006

Baker, J. G. (2005). The selectivity of beta-adrenoceptor antagonists at the human beta1, beta2 and beta3 adrenoceptors. *Br J Pharmacol, 144*(3), 317-322. doi:10.1038/sj.bjp.0706048

Banke, T. G., Bowie, D., Lee, H., Huganir, R. L., Schousboe, A., & Traynelis, S. F. (2000). Control of GluR1 AMPA receptor function by cAMP-dependent protein kinase. *J Neurosci, 20*(1), 89-102.

Barria, A., Derkach, V., & Soderling, T. (1997). Identification of the Ca2+/calmodulin-dependent protein kinase II regulatory phosphorylation site in the alpha-amino-3-hydroxyl-5-methyl-4-isoxazole-propionate-type glutamate receptor. *J Biol Chem, 272*(52), 32727-32730. doi:10.1074/jbc.272.52.32727

Bats, C., Groc, L., & Choquet, D. (2007). The interaction between Stargazin and PSD-95 regulates AMPA receptor surface trafficking. *Neuron, 53*(5), 719-734. doi:10.1016/j.neuron.2007.01.030

Beique, J. C., & Andrade, R. (2003). PSD-95 regulates synaptic transmission and plasticity in rat cerebral cortex. *J Physiol, 546*(Pt 3), 859-867. doi:10.1113/jphysiol.2002.031369

Ben-Yaacov, A., Gillor, M., Haham, T., Parsai, A., Qneibi, M., & Stern-Bach, Y. (2017). Molecular Mechanism of AMPA Receptor Modulation by TARP/Stargazin. *Neuron, 93*(5), 1126-1137 e1124. doi:10.1016/j.neuron.2017.01.032

Berridge, M. J. (1998). Neuronal calcium signaling. *Neuron, 21*(1), 13-26. doi:10.1016/s0896-6273(00)80510-3

Bhattacharyya, S., Biou, V., Xu, W., Schluter, O., & Malenka, R. C. (2009). A critical role for PSD-95/AKAP interactions in endocytosis of synaptic AMPA receptors. *Nat Neurosci, 12*(2), 172-181. doi:10.1038/nn.2249

Bissen, D., Foss, F., & Acker-Palmer, A. (2019). AMPA receptors and their minions: auxiliary proteins in AMPA receptor trafficking. *Cell Mol Life Sci, 76*(11), 2133-2169. doi:10.1007/s00018-019-03068-7

Bochain, A., Estey, L., Haronian, G., Reale, M., Rojas, C., & Cramer, J. (1981). Determination of catecholamine permeability coefficients for passive diffusion across phospholipid vesicle membranes. *J Membr Biol, 60*(1), 73-76. doi:10.1007/BF01870834

Bolshakov, V. Y., & Siegelbaum, S. A. (1994). Postsynaptic induction and presynaptic expression of hippocampal long-term depression. *Science, 264*(5162), 1148-1152. doi:10.1126/science.7909958

Boudkkazi, S., Brechet, A., Schwenk, J., & Fakler, B. (2014). Cornichon2 dictates the time course of excitatory transmission at individual hippocampal synapses. *Neuron, 82*(4), 848-858. doi:10.1016/j.neuron.2014.03.031

Bowen, A. B., Bourke, A. M., Hiester, B. G., Hanus, C., & Kennedy, M. J. (2017). Golgi-independent secretory trafficking through recycling endosomes in neuronal dendrites and spines. *Elife, 6*. doi:10.7554/eLife.27362

Brini, M., Cali, T., Ottolini, D., & Carafoli, E. (2014). Neuronal calcium signaling: function and dysfunction. *Cell Mol Life Sci, 71*(15), 2787-2814. doi:10.1007/s00018-013-1550-7

Buonarati, O. R., Hammes, E. A., Watson, J. F., Greger, I. H., & Hell, J. W. (2019). Mechanisms of postsynaptic localization of AMPA-type glutamate receptors and their regulation during long-term potentiation. *Sci Signal, 12*(562). doi:10.1126/scisignal.aar6889

Bymaster, F. P., Katner, J. S., Nelson, D. L., Hemrick-Luecke, S. K., Threlkeld, P. G., Heiligenstein, J. H., . . . Perry, K. W. (2002). Atomoxetine increases extracellular levels of norepinephrine and dopamine in prefrontal cortex of rat: a potential mechanism for efficacy in attention deficit/hyperactivity disorder. *Neuropsychopharmacology, 27*(5), 699-711. doi:10.1016/S0893-133X(02)00346-9

Calin-Jageman, I., & Lee, A. (2008). Ca(v)1 L-type Ca2+ channel signaling complexes in neurons. *J Neurochem, 105*(3), 573-583. doi:10.1111/j.1471-4159.2008.05286.x

Catterall, W. A. (2011). Voltage-gated calcium channels. *Cold Spring Harb Perspect Biol, 3*(8), a003947. doi:10.1101/cshperspect.a003947

Catterall, W. A., Perez-Reyes, E., Snutch, T. P., & Striessnig, J. (2005). International Union of Pharmacology. XLVIII. Nomenclature and structure-function relationships of voltage-gated calcium channels. *Pharmacol Rev, 57*(4), 411-425. doi:10.1124/pr.57.4.5

Chang, P. K., Verbich, D., & McKinney, R. A. (2012). AMPA receptors as drug targets in neurological disease--advantages, caveats, and future outlook. *Eur J Neurosci, 35*(12), 1908-1916. doi:10.1111/j.1460-9568.2012.08165.x

Chao, S. Z., Lu, W., Lee, H. K., Huganir, R. L., & Wolf, M. E. (2002). D(1) dopamine receptor stimulation increases GluR1 phosphorylation in postnatal nucleus accumbens cultures. *J Neurochem, 81*(5), 984-992. doi:10.1046/j.1471-4159.2002.00877.x

Chen, C. Y., Matt, L., Hell, J. W., & Rogawski, M. A. (2014). Perampanel inhibition of AMPA receptor currents in cultured hippocampal neurons. *PLoS One, 9*(9), e108021. doi:10.1371/journal.pone.0108021

Chen, L., Chetkovich, D. M., Petralia, R. S., Sweeney, N. T., Kawasaki, Y., Wenthold, R. J., . . . Nicoll, R. A. (2000). Stargazin regulates synaptic targeting of AMPA receptors by two distinct mechanisms. *Nature, 408*(6815), 936-943. doi:10.1038/35050030

Chen, M. L., & Yu, L. (2009). The use of drug metabolism for prediction of intestinal permeability (dagger). *Mol Pharm, 6*(1), 74-81. doi:10.1021/mp8001864

Chen, X., Levy, J. M., Hou, A., Winters, C., Azzam, R., Sousa, A. A., . . . Reese, T. S. (2015). PSD-95 family MAGUKs are essential for anchoring AMPA and NMDA receptor complexes at the postsynaptic density. *Proc Natl Acad Sci U S A, 112*(50), E6983-6992. doi:10.1073/pnas.1517045112

Chen, Y., Stevens, B., Chang, J., Milbrandt, J., Barres, B. A., & Hell, J. W. (2008). NS21: re-defined and modified supplement B27 for neuronal cultures. *J Neurosci Methods, 171*(2), 239-247. doi:10.1016/j.jneumeth.2008.03.013

Choi, J., Ko, J., Park, E., Lee, J. R., Yoon, J., Lim, S., & Kim, E. (2002). Phosphorylation of stargazin by protein kinase A regulates its interaction with PSD-95. *J Biol Chem, 277*(14), 12359-12363. doi:10.1074/jbc.M200528200

Choquet, D. (2018). Linking Nanoscale Dynamics of AMPA Receptor Organization to Plasticity of Excitatory Synapses and Learning. *J Neurosci, 38*(44), 9318-9329. doi:10.1523/JNEUROSCI.2119-18.2018

Choy, R. W., Park, M., Temkin, P., Herring, B. E., Marley, A., Nicoll, R. A., & von Zastrow, M. (2014). Retromer mediates a discrete route of local membrane delivery to dendrites. *Neuron, 82*(1), 55-62. doi:10.1016/j.neuron.2014.02.018

Citri, A., & Malenka, R. C. (2008). Synaptic plasticity: multiple forms, functions, and mechanisms. *Neuropsychopharmacology, 33*(1), 18-41. doi:10.1038/sj.npp.1301559

Colledge, M., Dean, R. A., Scott, G. K., Langeberg, L. K., Huganir, R. L., & Scott, J. D. (2000). Targeting of PKA to glutamate receptors through a MAGUK-AKAP complex. *Neuron, 27*(1), 107-119. doi:10.1016/s0896-6273(00)00013-1

Courousse, T., & Gautron, S. (2015). Role of organic cation transporters (OCTs) in the brain. *Pharmacol Ther, 146*, 94-103. doi:10.1016/j.pharmthera.2014.09.008

Craig, A. M., Blackstone, C. D., Huganir, R. L., & Banker, G. (1993). The distribution of glutamate receptors in cultured rat hippocampal neurons: postsynaptic clustering of AMPA-selective subunits. *Neuron, 10*(6), 1055-1068. doi:10.1016/0896-6273(93)90054-u

Dahlin, A., Xia, L., Kong, W., Hevner, R., & Wang, J. (2007). Expression and immunolocalization of the plasma membrane monoamine transporter in the brain. *Neuroscience, 146*(3), 1193-1211. doi:10.1016/j.neuroscience.2007.01.072

Davare, M. A., Avdonin, V., Hall, D. D., Peden, E. M., Burette, A., Weinberg, R. J., . . . Hell, J. W. (2001). A beta2 adrenergic receptor signaling complex assembled with the Ca2+ channel Cav1.2. *Science, 293*(5527), 98-101. doi:10.1126/science.293.5527.98

Davare, M. A., Dong, F., Rubin, C. S., & Hell, J. W. (1999). The A-kinase anchor protein MAP2B and cAMP-dependent protein kinase are associated with class C L-type calcium channels in neurons. *J Biol Chem, 274*(42), 30280-30287. doi:10.1074/jbc.274.42.30280

Davare, M. A., Horne, M. C., & Hell, J. W. (2000). Protein phosphatase 2A is associated with class C L-type calcium channels (Cav1.2) and antagonizes channel phosphorylation by cAMP-dependent protein kinase. *J Biol Chem, 275*(50), 39710-39717. doi:10.1074/jbc.M005462200

De Jongh, K. S., Murphy, B. J., Colvin, A. A., Hell, J. W., Takahashi, M., & Catterall, W. A. (1996). Specific phosphorylation of a site in the full-length form of the alpha 1 subunit of the cardiac L-type calcium channel by adenosine 3',5'-cyclic monophosphate-dependent protein kinase. *Biochemistry, 35*(32), 10392-10402. doi:10.1021/bi953023c

Dhuriya, Y. K., & Sharma, D. (2020). Neuronal Plasticity: Neuronal Organization is Associated with Neurological Disorders. *J Mol Neurosci, 70*(11), 1684-1701. doi:10.1007/s12031-020-01555-2

Di Biase, V., Tuluc, P., Campiglio, M., Obermair, G. J., Heine, M., & Flucher, B. E. (2011). Surface traffic of dendritic CaV1.2 calcium channels in hippocampal neurons. *J Neurosci, 31*(38), 13682-13694. doi:10.1523/JNEUROSCI.2300-11.2011

Diaz, E., Ge, Y., Yang, Y. H., Loh, K. C., Serafini, T. A., Okazaki, Y., . . . Scheiffele, P. (2002). Molecular analysis of gene expression in the developing pontocerebellar projection system. *Neuron, 36*(3), 417-434. doi:10.1016/s0896-6273(02)01016-4

Diering, G. H., & Huganir, R. L. (2018). The AMPA Receptor Code of Synaptic Plasticity. *Neuron, 100*(2), 314-329. doi:10.1016/j.neuron.2018.10.018

Doggrell, S. A., & Brown, L. (2000). D-Sotalol: death by the SWORD or deserving of further consideration for clinical use? *Expert Opin Investig Drugs, 9*(7), 1625-1634. doi:10.1517/13543784.9.7.1625

Dolphin, A. C. (2016). Voltage-gated calcium channels and their auxiliary subunits: physiology and pathophysiology and pharmacology. *J Physiol, 594*(19), 5369-5390. doi:10.1113/JP272262

Dolphin, A. C., & Lee, A. (2020). Presynaptic calcium channels: specialized control of synaptic neurotransmitter release. *Nat Rev Neurosci, 21*(4), 213-229. doi:10.1038/s41583-020-0278-2

Duan, H., Hu, T., Foti, R. S., Pan, Y., Swaan, P. W., & Wang, J. (2015). Potent and Selective Inhibition of Plasma Membrane Monoamine Transporter by HIV Protease Inhibitors. *Drug Metab Dispos, 43*(11), 1773-1780. doi:10.1124/dmd.115.064824

Duan, H., & Wang, J. (2010). Selective transport of monoamine neurotransmitters by human plasma membrane monoamine transporter and organic cation transporter 3. *J Pharmacol Exp Ther, 335*(3), 743-753. doi:10.1124/jpet.110.170142

Efendiev, R., Samelson, B. K., Nguyen, B. T., Phatarpekar, P. V., Baameur, F., Scott, J. D., & Dessauer, C. W. (2010). AKAP79 interacts with multiple adenylyl cyclase (AC) isoforms

and scaffolds AC5 and -6 to alpha-amino-3-hydroxyl-5-methyl-4-isoxazole-propionate (AMPA) receptors. *J Biol Chem, 285*(19), 14450-14458. doi:10.1074/jbc.M110.109769

Eisenhofer, G. (2001). The role of neuronal and extraneuronal plasma membrane transporters in the inactivation of peripheral catecholamines. *Pharmacol Ther, 91*(1), 35-62. doi:10.1016/s0163-7258(01)00144-9

El-Husseini, A. E., Schnell, E., Chetkovich, D. M., Nicoll, R. A., & Bredt, D. S. (2000). PSD-95 involvement in maturation of excitatory synapses. *Science, 290*(5495), 1364-1368.

Elias, G. M., Funke, L., Stein, V., Grant, S. G., Bredt, D. S., & Nicoll, R. A. (2006). Synapse-specific and developmentally regulated targeting of AMPA receptors by a family of MAGUK scaffolding proteins. *Neuron, 52*(2), 307-320. doi:10.1016/j.neuron.2006.09.012

Ellis, S. B., Williams, M. E., Ways, N. R., Brenner, R., Sharp, A. H., Leung, A. T., . . . et al. (1988). Sequence and expression of mRNAs encoding the alpha 1 and alpha 2 subunits of a DHP-sensitive calcium channel. *Science, 241*(4873), 1661-1664. doi:10.1126/science.2458626

Engel, K., & Wang, J. (2005). Interaction of organic cations with a newly identified plasma membrane monoamine transporter. *Mol Pharmacol, 68*(5), 1397-1407. doi:10.1124/mol.105.016832

Engel, K., Zhou, M., & Wang, J. (2004). Identification and characterization of a novel monoamine transporter in the human brain. *J Biol Chem, 279*(48), 50042-50049. doi:10.1074/jbc.M407913200

Ertel, E. A., Campbell, K. P., Harpold, M. M., Hofmann, F., Mori, Y., Perez-Reyes, E., . . . Catterall, W. A. (2000). Nomenclature of voltage-gated calcium channels. *Neuron, 25*(3), 533-535. doi:10.1016/s0896-6273(00)81057-0

Esteban, J. A., Shi, S. H., Wilson, C., Nuriya, M., Huganir, R. L., & Malinow, R. (2003). PKA phosphorylation of AMPA receptor subunits controls synaptic trafficking underlying plasticity. *Nat Neurosci, 6*(2), 136-143.

Frampton, J. E. (2015). Perampanel: A Review in Drug-Resistant Epilepsy. *Drugs, 75*(14), 1657-1668. doi:10.1007/s40265-015-0465-z

Friedman, J. I., Adler, D. N., & Davis, K. L. (1999). The role of norepinephrine in the pathophysiology of cognitive disorders: potential applications to the treatment of cognitive dysfunction in schizophrenia and Alzheimer's disease. *Biol Psychiatry, 46*(9), 1243-1252. doi:10.1016/s0006-3223(99)00232-2

Fuller, M. D., Emrick, M. A., Sadilek, M., Scheuer, T., & Catterall, W. A. (2010). Molecular mechanism of calcium channel regulation in the fight-or-flight response. *Sci Signal, 3*(141), ra70. doi:10.1126/scisignal.2001152

Funck-Brentano, C. (1993). Pharmacokinetic and pharmacodynamic profiles of d-sotalol and d,l-sotalol. *Eur Heart J, 14 Suppl H*, 30-35. doi:10.1093/eurheartj/14.suppl_h.30

Gannon, M., Che, P., Chen, Y., Jiao, K., Roberson, E. D., & Wang, Q. (2015). Noradrenergic dysfunction in Alzheimer's disease. *Front Neurosci, 9*, 220. doi:10.3389/fnins.2015.00220

Gasser, P. J. (2019). Roles for the uptake2 transporter OCT3 in regulation of dopaminergic neurotransmission and behavior. *Neurochem Int, 123*, 46-49. doi:10.1016/j.neuint.2018.07.008

Gasser, P. J., Hurley, M. M., Chan, J., & Pickel, V. M. (2017). Organic cation transporter 3 (OCT3) is localized to intracellular and surface membranes in select glial and neuronal cells within the basolateral amygdaloid complex of both rats and mice. *Brain Struct Funct, 222*(4), 1913-1928. doi:10.1007/s00429-016-1315-9

Gasser, P. J., Orchinik, M., Raju, I., & Lowry, C. A. (2009). Distribution of organic cation transporter 3, a corticosterone-sensitive monoamine transporter, in the rat brain. *J Comp Neurol, 512*(4), 529-555. doi:10.1002/cne.21921

Ge, Y., Tian, M., Liu, L., Wong, T. P., Gong, B., Wu, D., . . . Wang, Y. T. (2019). p97 regulates GluA1 homomeric AMPA receptor formation and plasma membrane expression. *Nat Commun, 10*(1), 4089. doi:10.1038/s41467-019-12096-7

Goujon, M., McWilliam, H., Li, W., Valentin, F., Squizzato, S., Paern, J., & Lopez, R. (2010). A new bioinformatics analysis tools framework at EMBL-EBI. *Nucleic Acids Res, 38*(Web Server issue), W695-699. doi:10.1093/nar/gkq313

Green, E. M., Barrett, C. F., Bultynck, G., Shamah, S. M., & Dolmetsch, R. E. (2007). The tumor suppressor eIF3e mediates calcium-dependent internalization of the L-type calcium channel CaV1.2. *Neuron, 55*(4), 615-632. doi:10.1016/j.neuron.2007.07.024

Greger, I. H., Watson, J. F., & Cull-Candy, S. G. (2017). Structural and Functional Architecture of AMPA-Type Glutamate Receptors and Their Auxiliary Proteins. *Neuron, 94*(4), 713-730. doi:10.1016/j.neuron.2017.04.009

Gregory, F. D., Pangrsic, T., Calin-Jageman, I. E., Moser, T., & Lee, A. (2013). Harmonin enhances voltage-dependent facilitation of Cav1.3 channels and synchronous exocytosis in mouse inner hair cells. *J Physiol, 591*(13), 3253-3269. doi:10.1113/jphysiol.2013.254367

Groc, L., & Choquet, D. (2020). Linking glutamate receptor movements and synapse function. *Science, 368*(6496). doi:10.1126/science.aay4631

Grover, L. M., & Teyler, T. J. (1990). Two components of long-term potentiation induced by different patterns of afferent activation. *Nature, 347*(6292), 477-479. doi:10.1038/347477a0

Grundemann, D., Schechinger, B., Rappold, G. A., & Schomig, E. (1998). Molecular identification of the corticosterone-sensitive extraneuronal catecholamine transporter. *Nat Neurosci, 1*(5), 349-351. doi:10.1038/1557

Hall, D. D., Davare, M. A., Shi, M., Allen, M. L., Weisenhaus, M., McKnight, G. S., & Hell, J. W. (2007). Critical role of cAMP-dependent protein kinase anchoring to the L-type calcium

channel Cav1.2 via A-kinase anchor protein 150 in neurons. *Biochemistry, 46*(6), 1635-1646. doi:10.1021/bi062217x

Hall, D. D., Feekes, J. A., Arachchige Don, A. S., Shi, M., Hamid, J., Chen, L., . . . Hell, J. W. (2006). Binding of protein phosphatase 2A to the L-type calcium channel Cav1.2 next to Ser1928, its main PKA site, is critical for Ser1928 dephosphorylation. *Biochemistry, 45*(10), 3448-3459. doi:10.1021/bi051593z

Han, D., Xue, X., Yan, Y., & Li, G. (2019). Dysfunctional Cav1.2 channel in Timothy syndrome, from cell to bedside. *Exp Biol Med (Maywood), 244*(12), 960-971. doi:10.1177/1535370219863149

Hayer-Zillgen, M., Bruss, M., & Bonisch, H. (2002). Expression and pharmacological profile of the human organic cation transporters hOCT1, hOCT2 and hOCT3. *Br J Pharmacol, 136*(6), 829-836. doi:10.1038/sj.bjp.0704785

He, K., Song, L., Cummings, L. W., Goldman, J., Huganir, R. L., & Lee, H. K. (2009). Stabilization of Ca2+-permeable AMPA receptors at perisynaptic sites by GluR1-S845 phosphorylation. *Proc Natl Acad Sci U S A, 106*(47), 20033-20038. doi:10.1073/pnas.0910338106

Hell, J. W., Westenbroek, R. E., Breeze, L. J., Wang, K. K., Chavkin, C., & Catterall, W. A. (1996). N-methyl-D-aspartate receptor-induced proteolytic conversion of postsynaptic class C L-type calcium channels in hippocampal neurons. *Proc Natl Acad Sci U S A, 93*(8), 3362-3367. doi:10.1073/pnas.93.8.3362

Hell, J. W., Westenbroek, R. E., Warner, C., Ahlijanian, M. K., Prystay, W., Gilbert, M. M., . . . Catterall, W. A. (1993). Identification and differential subcellular localization of the neuronal class C and class D L-type calcium channel alpha 1 subunits. *J Cell Biol, 123*(4), 949-962. doi:10.1083/jcb.123.4.949

Henley, J. M., & Wilkinson, K. A. (2013). AMPA receptor trafficking and the mechanisms underlying synaptic plasticity and cognitive aging. *Dialogues Clin Neurosci, 15*(1), 11-27.

Henley, J. M., & Wilkinson, K. A. (2016). Synaptic AMPA receptor composition in development, plasticity and disease. *Nat Rev Neurosci, 17*(6), 337-350. doi:10.1038/nrn.2016.37

Herring, B. E., & Nicoll, R. A. (2016). Long-Term Potentiation: From CaMKII to AMPA Receptor Trafficking. *Annu Rev Physiol, 78*, 351-365. doi:10.1146/annurev-physiol-021014-071753

Herring, B. E., Shi, Y., Suh, Y. H., Zheng, C. Y., Blankenship, S. M., Roche, K. W., & Nicoll, R. A. (2013). Cornichon proteins determine the subunit composition of synaptic AMPA receptors. *Neuron, 77*(6), 1083-1096. doi:10.1016/j.neuron.2013.01.017

Hiester, B. G., Bourke, A. M., Sinnen, B. L., Cook, S. G., Gibson, E. S., Smith, K. R., & Kennedy, M. J. (2017). L-Type Voltage-Gated Ca(2+) Channels Regulate Synaptic-Activity-Triggered Recycling Endosome Fusion in Neuronal Dendrites. *Cell Rep, 21*(8), 2134-2146. doi:10.1016/j.celrep.2017.10.105

Hill, J. E., Makky, K., Shrestha, L., Hillard, C. J., & Gasser, P. J. (2011). Natural and synthetic corticosteroids inhibit uptake 2-mediated transport in CNS neurons. *Physiol Behav, 104*(2), 306-311. doi:10.1016/j.physbeh.2010.11.012

Hill, S. J., Williams, C., & May, L. T. (2010). Insights into GPCR pharmacology from the measurement of changes in intracellular cyclic AMP; advantages and pitfalls of differing methodologies. *Br J Pharmacol, 161*(6), 1266-1275. doi:10.1111/j.1476-5381.2010.00779.x

Howard, M. A., Elias, G. M., Elias, L. A., Swat, W., & Nicoll, R. A. (2010). The role of SAP97 in synaptic glutamate receptor dynamics. *Proc Natl Acad Sci U S A, 107*(8), 3805-3810. doi:10.1073/pnas.0914422107

Huganir, R. L., & Nicoll, R. A. (2013). AMPARs and synaptic plasticity: the last 25 years. *Neuron, 80*(3), 704-717. doi:10.1016/j.neuron.2013.10.025

Hussain, N. K., Diering, G. H., Sole, J., Anggono, V., & Huganir, R. L. (2014). Sorting Nexin 27 regulates basal and activity-dependent trafficking of AMPARs. *Proc Natl Acad Sci U S A, 111*(32), 11840-11845. doi:10.1073/pnas.1412415111

Irannejad, R., Pessino, V., Mika, D., Huang, B., Wedegaertner, P. B., Conti, M., & von Zastrow, M. (2017). Functional selectivity of GPCR-directed drug action through location bias. *Nat Chem Biol, 13*(7), 799-806. doi:10.1038/nchembio.2389

Jacobi, E., & von Engelhardt, J. (2021). Modulation of information processing by AMPA receptor auxiliary subunits. *J Physiol, 599*(2), 471-483. doi:10.1113/JP276698

Jayanthi, L. D., & Ramamoorthy, S. (2005). Regulation of monoamine transporters: influence of psychostimulants and therapeutic antidepressants. *AAPS J, 7*(3), E728-738. doi:10.1208/aapsj070373

Johnson, M. (2006). Molecular mechanisms of beta(2)-adrenergic receptor function, response, and regulation. *J Allergy Clin Immunol, 117*(1), 18-24; quiz 25. doi:10.1016/j.jaci.2005.11.012

Joiner, M. L., Lise, M. F., Yuen, E. Y., Kam, A. Y., Zhang, M., Hall, D. D., . . . Hell, J. W. (2010). Assembly of a beta2-adrenergic receptor--GluR1 signalling complex for localized cAMP signalling. *EMBO J, 29*(2), 482-495. doi:10.1038/emboj.2009.344

Jordan, M., Schallhorn, A., & Wurm, F. M. (1996). Transfecting mammalian cells: optimization of critical parameters affecting calcium-phosphate precipitate formation. *Nucleic Acids Res, 24*(4), 596-601. doi:10.1093/nar/24.4.596

Jurado, S. (2017). AMPA Receptor Trafficking in Natural and Pathological Aging. *Front Mol Neurosci, 10*, 446. doi:10.3389/fnmol.2017.00446

Kabir, Z. D., Martinez-Rivera, A., & Rajadhyaksha, A. M. (2017). From Gene to Behavior: L-Type Calcium Channel Mechanisms Underlying Neuropsychiatric Symptoms. *Neurotherapeutics, 14*(3), 588-613. doi:10.1007/s13311-017-0532-0

Kalashnikova, E., Lorca, R. A., Kaur, I., Barisone, G. A., Li, B., Ishimaru, T., . . . Diaz, E. (2010). SynDIG1: an activity-regulated, AMPA- receptor-interacting transmembrane protein that regulates excitatory synapse development. *Neuron, 65*(1), 80-93. doi:10.1016/j.neuron.2009.12.021

Kamp, T. J., & Hell, J. W. (2000). Regulation of cardiac L-type calcium channels by protein kinase A and protein kinase C. *Circ Res, 87*(12), 1095-1102. doi:10.1161/01.res.87.12.1095

Kang, M. G., Chen, C. C., Wakamori, M., Hara, Y., Mori, Y., & Campbell, K. P. (2006). A functional AMPA receptor-calcium channel complex in the postsynaptic membrane. *Proc Natl Acad Sci U S A, 103*(14), 5561-5566. doi:10.1073/pnas.0601289103

Kato, A. S., Gill, M. B., Yu, H., Nisenbaum, E. S., & Bredt, D. S. (2010). TARPs differentially decorate AMPA receptors to specify neuropharmacology. *Trends Neurosci, 33*(5), 241-248. doi:10.1016/j.tins.2010.02.004

Kirk, L. M., Ti, S. W., Bishop, H. I., Orozco-Llamas, M., Pham, M., Trimmer, J. S., & Diaz, E. (2016). Distribution of the SynDIG4/proline-rich transmembrane protein 1 in rat brain. *J Comp Neurol, 524*(11), 2266-2280. doi:10.1002/cne.23945

Koepsell, H. (2021). General Overview of Organic Cation Transporters in Brain. *Handb Exp Pharmacol*. doi:10.1007/164_2021_449

Koepsell, H. (2021). General Overview of Organic Cation Transporters in Brain (pp. 1-39). Berlin, Heidelberg: Springer Berlin Heidelberg.

Kristensen, A. S., Andersen, J., Jorgensen, T. N., Sorensen, L., Eriksen, J., Loland, C. J., . . . Gether, U. (2011). SLC6 neurotransmitter transporters: structure, function, and regulation. *Pharmacol Rev, 63*(3), 585-640. doi:10.1124/pr.108.000869

Lee, H. K., Barbarosie, M., Kameyama, K., Bear, M. F., & Huganir, R. L. (2000). Regulation of distinct AMPA receptor phosphorylation sites during bidirectional synaptic plasticity. *Nature, 405*(6789), 955-959. doi:10.1038/35016089

Lemke, T., Welling, A., Christel, C. J., Blaich, A., Bernhard, D., Lenhardt, P., . . . Moosmang, S. (2008). Unchanged beta-adrenergic stimulation of cardiac L-type calcium channels in Ca v 1.2 phosphorylation site S1928A mutant mice. *J Biol Chem, 283*(50), 34738-34744. doi:10.1074/jbc.M804981200

Leonard, A. S., Davare, M. A., Horne, M. C., Garner, C. C., & Hell, J. W. (1998). SAP97 is associated with the alpha-amino-3-hydroxy-5-methylisoxazole-4-propionic acid receptor GluR1 subunit. *J Biol Chem, 273*(31), 19518-19524. doi:10.1074/jbc.273.31.19518

Li, G. R., & Dong, M. Q. (2010). Pharmacology of cardiac potassium channels. *Adv Pharmacol, 59*, 93-134. doi:10.1016/S1054-3589(10)59004-5

Liao, P., & Soong, T. W. (2010). Understanding alternative splicing of Cav1.2 calcium channels for a new approach towards individualized medicine. *J Biomed Res, 24*(3), 181-186. doi:10.1016/S1674-8301(10)60027-9

Lieb, A., Scharinger, A., Sartori, S., Sinnegger-Brauns, M. J., & Striessnig, J. (2012). Structural determinants of CaV1.3 L-type calcium channel gating. *Channels (Austin), 6*(3), 197-205. doi:10.4161/chan.21002

Liu, W., Okochi, H., Benet, L. Z., & Zhai, S. D. (2012). Sotalol permeability in cultured-cell, rat intestine, and PAMPA system. *Pharm Res, 29*(7), 1768-1774. doi:10.1007/s11095-012-0699-3

Loo, L. S., Tang, N., Al-Haddawi, M., Dawe, G. S., & Hong, W. (2014). A role for sorting nexin 27 in AMPA receptor trafficking. *Nat Commun, 5*, 3176. doi:10.1038/ncomms4176

Lovero, K. L., Blankenship, S. M., Shi, Y., & Nicoll, R. A. (2013). SynDIG1 promotes excitatory synaptogenesis independent of AMPA receptor trafficking and biophysical regulation. *PLoS One, 8*(6), e66171. doi:10.1371/journal.pone.0066171

Lu, W., Shi, Y., Jackson, A. C., Bjorgan, K., During, M. J., Sprengel, R., . . . Nicoll, R. A. (2009). Subunit composition of synaptic AMPA receptors revealed by a single-cell genetic approach. *Neuron, 62*(2), 254-268. doi:10.1016/j.neuron.2009.02.027

Lu, Y., Allen, M., Halt, A. R., Weisenhaus, M., Dallapiazza, R. F., Hall, D. D., . . . Hell, J. W. (2007). Age-dependent requirement of AKAP150-anchored PKA and GluR2-lacking AMPA receptors in LTP. *EMBO J, 26*(23), 4879-4890. doi:10.1038/sj.emboj.7601884

Mammen, A. L., Kameyama, K., Roche, K. W., & Huganir, R. L. (1997). Phosphorylation of the alpha-amino-3-hydroxy-5-methylisoxazole4-propionic acid receptor GluR1 subunit by calcium/calmodulin-dependent kinase II. *J Biol Chem, 272*(51), 32528-32533. doi:10.1074/jbc.272.51.32528

Man, K. N. M., Navedo, M. F., Horne, M. C., & Hell, J. W. (2020). beta2 Adrenergic Receptor Complexes with the L-Type Ca(2+) Channel CaV1.2 and AMPA-Type Glutamate Receptors: Paradigms for Pharmacological Targeting of Protein Interactions. *Annu Rev Pharmacol Toxicol, 60*, 155-174. doi:10.1146/annurev-pharmtox-010919-023404

Martinez-Rivera, A., Hao, J., Tropea, T. F., Giordano, T. P., Kosovsky, M., Rice, R. C., . . . Rajadhyaksha, A. M. (2017). Enhancing VTA Cav1.3 L-type Ca(2+) channel activity promotes cocaine and mood-related behaviors via overlapping AMPA receptor mechanisms in the nucleus accumbens. *Mol Psychiatry, 22*(12), 1735-1745. doi:10.1038/mp.2017.9

Matt, L., Kirk, L. M., Chenaux, G., Speca, D. J., Puhger, K. R., Pride, M. C., . . . Diaz, E. (2018). SynDIG4/Prrt1 Is Required for Excitatory Synapse Development and Plasticity Underlying Cognitive Function. *Cell Rep, 22*(9), 2246-2253. doi:10.1016/j.celrep.2018.02.026

Matthaeus, F., Schloss, P., & Lau, T. (2015). Differential Uptake Mechanisms of Fluorescent Substrates into Stem-Cell-Derived Serotonergic Neurons. *ACS Chem Neurosci, 6*(12), 1906-1912. doi:10.1021/acschemneuro.5b00219

Matthies, H. J., Han, Q., Shields, A., Wright, J., Moore, J. L., Winder, D. G., . . . Blakely, R. D. (2009). Subcellular localization of the antidepressant-sensitive norepinephrine transporter. *BMC Neurosci, 10*, 65. doi:10.1186/1471-2202-10-65

Michailidis, I. E., Abele-Henckels, K., Zhang, W. K., Lin, B., Yu, Y., Geyman, L. S., . . . Yang, J. (2014). Age-related homeostatic midchannel proteolysis of neuronal L-type voltage-gated Ca(2)(+) channels. *Neuron, 82*(5), 1045-1057. doi:10.1016/j.neuron.2014.04.017

Moosmang, S., Haider, N., Klugbauer, N., Adelsberger, H., Langwieser, N., Muller, J., . . . Kleppisch, T. (2005). Role of hippocampal Cav1.2 Ca2+ channels in NMDA receptor-independent synaptic plasticity and spatial memory. *J Neurosci, 25*(43), 9883-9892. doi:10.1523/JNEUROSCI.1531-05.2005

Mubarik, A., Kerndt, C. C., & Cassagnol, M. (2021). Sotalol *StatPearls*. Treasure Island (FL).

Murphy, J. A., Stein, I. S., Lau, C. G., Peixoto, R. T., Aman, T. K., Kaneko, N., . . . Zukin, R. S. (2014). Phosphorylation of Ser1166 on GluN2B by PKA is critical to synaptic NMDA receptor function and Ca2+ signaling in spines. *J Neurosci, 34*(3), 869-879. doi:10.1523/JNEUROSCI.4538-13.2014

Nair, D., Hosy, E., Petersen, J. D., Constals, A., Giannone, G., Choquet, D., & Sibarita, J. B. (2013). Super-resolution imaging reveals that AMPA receptors inside synapses are dynamically organized in nanodomains regulated by PSD95. *J Neurosci, 33*(32), 13204-13224. doi:10.1523/JNEUROSCI.2381-12.2013

Nanou, E., & Catterall, W. A. (2018). Calcium Channels, Synaptic Plasticity, and Neuropsychiatric Disease. *Neuron, 98*(3), 466-481. doi:10.1016/j.neuron.2018.03.017

Nemeroff, C. B., & Owens, M. J. (2004). Pharmacologic differences among the SSRIs: focus on monoamine transporters and the HPA axis. *CNS Spectr, 9*(6 Suppl 4), 23-31. doi:10.1017/s1092852900025475

Nguyen, P. V., & Connor, S. A. (2019). Noradrenergic Regulation of Hippocampus-Dependent Memory. *Cent Nerv Syst Agents Med Chem, 19*(3), 187-196. doi:10.2174/1871524919666190719163632

Nicoll, R. A., Tomita, S., & Bredt, D. S. (2006). Auxiliary subunits assist AMPA-type glutamate receptors. *Science, 311*(5765), 1253-1256. doi:10.1126/science.1123339

Nishimune, A., Isaac, J. T., Molnar, E., Noel, J., Nash, S. R., Tagaya, M., . . . Henley, J. M. (1998). NSF binding to GluR2 regulates synaptic transmission. *Neuron, 21*(1), 87-97. doi:10.1016/s0896-6273(00)80517-6

Nystoriak, M. A., Nieves-Cintron, M., Patriarchi, T., Buonarati, O. R., Prada, M. P., Morotti, S., . . . Navedo, M. F. (2017). Ser1928 phosphorylation by PKA stimulates the L-type Ca2+ channel CaV1.2 and vasoconstriction during acute hyperglycemia and diabetes. *Sci Signal, 10*(463). doi:10.1126/scisignal.aaf9647

O'Dell, T. J., Connor, S. A., Guglietta, R., & Nguyen, P. V. (2015). beta-Adrenergic receptor signaling and modulation of long-term potentiation in the mammalian hippocampus. *Learn Mem, 22*(9), 461-471. doi:10.1101/lm.031088.113

Oh, M. C., Derkach, V. A., Guire, E. S., & Soderling, T. R. (2006). Extrasynaptic membrane trafficking regulated by GluR1 serine 845 phosphorylation primes AMPA receptors for long-term potentiation. *J Biol Chem, 281*(2), 752-758. doi:10.1074/jbc.M509677200

Oliveria, S. F., Dell'Acqua, M. L., & Sather, W. A. (2007). AKAP79/150 anchoring of calcineurin controls neuronal L-type Ca2+ channel activity and nuclear signaling. *Neuron, 55*(2), 261-275. doi:10.1016/j.neuron.2007.06.032

Patriarchi, T., Buonarati, O. R., & Hell, J. W. (2018). Postsynaptic localization and regulation of AMPA receptors and Cav1.2 by beta2 adrenergic receptor/PKA and Ca(2+)/CaMKII signaling. *EMBO J, 37*(20). doi:10.15252/embj.201899771

Patriarchi, T., Qian, H., Di Biase, V., Malik, Z. A., Chowdhury, D., Price, J. L., . . . Hell, J. W. (2016). Phosphorylation of Cav1.2 on S1928 uncouples the L-type Ca2+ channel from the beta2 adrenergic receptor. *EMBO J, 35*(12), 1330-1345. doi:10.15252/embj.201593409

Perez-Reyes, E., Castellano, A., Kim, H. S., Bertrand, P., Baggstrom, E., Lacerda, A. E., . . . Birnbaumer, L. (1992). Cloning and expression of a cardiac/brain beta subunit of the L-type calcium channel. *J Biol Chem, 267*(3), 1792-1797.

Price, C. J., Kim, P., & Raymond, L. A. (1999). D1 dopamine receptor-induced cyclic AMP-dependent protein kinase phosphorylation and potentiation of striatal glutamate receptors. *J Neurochem, 73*(6), 2441-2446. doi:10.1046/j.1471-4159.1999.0732441.x

Qian, H., Patriarchi, T., Price, J. L., Matt, L., Lee, B., Nieves-Cintron, M., . . . Hell, J. W. (2017). Phosphorylation of Ser1928 mediates the enhanced activity of the L-type Ca2+ channel Cav1.2 by the beta2-adrenergic receptor in neurons. *Sci Signal, 10*(463). doi:10.1126/scisignal.aaf9659

Ranjbar-Slamloo, Y., & Fazlali, Z. (2019). Dopamine and Noradrenaline in the Brain; Overlapping or Dissociate Functions? *Front Mol Neurosci, 12*, 334. doi:10.3389/fnmol.2019.00334

Roche, K. W., O'Brien, R. J., Mammen, A. L., Bernhardt, J., & Huganir, R. L. (1996). Characterization of multiple phosphorylation sites on the AMPA receptor GluR1 subunit. *Neuron, 16*(6), 1179-1188. doi:10.1016/s0896-6273(00)80144-0

Ross, J. A., McGonigle, P., & Van Bockstaele, E. J. (2015). Locus Coeruleus, norepinephrine and Abeta peptides in Alzheimer's disease. *Neurobiol Stress, 2*, 73-84. doi:10.1016/j.ynstr.2015.09.002

Ross, J. A., & Van Bockstaele, E. J. (2020). The Locus Coeruleus- Norepinephrine System in Stress and Arousal: Unraveling Historical, Current, and Future Perspectives. *Front Psychiatry, 11*, 601519. doi:10.3389/fpsyt.2020.601519

Roubert, C., Cox, P. J., Bruss, M., Hamon, M., Bonisch, H., & Giros, B. (2001). Determination of residues in the norepinephrine transporter that are critical for tricyclic antidepressant affinity. *J Biol Chem, 276*(11), 8254-8260. doi:10.1074/jbc.M009798200

Scheefhals, N., & MacGillavry, H. D. (2018). Functional organization of postsynaptic glutamate receptors. *Mol Cell Neurosci, 91*, 82-94. doi:10.1016/j.mcn.2018.05.002

Schluter, O. M., Xu, W., & Malenka, R. C. (2006). Alternative N-terminal domains of PSD-95 and SAP97 govern activity-dependent regulation of synaptic AMPA receptor function. *Neuron, 51*(1), 99-111. doi:10.1016/j.neuron.2006.05.016

Schnell, E., Sizemore, M., Karimzadegan, S., Chen, L., Bredt, D. S., & Nicoll, R. A. (2002). Direct interactions between PSD-95 and stargazin control synaptic AMPA receptor number. *Proc Natl Acad Sci U S A, 99*(21), 13902-13907. doi:10.1073/pnas.172511199

Schwenk, J., Harmel, N., Zolles, G., Bildl, W., Kulik, A., Heimrich, B., . . . Klocker, N. (2009). Functional proteomics identify cornichon proteins as auxiliary subunits of AMPA receptors. *Science, 323*(5919), 1313-1319. doi:10.1126/science.1167852

Seaman, M. N. (2012). The retromer complex - endosomal protein recycling and beyond. *J Cell Sci, 125*(Pt 20), 4693-4702. doi:10.1242/jcs.103440

Senatore, A., Boone, A. N., & Spafford, J. D. (2011). Optimized transfection strategy for expression and electrophysiological recording of recombinant voltage-gated ion channels in HEK-293T cells. *J Vis Exp*(47). doi:10.3791/2314

Shang, T., Uihlein, A. V., Van Asten, J., Kalyanaraman, B., & Hillard, C. J. (2003). 1-Methyl-4-phenylpyridinium accumulates in cerebellar granule neurons via organic cation transporter 3. *J Neurochem, 85*(2), 358-367. doi:10.1046/j.1471-4159.2003.01686.x

Shepherd, J. D., & Huganir, R. L. (2007). The cell biology of synaptic plasticity: AMPA receptor trafficking. *Annu Rev Cell Dev Biol, 23*, 613-643. doi:10.1146/annurev.cellbio.23.090506.123516

Shi, S., Hayashi, Y., Esteban, J. A., & Malinow, R. (2001). Subunit-specific rules governing AMPA receptor trafficking to synapses in hippocampal pyramidal neurons. *Cell, 105*(3), 331-343. doi:10.1016/s0092-8674(01)00321-x

Sievers, F., Wilm, A., Dineen, D., Gibson, T. J., Karplus, K., Li, W., . . . Higgins, D. G. (2011). Fast, scalable generation of high-quality protein multiple sequence alignments using Clustal Omega. *Mol Syst Biol, 7*, 539. doi:10.1038/msb.2011.75

Simms, B. A., & Zamponi, G. W. (2014). Neuronal voltage-gated calcium channels: structure, function, and dysfunction. *Neuron, 82*(1), 24-45. doi:10.1016/j.neuron.2014.03.016

Sinnegger-Brauns, M. J., Hetzenauer, A., Huber, I. G., Renstrom, E., Wietzorrek, G., Berjukov, S., . . . Striessnig, J. (2004). Isoform-specific regulation of mood behavior and pancreatic beta cell and cardiovascular function by L-type Ca 2+ channels. *J Clin Invest, 113*(10), 1430-1439. doi:10.1172/JCI20208

Sinnegger-Brauns, M. J., Huber, I. G., Koschak, A., Wild, C., Obermair, G. J., Einzinger, U., . . . Striessnig, J. (2009). Expression and 1,4-dihydropyridine-binding properties of brain L-type calcium channel isoforms. *Mol Pharmacol, 75*(2), 407-414. doi:10.1124/mol.108.049981

Splawski, I., Timothy, K. W., Sharpe, L. M., Decher, N., Kumar, P., Bloise, R., . . . Keating, M. T. (2004). Ca(V)1.2 calcium channel dysfunction causes a multisystem disorder including arrhythmia and autism. *Cell, 119*(1), 19-31. doi:10.1016/j.cell.2004.09.011

Striessnig, J., Pinggera, A., Kaur, G., Bock, G., & Tuluc, P. (2014). L-type Ca(2+) channels in heart and brain. *Wiley Interdiscip Rev Membr Transp Signal, 3*(2), 15-38. doi:10.1002/wmts.102

Sun, X., Milovanovic, M., Zhao, Y., & Wolf, M. E. (2008). Acute and chronic dopamine receptor stimulation modulates AMPA receptor trafficking in nucleus accumbens neurons cocultured with prefrontal cortex neurons. *J Neurosci, 28*(16), 4216-4230. doi:10.1523/JNEUROSCI.0258-08.2008

Tavalin, S. J., Colledge, M., Hell, J. W., Langeberg, L. K., Huganir, R. L., & Scott, J. D. (2002). Regulation of GluR1 by the A-kinase anchoring protein 79 (AKAP79) signaling complex shares properties with long-term depression. *J Neurosci, 22*(8), 3044-3051. doi:20026277

Temkin, P., Lauffer, B., Jager, S., Cimermancic, P., Krogan, N. J., & von Zastrow, M. (2011). SNX27 mediates retromer tubule entry and endosome-to-plasma membrane trafficking of signalling receptors. *Nat Cell Biol, 13*(6), 715-721. doi:10.1038/ncb2252

Temkin, P., Morishita, W., Goswami, D., Arendt, K., Chen, L., & Malenka, R. (2017). The Retromer Supports AMPA Receptor Trafficking During LTP. *Neuron, 94*(1), 74-82 e75. doi:10.1016/j.neuron.2017.03.020

Tomita, S., Chen, L., Kawasaki, Y., Petralia, R. S., Wenthold, R. J., Nicoll, R. A., & Bredt, D. S. (2003). Functional studies and distribution define a family of transmembrane AMPA receptor regulatory proteins. *J Cell Biol, 161*(4), 805-816. doi:10.1083/jcb.200212116

Tomita, S., Nicoll, R. A., & Bredt, D. S. (2001). PDZ protein interactions regulating glutamate receptor function and plasticity. *J Cell Biol, 153*(5), F19-24. doi:10.1083/jcb.153.5.f19

Traynelis, S. F., Wollmuth, L. P., McBain, C. J., Menniti, F. S., Vance, K. M., Ogden, K. K., . . . Dingledine, R. (2010). Glutamate receptor ion channels: structure, regulation, and function. *Pharmacol Rev, 62*(3), 405-496. doi:10.1124/pr.109.002451

Tseng, P. Y., Henderson, P. B., Hergarden, A. C., Patriarchi, T., Coleman, A. M., Lillya, M. W., . . . Horne, M. C. (2017). alpha-Actinin Promotes Surface Localization and Current Density of the Ca(2+) Channel CaV1.2 by Binding to the IQ Region of the alpha1 Subunit. *Biochemistry, 56*(28), 3669-3681. doi:10.1021/acs.biochem.7b00359

Tsvetanova, N. G., & von Zastrow, M. (2014). Spatial encoding of cyclic AMP signaling specificity by GPCR endocytosis. *Nat Chem Biol, 10*(12), 1061-1065. doi:10.1038/nchembio.1665

Vagnozzi, A. N., & Pratico, D. (2019). Endosomal sorting and trafficking, the retromer complex and neurodegeneration. *Mol Psychiatry, 24*(6), 857-868. doi:10.1038/s41380-018-0221-3

van Bommel, B., & Mikhaylova, M. (2016). Talking to the neighbours: The molecular and physiological mechanisms of clustered synaptic plasticity. *Neurosci Biobehav Rev, 71*, 352-361. doi:10.1016/j.neubiorev.2016.09.016

Vialou, V., Amphoux, A., Zwart, R., Giros, B., & Gautron, S. (2004). Organic cation transporter 3 (Slc22a3) is implicated in salt-intake regulation. *J Neurosci, 24*(11), 2846-2851. doi:10.1523/JNEUROSCI.5147-03.2004

Vieira, L. S., & Wang, J. (2021). Brain Plasma Membrane Monoamine Transporter in Health and Disease (pp. 1-28). Berlin, Heidelberg: Springer Berlin Heidelberg.

Voglis, G., & Tavernarakis, N. (2006). The role of synaptic ion channels in synaptic plasticity. *EMBO Rep, 7*(11), 1104-1110. doi:10.1038/sj.embor.7400830

Waites, C. L., Specht, C. G., Hartel, K., Leal-Ortiz, S., Genoux, D., Li, D., . . . Garner, C. C. (2009). Synaptic SAP97 isoforms regulate AMPA receptor dynamics and access to presynaptic glutamate. *J Neurosci, 29*(14), 4332-4345. doi:10.1523/JNEUROSCI.4431-08.2009

Walsh, D. M., & Selkoe, D. J. (2007). A beta oligomers - a decade of discovery. *J Neurochem, 101*(5), 1172-1184. doi:10.1111/j.1471-4159.2006.04426.x

Wang, D., Govindaiah, G., Liu, R., De Arcangelis, V., Cox, C. L., & Xiang, Y. K. (2010). Binding of amyloid beta peptide to beta2 adrenergic receptor induces PKA-dependent AMPA receptor hyperactivity. *FASEB J, 24*(9), 3511-3521. doi:10.1096/fj.10-156661

Wang, J. (2016). The plasma membrane monoamine transporter (PMAT): Structure, function, and role in organic cation disposition. *Clin Pharmacol Ther, 100*(5), 489-499. doi:10.1002/cpt.442

Wassal, R. D., Teramoto, N., & Cunnane, T. C. (2009). Noradrenaline *Encyclopedia of Neuroscience* (pp. 1221-1230): Elsevier Ltd.

Wei, X., Neely, A., Lacerda, A. E., Olcese, R., Stefani, E., Perez-Reyes, E., & Birnbaumer, L. (1994). Modification of Ca2+ channel activity by deletions at the carboxyl terminus of the cardiac alpha 1 subunit. *J Biol Chem, 269*(3), 1635-1640.

Wenthold, R. J., Petralia, R. S., Blahos, J., II, & Niedzielski, A. S. (1996). Evidence for multiple AMPA receptor complexes in hippocampal CA1/CA2 neurons. *J Neurosci, 16*(6), 1982-1989.

Wenthold, R. J., Yokotani, N., Doi, K., & Wada, K. (1992). Immunochemical characterization of the non-NMDA glutamate receptor using subunit-specific antibodies. Evidence for a hetero-oligomeric structure in rat brain. *J Biol Chem, 267*(1), 501-507.

Willoughby, D., Masada, N., Wachten, S., Pagano, M., Halls, M. L., Everett, K. L., . . . Cooper, D. M. (2010). AKAP79/150 interacts with AC8 and regulates Ca2+-dependent cAMP synthesis in pancreatic and neuronal systems. *J Biol Chem, 285*(26), 20328-20342. doi:10.1074/jbc.M110.120725

Woolfrey, K. M., & Dell'Acqua, M. L. (2015). Coordination of Protein Phosphorylation and Dephosphorylation in Synaptic Plasticity. *J Biol Chem, 290*(48), 28604-28612. doi:10.1074/jbc.R115.657262

Wright, A., & Vissel, B. (2012). The essential role of AMPA receptor GluR2 subunit RNA editing in the normal and diseased brain. *Front Mol Neurosci, 5*, 34. doi:10.3389/fnmol.2012.00034

Wu, X., Kekuda, R., Huang, W., Fei, Y. J., Leibach, F. H., Chen, J., . . . Ganapathy, V. (1998). Identity of the organic cation transporter OCT3 as the extraneuronal monoamine transporter (uptake2) and evidence for the expression of the transporter in the brain. *J Biol Chem, 273*(49), 32776-32786. doi:10.1074/jbc.273.49.32776

Xu, H., Ginsburg, K. S., Hall, D. D., Zimmermann, M., Stein, I. S., Zhang, M., . . . Hell, J. W. (2010). Targeting of protein phosphatases PP2A and PP2B to the C-terminus of the L-

type calcium channel Ca v1.2. *Biochemistry, 49*(48), 10298-10307. doi:10.1021/bi101018c

Zhang, H., & Bramham, C. R. (2020). Bidirectional Dysregulation of AMPA Receptor-Mediated Synaptic Transmission and Plasticity in Brain Disorders. *Front Synaptic Neurosci, 12*, 26. doi:10.3389/fnsyn.2020.00026

Zhang, H., Zhang, C., Vincent, J., Zala, D., Benstaali, C., Sainlos, M., . . . Choquet, D. (2018). Modulation of AMPA receptor surface diffusion restores hippocampal plasticity and memory in Huntington's disease models. *Nat Commun, 9*(1), 4272. doi:10.1038/s41467-018-06675-3

Zhang, M., Patriarchi, T., Stein, I. S., Qian, H., Matt, L., Nguyen, M., . . . Hell, J. W. (2013). Adenylyl cyclase anchoring by a kinase anchor protein AKAP5 (AKAP79/150) is important for postsynaptic beta-adrenergic signaling. *J Biol Chem, 288*(24), 17918-17931. doi:10.1074/jbc.M112.449462

Zhang, Y., Matt, L., Patriarchi, T., Malik, Z. A., Chowdhury, D., Park, D. K., . . . Hell, J. W. (2014). Capping of the N-terminus of PSD-95 by calmodulin triggers its postsynaptic release. *EMBO J, 33*(12), 1341-1353. doi:10.1002/embj.201488126

Zhao, W. Q., Santini, F., Breese, R., Ross, D., Zhang, X. D., Stone, D. J., . . . Ray, W. J. (2010). Inhibition of calcineurin-mediated endocytosis and alpha-amino-3-hydroxy-5-methyl-4-isoxazolepropionic acid (AMPA) receptors prevents amyloid beta oligomer-induced synaptic disruption. *J Biol Chem, 285*(10), 7619-7632. doi:10.1074/jbc.M109.057182

Zhou, J. (2004). Norepinephrine transporter inhibitors and their therapeutic potential. *Drugs Future, 29*(12), 1235-1244. doi:10.1358/dof.2004.029.12.855246

Zuccotti, A., Clementi, S., Reinbothe, T., Torrente, A., Vandael, D. H., & Pirone, A. (2011). Structural and functional differences between L-type calcium channels: crucial issues for future selective targeting. *Trends Pharmacol Sci, 32*(6), 366-375. doi:10.1016/j.tips.2011.02.012